Enzymes for the synthesis of bioactive compounds

I n a u g u r a l d i s s e r t a t i o n

zur

Erlangung des akademischen Grades eines

Doktors der Naturwissenschaften (Dr. rer. nat.)

der

Mathematisch-Naturwissenschaftlichen Fakultät

der

Universität Greifswald

vorgelegt von

Agata Wszołek

geboren am 16.10.1987

in Gorzów Wielkopolski, Polen

Greifswald, 28.09.2020

Dekan:	Prof. Dr. Werner Weitschies
1. Gutachter:	Prof. Dr. Uwe T. Bornscheuer
2. Gutachter:	Prof. Dr. Vlada B. Urlacher
Tag der Promotion	28.09.2020

Contents

List of Abbreviations

ADP	Adenosine 5'-Diphosphate
AK	Arginine Kinase
Amp	Ampicillin
APS	Ammonium persulfate
ATP	Adenosine 5'-Triphosphate
ASS	Argininosuccinate synthase
ASL	Argininosuccinate lyase
Aq. dest.	Distilled water
BA	Bile acids
B. megaterium	*Bacillus megaterium*
BLAST	Basic Local Alignment Search Tool
BM3	P450 from *Bacillus megaterium*
CO	Carbon monoxide
CYP	Cytochrome P450 monooxygenase
DCPIP	2,6-Dichlorofenoloindofenol
DMF	Dimethylformamide
DMSO	Dimethyl sulfoxide
DNA	Deoxyribonucleic acid
DTT	1,4-Dithiothreitol
dNTP	Deoxyribonucleoside triphosphate
E. coli	*Escherichia coli*
e.g.	exempli gratia
EDTA	Ethylenediaminetetraacetic acid
ee	Enantiomeric excess
EPSPS	5-enolpyruvylshikimate 3-phosphate synthase
FAD	Flavin adenine dinucleotide
FDA	Food and Drug Administration
FMN	Flavin mononucleotide
FPLC	Fast protein liquid chromatography
GC	Gas chromatography
GC-MS	Gas chromatography-mass spectrometry
HPLC	High performance liquid chromatography
HRP	Horseradish peroxidase
IMAC	Immobilized metal affinity chromatography
IPTG	Isopropyl β-D-1-thiogalactopyranoside
Kan	Kanamycin
Kb	Kilobases
LB	Lysogeny broth
LDH	L-Lactic Dehydrogenase
kDa	Kilodalton
mA	Milliampere
NAD(P)H	Nicotinamide adenine dinucleotide (phosphate)
$NAD(P)^+$	Oxidized NAD(P)H
NMR	Nuclear magnetic resonance
OD600	Optical density at $\lambda = 600nm$
ORF	Open reading frame
P. pastoris	*Pichia pastoris*
P. putida	*Pseudomonas putida*
PdX	Putidaredoxin from *Pseudomonas putida*

PdR	Putidaredoxin Reductase *Pseudomonas putida*
PAGE	Polyacrylamide gel electrophoresis
PEP	Phospho(enol)pyruvate
PCR	Polymerase chain reaction
PDB	Protein Data Bank
pH	Pondus hydrogenii
pI	Isoelectric point
PK	Pyruvate Kinase
SDS	Sodium dodecyl sulfate
TAE	Tris-Acetate-EDTA
TB	Terrific broth
TEMED	N,N,N',N'-Tetramethylethane-1,2-diamine
Triton X10	O-[4-(1,1,3,3Tetramethylbutyl) phenoxy]polyethoxyethanol
TLC	Thin layer chromatography
UV/Vis	Ultraviolet/visible
V	Volt
w/o	Without
wt	Wild-type
Zeo	Zeocin
YNB	Yeast nitrogen base
YPD	Yeast-Extract-Peptone-Dextrose
ß-NADH	ß-Nicotinamide Adenine Dinucleotide, Reduced Form
ß-NAD	ß-Nicotinamide Adenine Dinucleotide, Oxidized Form
δ-Ala	δ-Aminolevulinic acid

Additionally, SI-units and the standard one- and three-letter codes for amino acids and abbreviations for nucleotides were used.

1 Introduction

With the rapid development of industrialization, environmental pollution has become a global concern. The chemical industry and other related industries supply a huge variety of essential products, from petroleum to pharmaceuticals. However, these manufacturing processes also lead to millions of tons of waste, which have the potential to be harmful to the environment, human health and to all living species (Clark 1999). Green chemistry has become a worldwide approach that leads to design and manufacture of cost-competitive chemical products and processes to reduce or to eliminate the use and generation of substances hazardous to human health and environment (Chanshetti 2014). Enzymes can replace chemo-catalysts in synthetic routes and enable new synthetic pathways, which may be shorter, more efficient and more sustainable. Moreover, combining chemo- and bio-catalysis generates opportunities for the design of new synthetic routes (Bornscheuer et al. 2012; Choi et al. 2015; Truppo 2017). Due to their ability to catalyze important synthetic chemical reactions under mild conditions compared with chemical catalysts that need harsher conditions, such as high temperature and pressure, enzymes became important tools in the industrial synthesis of pharmaceutical, cosmetic, food and bulk chemicals. What is more, enzymes are biodegradable and have nontoxic nature, which makes them good alternatives to hazardous chemical pollutants (Singh et al. 2016; Timson 2019). However, the number of applications of enzymes is limited because of the enzyme availability, substrate scope, and operational stability. Recent scientific breakthroughs in genomics, directed protein evolution and technology advances as bioinformatic tools should help to overcome these limitations. Worldwide, the challenge for chemists is to develop synthetic methodology and „green" processes that posess environmental and economic benefits, which are now required as: reduction of materials and energy intensity of chemical processes and by-products, minimization or elimination of harmful chemicals emission in the environment (Schmid et al. 2001; Thomas et al. 2002; Singh et al. 2016). The biocatalytic transformations have been employed in industries and medicine for the sake of development of new production routes to fine chemicals, pharmaceutical ingredients and precursors, agrochemicals, and even bulk commodities. Figure 1 summarizes several applications of enzymes based on different industrial sectors. Due to this versatility of applications, enzymes can be considered as a powerful technology for a biobased economy (Wohlgemuth 2009).

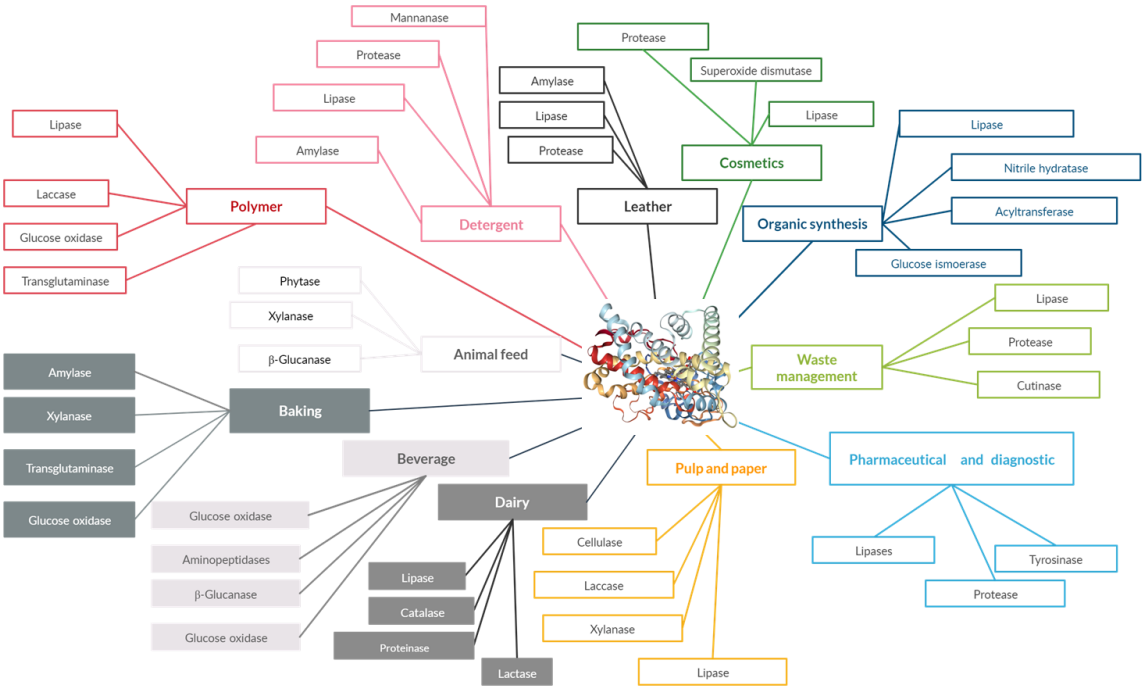

Figure 1:Industrial applications of microbial enzymes. Data adapted from Singh et al. 2016.(Singh et al. 2016)

For the majority of enzyme classes, almost 75% of all industrial enzymes are hydrolytic enzymes. Alcohol dehydrogenase, amylases, cellulases, lipases, ketoreductases, proteases and xylanases, dominate the enzyme market, accounting for more than 70% of all enzyme sales (Bornscheuer et al. 2012; Li et al. 2012; Singh et al. 2016; Buller et al. 2017).

Over the last decades, oxidoreductases have been more regularly taken into account in the design of novel process routes (e.g., alcohol dehydrogenases, BVMOs, ketoreductases, laccases, peroxidases) whereas a few lyases (e.g., pectate lyase for raw cotton bio scouring, pectin lyase for the food industry) have been commercially introduced but have not yet been sufficiently developed to become widely applicable in manufacturing (Galante and Formantici 2005; Kirschner and Bornscheuer 2008; Kashyap and Mishra 2011; Bornscheuer et al. 2012; Staudt et al. 2013; Patel et al. 2016; Buller et al. 2017; Zhao et al. 2018; Atalla et al. 2019). Diverse industries demand the discovery and application of novel enzymes. Today, advances in microbial genome engineering techniques allow the easy modification of genes in the biosynthesis pathway to maximize the production of high-value molecules in the host.

In particlular, hydroxylated compounds are of great value, but selective hydroxylation of organic molecules is a challenge in the classical organic chemistry. Therefore, enzymes which catalyse selective hydroxylation are highly needed.

Since oxidoreductases, more precisely P450 monooxygenases, can perform selective hydroxylation of non-activated carbons, they are a class of enzymes with potential in the production of a variety of fine chemicals and pharmaceuticals (Martínez et al. 2017).

Lyases are excellent candidates for the commercial production of optically active compounds. Lyases catalyze the cleavage or formation of C-C, C-N, C-O and other bonds to yield double bonds. They also catalyze the addition of groups to double bonds. Moreover, they do not require (expensive) cofactors and give an absolute stereospecificity with a theoretical yield of 100%, which is much more efficient compared to enantiomeric resolutions of only 50% productive rate. Therefore, lyases are attracting considerable interest as biocatalysts for the production of optically active compounds. Lyases such as hydroxynitril lyase, aspartase, nitrile hydratase, pyruvate decarboxylases have already found application in a few large commercial processes (van der Werf et al. 1994; Mahdi and Kelly 2008).

Moreover, industry demands the discovery of more selective and efficient novel catalysts and processes for the manufacture of phosphorylated, enantiomerically pure fine chemicals and metabolites. The synthesis and analysis of phosphorylated metabolites, which play a central role in metabolism, signaling, regulation and maintenance, is still of major interest today. Therefore, synthetic methodologies for the phosphorylation of small molecules continue to be important. While chemical synthesis of these small molecules is challenging and requires the use of protecting groups, biocatalytic phosphorylation can be highly site-selective and does not need protecting groups. A large number of phosphorylases, phosphatases, and phosphotransfer-kinases have been described as enzymes for the biocatalytic synthesis of phosphorylated metabolites. Therefore, employing kinases in the industrial biocatalytic production of phosphorylated metabolites would be highly beneficial (Wohlgemuth 2017; Wohlgemuth et al. 2017; Roy et al. 2019).

Taking into consideration the above arguments, the objective of this thesis was to achieve efficient, selective and environmentally friendly processes, which enable

obtaining bioactive compounds such as metabolites and fine chemicals using diverse classes of enzymes such as P450 monooxygenases, lyases and kinases.

1.1 Enzymes in organic synthesis

Because of the unique properties of enzymes, such as high regio-, chemo- and stereoselectivity, fast action, and their environmentally friendly character, enzymes are used in many industries. According to the type of the catalyzed reaction, enzymes can be classified into seven types (Figure 2). There are many commercially potencially useful microbial enzymes in the metagenomic database, but as of today, 75% of the industrial enzymes are hydrolytic enzymes (Li et al. 2012). In this thesis, the oxidoreductases, tansferases and lyases will be detailed and their scope of industrial application will be discussed (indicated in green in Figure 2).

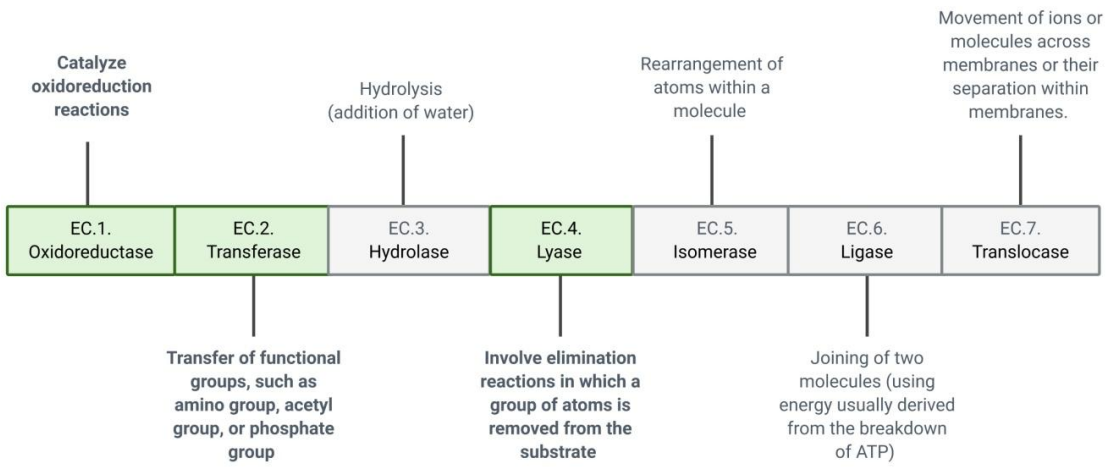

Figure 2: Systematic name is given according to the reaction in the seven classes of the enzymes.

1.2 Oxidoreductases: P450-monooxygenases

Oxidoreductases are a broad class of enzymes that catalyze biological oxidation/reduction processes. The main reason for the interest in oxidoreductases and their industrial application is their ability to catalyze regio-, chemo-, and stereoselective reactions where chemical catalysts often fail. Therefore, oxidoreductases are often considered as a perfect tool for green chemistry and have already several applications in the industry (e.g. the synthesis of products such as *cis*-dihydrodiols, catechols, epoxides) (May and Padgette 1983; May 1999; Xu 2005; Nolan and O'Connor 2008; Martínez et al. 2017). Oxygenases belong to the oxidoreductase class of enzymes, which introduce one (monooxygenases, e.g. P450, BVMO) or two (dioxygenases, e.g. toluene dioxygenase, naphthalene dioxygenase) oxygen atoms into their substrates. Typically NADH or NADPH serve as reduction equivalents through electron transfer proteins (such as reductase) (Williams et al. 1990; Lee 2006; de Souza et al. 2017).

The cytochromes P450 monooxygenases constitute a large family of cysteinato-heme enzymes. In all these enzymes, the prosthetic group is constituted of iron(III) protoporphyrin IX covalently linked to the protein by the sulfur atom of a proximal cysteine ligand (Guengerich and Munro 2013; Munro et al. 2013). They are b-type hemoproteins, and they owe their name to the intense light absorption at 450 nm from their unusual spectral properties displaying a typical absorption at maximum 450 nm of the reduced CO-bound heme-complex. They play a key role in the oxidative transformation of endogenous and exogenous molecules. As the means of oxidation, P450 uses molecular oxygen, introducing one atom of oxygen into the substrate and reduces the second oxygen to a water molecule, utilizing two electrons derived from the cofactors NADH or NADPH and transfer them to the heme iron of the P450 (Equation 1)(Meunier et al. 2004; Urlacher and Girhard 2012; Erdogan 2019).

$$\mathbf{RH + O_2 + NAD(P)H + H^+ \rightarrow ROH + NAD(P)^+ + H_2O}$$

Equation 1: General reaction of P450-monooxygenase-catalyzed reactions.

1.2.1 Catalytic cycle of cytochrome P450 enzymes

The catalytic cycle of a typical P450 is shown in Figure 3.I.

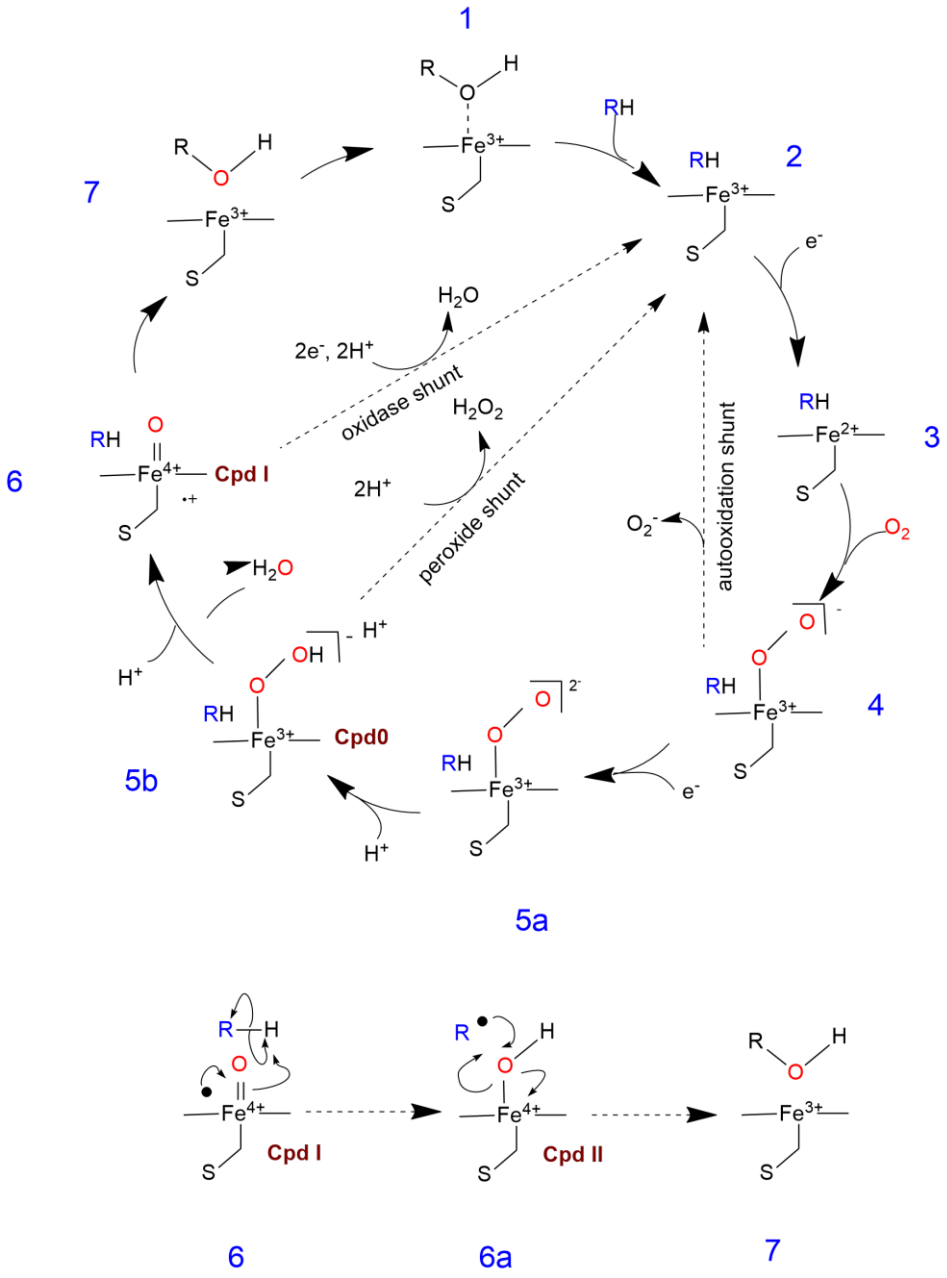

Figure 3.I: Scheme of the catalytic cycle of cytochrome P450 monooxygenases. The 'uncoupling pathways' are shown with dotted lines. 3.II: Scheme of the 'oxygen rebound' mechanism. The ferryl-oxo intermediate (CpdI) is considered to be the active oxidant that abstracts hydrogen from the substrate (R-H), which is followed by quick radical recombination and release of the oxygenated (frequently hydroxylated) product (R-OH) Adapted from Munro et al. (2013) (Munro et al. 2013).

The P450 cycle begins with the heme in the resting form (1) and shows successive events of substrate (RH) binding (2) with distal water ligand dissociation. Substrate binding induces electron transfer from NAD(P)H via cytochrome P450 reductase or another associated reductase (3). Molecular oxygen binds to the ferrous heme center to form a ferric peroxo state (4); next a second electron is transferred from either cytochrome P450 reductase, ferredoxins or cytochrome b5, reducing the Fe-O_2 adduct to give a short-lived peroxo state (5a). The peroxo group is rapidly protonated to generate the transient compound 0 (ferric hydroperoxo) species (5b). Further protonation of this intermediate leads to a release of one water molecule and forming of the highly reactive species referred to as P450 Compound I. These are used as the catalyst for oxygen insertion (6) to generate ROH product (7). The final step is a dissociation of the oxidized substrate from the active site of CYP, wherein the enzyme returns to its initial ferric state (Fe^{3+}) and is thus equipped to react again. The oxygen rebound mechanism (hydroxylated product formation and release) is shown in Figure. 3.II (under the catalytic cycle of P450). Hydrogen abstraction from the substrate takes place by compound I (6) to form compound II (6a), prior to rebound of the hydroxyl to the substrate radical to form the hydroxylated product (Werck-Reichhart and Feyereisen 2000; Isin and Guengerich 2008; Munro et al. 2013; Dubey and Shaik 2019).

The normal reaction mechanism of cytochrome P450 operates by utilizing two reducing equivalents to deplete atmospheric dioxygen, producing one molecule of water and an oxygenated product in an overall stoichiometry of 2 electrons:1 dioxygen:1 product (Grinkova et al. 2013). Often, electrons generated by the redox partner, are not transferred effectively. Therefore, the catalytic cycle may be hindered in some cases by three so called “uncoupling” pathways (depicted by dotted lines in Figure 3), yielding hydrogen peroxide or superoxide anion without substrate metabolism. The first is the “oxidase shunt” pathway, where Compound I (6) is protonated and reduced to produce a water molecule. The alternative route for monooxygenation is via the “peroxide shunt”, interaction with single-oxygen donors such as H_2O_2 or related oxygen donors, which leads to the formation of the iron-oxo intermediate (compound 0 (5b), from the ferric substrate-bound form (2). Interestingly, it has been shown that there are a few examples of P450s (P450 peroxygenases) that are able to use hydrogen peroxide for their benefit and drive the reverse reaction, generating Compound 0 (5b) directly from the initially substrate-bound (2) intermediate (Makris et al. 2005). The third uncoupling pathway is the “autooxidation shunt” path, where the ferric-superoxy complex (4) produces a superoxide

anion and the enzyme returns to the resting state (2). The formation of reactive oxygen species (uncoupling) is an unfavorable side reaction (Morlock et al. 2018). The coupling efficiency is a measure of the number of electrons donated from NAD(P)H, which are successfully used for the catalysis of a bound organic substrate (Albertolle and Peter Guengerich 2018). Whereas uncoupling can lead to inactivation of the enzyme, the coupling efficiency of a P450 is an important determinant of the enzymes rate of catalysis. The coupling efficiency is a measure of the number of electrons donated from NAD(P)H, which are successfully used for the catalysis of a bound organic substrate (Cook et al. 2016). It has been shown in the past that the bacterial P450 has higher coupling efficiencies for native substrates compared to mammalian (Albertolle and Peter Guengerich 2018). Moreover, for self-sufficient systems like the cytochrome P450 BM3, the coupling efficiency can be 100% (Ciaramella et al. 2017), whereas for other P450 multi-component systems, the coupling efficiency can be very low (0.5–3%) (Gruenke et al. 1995). For instance, BM3, which acts as a fatty acids oxygenase displaying a high activity (>1000 turnovers/min), has a coupling efficiency nearly 100%, meaning that all electrons donated from the nicotinamide cofactor are used for catalysis (Ciaramella et al. 2017). Moreover, different mutants of P450 BM3 have a coupling efficiency against testosterone rangeing from 13.5% to 83.5% (Ciaramella et al. 2017).

1.2.2 Classification of cytochrome P450 enzymes

Depending on structural characteristics and their type of redox partners, P450s can be classified according to their number of component systems: single-, two- or three protein systems. Prokaryotic P450s are generally three-component systems, whereas eukaryotic P450s like hepatic P450s and many plant and fungal P450s are working as two component systems. There are also self-sufficient isozymes, where the heme and reductase domains are fused. According to Hannemann et al., depending on the reductase, cytochrome P450 systems can be divided into at least ten different classes (Figure 4)(Hannemann et al. 2007).

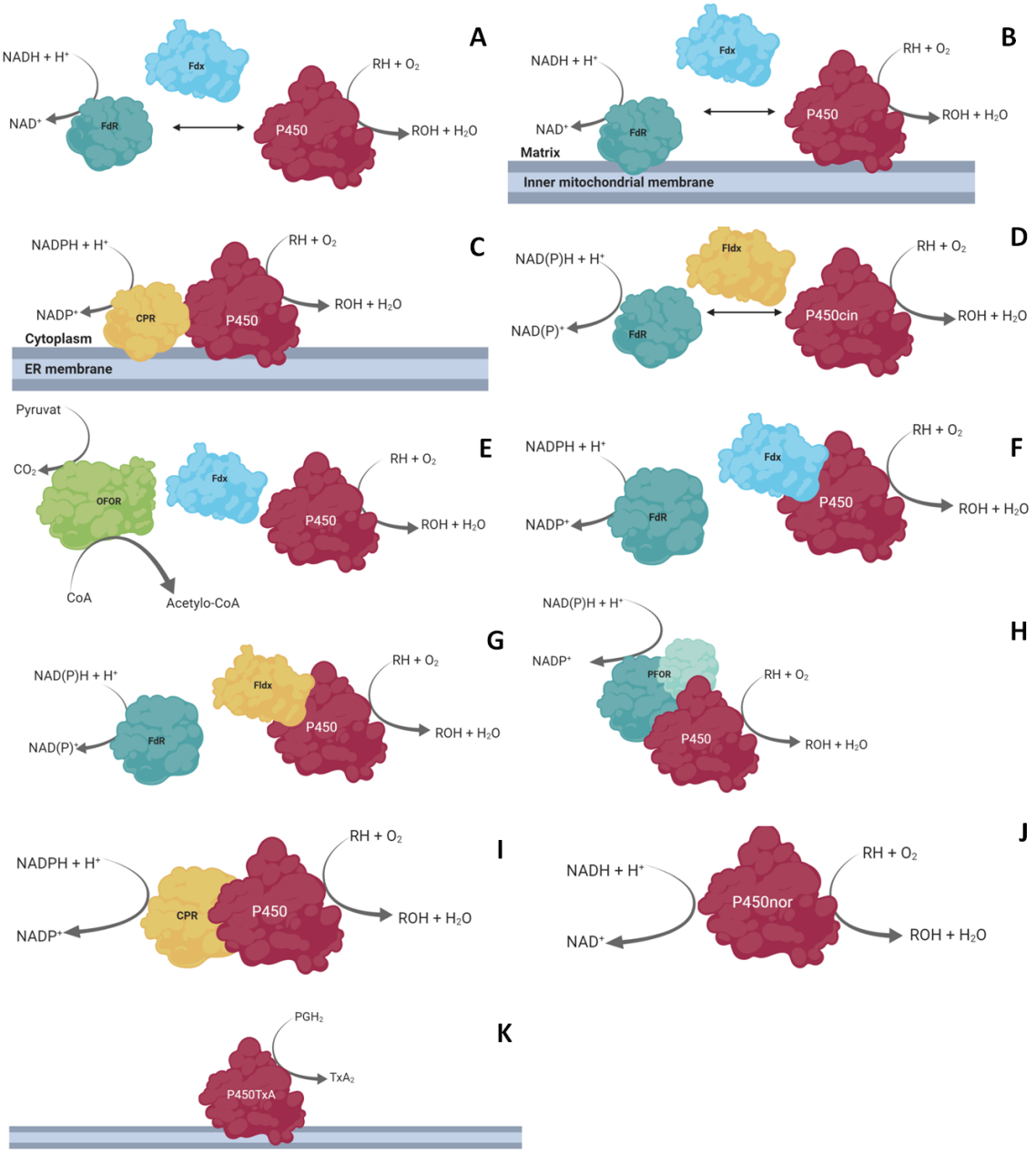

Figure 4: Scheme showing the different cytochrome P450 classes, further described in section 1.1.2 Adapted from Hannemann et al. (2007).

Class I contains most of the known bacterial P450s and also a number of eukaryotic mitochondrial systems (Figure 4, A and B respectively). All these systems are comprised of three separate proteins: the FAD-dependent ferredoxin reductase (FdR) that transfers the electrons from NADH or NADPH to the ferredoxin (Fdx) (containing an iron–sulfur cluster), which provides the reducing equivalents to the P450 heme domain. In the bacterial systems, all three proteins are soluble (Figure 4A). In eukaryotes though, only the ferredoxin is a soluble protein, while the reductase is membrane-associated and the cytochrome P450 is incorporated in the mitochondrial membrane (Figure 4B).

Examples of class I P450s are P450cam from *Pseudomonas putida* (bacterial system) and CYP11A1 (P450scc) (mitochondrial eukaryotic system) (Hannemann et al. 2007).

The Class II system, most commonly found in eukaryotes, contains two integral membrane proteins (Figure 4C): the cytochrome P450 and the NADPH- cytochrome P450 reductase (CPR). CPR contains the prosthetic groups FAD and FMN, which transfer both required redox equivalents from NADPH to one of the isoforms of cytochrome P450.

The Class III system was reported for the first time by Hawkes et al in 2002 (Hawkes et al. 2002). This class is similar to the bacterial Class I (Figure 4D), when it comes to comprising three separate proteins, a FAD-dependent ferredoxin reductase, a small intermediate redox protein (Fldx) and P450. The difference, however, is that the Class III systems utilize an FMN-dependent redox protein referred to as flavodoxin (Fldx), rather than the iron–sulfur cluster containing Class I-type ferredoxin (Fdx) (Cook et al. 2016). An example of Class III P450s is P450cin from *Citrobacter braakii*.

The Class IV is the only class of P450, which has been shown to utilize redox partners specific for an electron donor different than NAD(P)H. Namely, the reductase system obtains electrons from pyruvic acid rather than from NAD(P)H (Figure 4E). Example of Class IV was identified by investigating the first thermophilic CYP119 from the extreme acidothermophilic archaeon *Sulfolobus solfataricus*(Park et al. 2002; Hannemann et al. 2007).

In Class V, in contrast to the classical three-component Class I system, P450 includes two components: a NAD(P)H-dependent reductase (Fdr) and a P450 domain bound to C-terminal ferredoxin (Fdx) via an alanine-rich linker region, which acts as a flexible hinge allowing interactions between the two domains (Figure 4F). A member of this class was described for the first time by Jacson et.al. in 2002 (Jackson et al. 2002).

The Class VI system (Figure 4G) is similar to class V, but the C-terminal-bound ferredoxin (Fdx) is replaced with an N-terminal-bound flavodoxin (Fldx)(Cook et al. 2016).

The P450 Class VII (Figure 4H) presents a completely novel domain architecture: the P450 domain is C-terminally bound to phthalate dioxygenase reductase domain (PFOR). It has three distinct domains: an NADH-binding domain, an FMN-binding domain and an Fdx domain containing an iron-sulfur cluster. The member of Class VII was reported for the first time by Roberts et al. in 2002 and named as P450RhF (Roberts et al. 2002).

As the monooxygenases, members of Class VIII are catalytically self-sufficient. This means that P450 domain is fused to a eukaryotic-like diflavin reductase partner – cytochrome P450 reductase (CPR) – in a single polypeptide chain (Figure 4I) (Cook et al. 2016). The most intensively studied member of this class is the BM3 (CYP102A1) from *Bacillus megaterium* (Fulco and Miura 1974).

The Class IX systems (Figure 4J) are unique since they require no redox protein partners for transfer of electrons from NAD(P)H and consist solely of nitric oxide (NO) reductases. A member of this class was described for the first time in the filamentous fungus *Fusarium oxysporum* (Kizawa et al. 1991).

Class X consists of cytochrome P450 enzymes, which do not require the transport of electrons via redox proteins but use differing intramolecular transfer systems instead (they require neither O_2 nor NAD(P)H) (Figure 3K). Members of Class X P450 utilize the acyl hydroperoxide groups of their substrates as oxygen donors to form a new carbon-oxygen bond (Hannemann et al. 2007; Cook et al. 2016).

1.2.3 Biotechnological application of Cytochromes P450

P450 monooxygenases catalyze the hydroxylation or epoxidation of non-activated carbon atoms with high selectivity. They act on a broad range of chemically diverse substrates like fatty acids, alkanes, or monoterpenes to yield vitamins, steroids, antibiotics, diverse drugs and xenobiotics. Moreover, they have shown great potential in bioremediation, which makes them promising candidates in biotechnological applications (Figure 5) (Bernhardt 2006; Bhattacharya and Yadav 2017; Urlacher and Girhard 2019).

Despite this potential of P450 enzymes, industrial application of those enzymes is often limited by widely recognized technical bottlenecks. Lack of stability, low activity, narrow substrate specificity, expensive cofactor requirements, solvent tolerance and limitations in the electron transfer and electron supply are some of the main reasons why the industrial application of this enzyme system is challenging. Alternately, use of a whole-cell system allows to overcome some of these limitations providing a cofactor regeneration system (co-expression of redox partners) and a protected environment to enhance the stability of the biocatalyst (Urlacher and Girhard 2011; Bracco et al. 2013a; Lundemo et al. 2015).

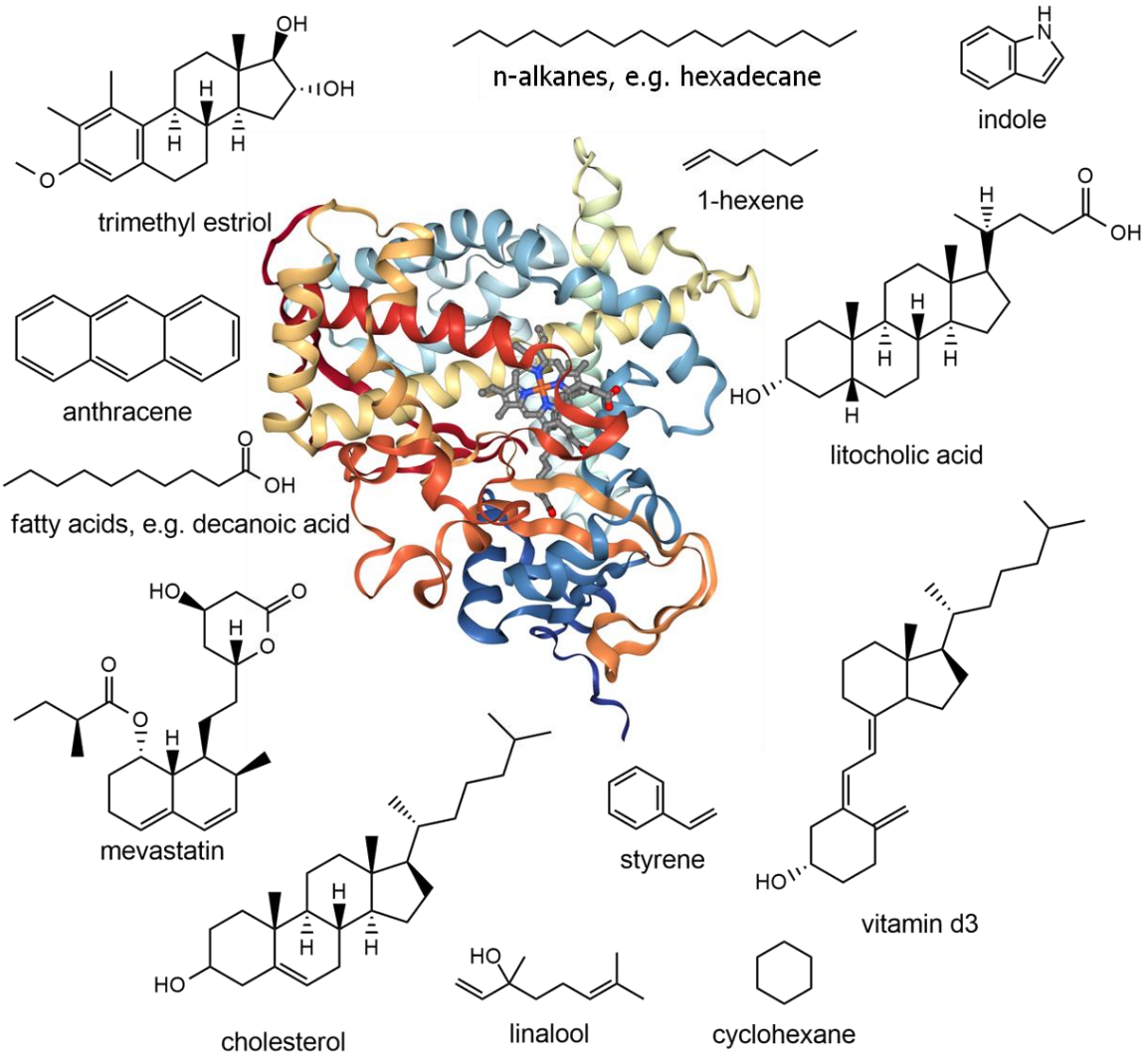

Figure 5: Examples for substrates of P450 monooxygenases: CYP2B6 was shown to catalyse the side chain oxidation of styrene (Nakajima et al. 1994); members of the CYP3, CYP7, CYP8, CYP27, CYP39, and CYP46 families CYP7A1, CYP7B1, and CYP39A1 initiate the synthesis of bile acids from cholesterol (Nebert and Russell 2002); BM3 oxidizing indole (Li et al. 2005); CYP105A1, catalyzes a three-step hydroxylation of vitamin D3 (Hayashi et al. 2010); BM3 mutant (containing 11 mutations), catalyse hydroxylation of a range of alkanes from octane through to propane, including cyclohexane (Butler et al. 2013); BM3 CYP505 catalyse hydroxylation of fatty acids (Boddupalli et al. 1992; Kitazume et al. 2002); a new member of the CYP116B subfamily—P450LaMO oxidize linalool (Yin et al. 2014); CYP members of *P. placenta* (CYP5150, CYP5027, and CYP5350) are involved in the oxidation of a series of PAHs such as anthracene, carbazole, phenanthrene, and pyrene (Ide et al. 2012); CYP107DY1 show catalytic activity towards mevastatin (Milhim et al. 2016); CYP3A4 catalyse hydroxylation of LCA (Araya and Wikvall 1999); a BM3 mutant exhibited activity with the steroid derivative trimethyl estriol (Lewis et al. 2010).

1.2.4 Hydroxylation of steroid molecules such as the bile acids using P450 monooxygenase CYP107D1(OleP) from *Streptomyces antibioticus*

In mammals, cholesterol provides essential building blocks for the synthesis of vitamin D and steroid hormones, yet most of the cholesterol is converted to bile acids (BAs). Bile acids and steroid hormones of higher vertebrates differ strongly in the shape of their ring structures. While bile acids have the 5β-steroid structure in common, also known as the 5β-cholane scaffold, steroid hormones possess the 5α-steroid structure, making the ring system of the 5α-steroids flatter than that of the 5β-steroids. BAs can take over various roles in the human body; they can, e.g. act as emulsifiers of lipid aggregates or transporters of lipids, function as hormones in cholesterol biosynthesis or promote liver regeneration (Russell 2009; Wang et al. 2013).

Yet, bile acids are also suspected of acting as potential carcinogens and have been linked to liver cancer. Especially secondary bile acids, which result from bacterial biotransformations in the colon, have been associated with gastrointestinal cancers (Bernstein et al. 2005; Wang et al. 2013; Ajouz et al. 2014; Ridlon et al. 2015). Therefore, bile acids became attractive therapeutic targets for metabolic disorders (Trauner et al. 2010; Li and Apte 2015; Takahashi et al. 2016). Many bacterial P450s are known, which can convert steroid hormones regio- and stereo-selectively. However, the knowledge of bacterial P450s, which can selectively convert bile acids, is scarce (Anzenbacher and Anzenbacherová 2001). Hydroxylation of bile acids on the 6-α, 6-β and 7-β positions by various cytochrome (CYP) isoforms is the major BA detoxification pathway leading to the formation of the hydroxylated bile acids as hyocholic acid (HCA), muricholic acid (MCA) and ursodeoxycholic acid (UDCA) (Thakare et al. 2018). UDCA is by now the only drug approved by FDA for the treatment of primary sclerosing cholangitis and the medicamentous, non-surgical dissolution of gallstones. Currently, UDCA is prepared industrially from cholic acid following a seven-step chemical procedure with an overall yield of <30% (Munro et al. 2013). In goal, to reduce the number of steps to produce ursodeoxycholic acid, biotransformation has been successfully used (Bortolini et al. 1997). Novel enzymatic bioconversions of free saturated bile acids are highly needed to obtain pharmaceutically significant compounds. Excellent tools to obtain hydroxylated bile acids are cytochrome P450 monooxygenases (P450s), which can catalyze the regio-

and stereospecific oxidation of non-activated hydrocarbons under mild conditions, which is a challenging task for chemical catalysts (Urlacher and Girhard 2012).

One important family of bacterial P450s is the CYP107 family, as members of this family catalyze a variety of reactions in the secondary metabolism of bacteria, i.a, they are involved in the biosynthesis of many antibiotics (Parajuli et al.; Palaniappan et al. 2003; Arakawa et al. 2006; Furuya et al. 2008). Moreover, enzymes of this family have the potential to be applied in the production of therapeutic drugs, vitamins and drug metabolites (Fujii et al. 2009; Milhim et al. 2016). Interestingly, a member of CYP107 (CYP107D1) can catalyze the unspecific hydroxylation of testosterone at the positions 6β, 7β, 12β and 15β by CYP107D1 (Figure 6.) (Agematu et al. 2006).

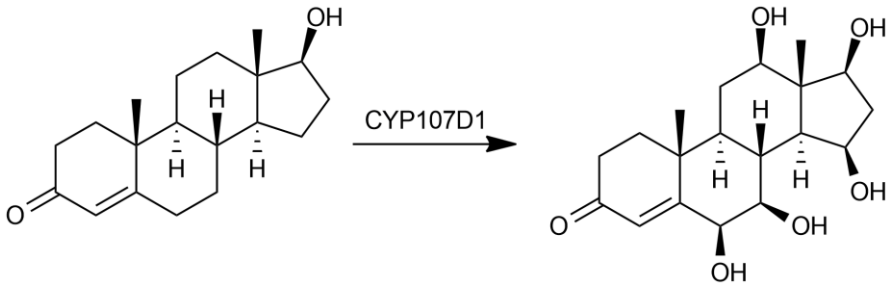

Figure 6: Hydroxylation of Testosterone by CYP107D1(Agematu et al. 2006).

What is more, not long ago, the crystal structure of CYP107D1 (pdb-code:4XE3, 5MNV-Figure 7) has been revealed.

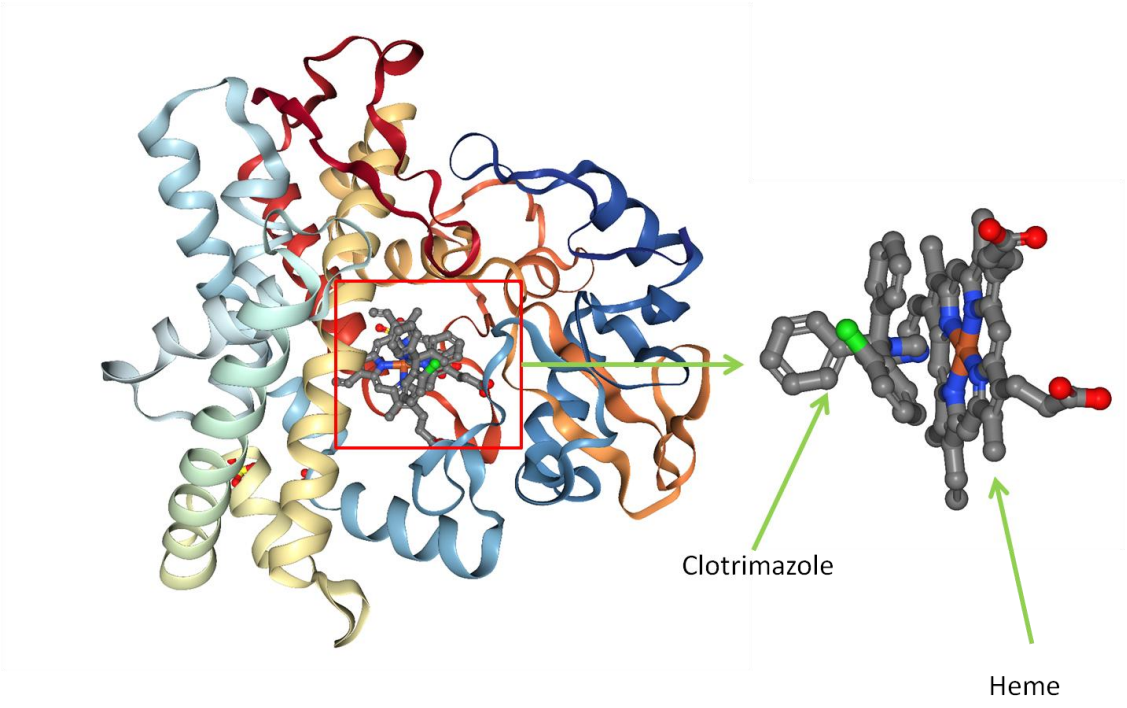

Figure 7: Crystallographic structure of clotrimazole bond OleP (Montemiglio et al. 2015).

The CYP107D1 (OleP) was discovered as the catalyzing enzyme responsible for the stereo- and regioselective epoxygenation of the aliphatic C8-C8a bond in the macrolide antibiotic oleandomycin (Montemiglio et al. 2015; Parisi et al. 2019). However, since CYP107D1 has been also shown to catalyze the hydroxylation of steroids compounds, and its crystal structure is known, it makes this P450 an even more interesting candidate to investigate. The aim of this study was to explore the potential of this enzyme to synthesize hydroxylated steroid compounds such as bile acids dedicated to pharmaceutical applications.

1.2.5 Hydroxylation of fatty acids using self-sufficient P450 monooxygenase from *Fusarium graminearum*

Fatty acids bearing a hydroxyl group display some special properties, such as higher viscosity and reactivity, compared to non-substituted fatty acids. Hence, hydroxy fatty acids have become important building blocks for biodegradable polymer materials and for the cosmetic, chemical, pharmaceutical and food industries (Cao and Zhang 2013). However, most of these fatty acids are not commercially available because they are difficult to be synthesized via chemical routes. In contrast, a number of microorganisms are capable to produce hydroxy fatty acids from fatty acids or vegetable oils. Production of hydroxy fatty acids by microbial biotransformation offer the potential for transformation with high specificity and reduce the manufacturing cost compared to chemical synthesis routes (Cao and Zhang 2013; Kim and Oh 2013). Therefore, identification of novel enzymes to produce diverse hydroxy fatty acids is essential. Cytochrome P450 monooxygenases (P450s) take part in the stereospecific and regiospecific hydroxylation of non-activated hydroxycarbons, including fatty acids, under mild conditions (Van Den Brink et al. 1998; Honda Malca et al. 2012; Bernhardt and Urlacher 2014). Self-sufficient systems, where the P450 domain is naturally fused to its redox partners, are of particular interest since self-sufficient P450s are more efficient and stable than conventional P450s (Urlacher and Girhard 2012). However, until now, only two self-sufficient P450s are well described and can be implemented in industry.

These P450s have been studied in the bacterium *Bacillus megaterium* BM3 (CYP102A1) and the plant pathogenic fungus *Fusarium oxysporum* P450foxy (CYP505A1). Interestingly, both enzymes catalyze subterminal hydroxylations at the ω-1 to ω-3 carbons of saturated and unsaturated fatty acids (Durairaj et al., 2015; Nakayama et al. 1996; Yadav et al. 2003; Lisowska et al. 2006)(Durairaj et al. 2015). Fungal genome sequencing projects have revealed the existence of more than 6000 fungal genes coding for putative P450s which are yet to be explored for the discovery of novel catalytic enzymes.

Fusarium graminearum seems to be an excellent model organism because its genome has been sequenced, and genetic modification is relatively easy. The *F. graminearum* genome is expected to contain 119 putative CYP genes, and only nine *F. graminearum* CYPs have been functionally characterized (Shin et al. 2018). It is an excellent starting point for the discovery of novel self-sufficient P450, which show the

highest turnover numbers and coupling efficiency and allow CYPs to run with increased efficiency. Moreover, the most efficient way to use P450s for production of hydroxy fatty acids is to use the enzymes as whole-cell biocatalysts (Hammerer et al. 2018).

1.3 Transferases: Kinases

Kinases are ubiquitous groups of enzymes, which catalyse the transfer of phosphate groups from high-energy, phosphate-donating molecules to specific substrates. This process is known as phosphorylation, where the substrate gains a phosphate group and the high-energy ATP molecule donates a phosphate group, produces a phosphorylated substrate and ADP. Kinase catalyzed phosphorylation of proteins, lipids, carbohydrates, nucleotides and can affect its activity, reactivity and its ability to bind other molecules. Therefore, kinases and their phosphorylated metabolites are critical in metabolism, cell signalling, protein regulation, cellular transport, secretory processes and many other cellular pathways, which makes them very important to human physiology (Cohen 2002; Fry et al. 2012; Attwood 2013; Baltussen et al. 2018; Roy et al. 2019). These phosphorylated metabolites can be directly isolated from natural resources. However, the yield of those high-value molecules through direct isolation is poor due to slow biomass accumulation and insufficient synthesis by the native host. Alternatively, phosphorylated metabolites can be obtained from chemical synthesis. However, selective phosphorylation in organic synthesis is challenging, involves numerous transformations for producing complex artificial compounds, which results in poor yield of phosphorylated metabolites(Wohlgemuth 2017).

Therefore, making use of ubiquitous in nature and highly site-selective kinases for the synthesis of phosphorylated metabolites is a very promising route. Considering above, in this PhD thesis, two kinases were examined, and their ability for industrial production of phosphorylated metabolites.

1.3.1 Biocatalytic production of phosphorylated metabolites using kinases.

Since chemical synthesis of phosphorylated metabolites is tedious, biocatalytic phosphorylation has a great advantage in improving molecular economy, safety, health, and environmental issues. Many phosphorylating enzymes such as kinases can be applied for mild biocatalytic phosphorylation reactions of metabolites without protecting groups and with high chemoselectivity, regioselectivity, and enantioselectivity (Wohlgemuth 2017; Wohlgemuth et al. 2017). Kinases requires nucleoside triphosphates as cofactors. ATP is the most important biological phosphate donor and is a required cofactor for numerous enzymatic reactions in metabolism, specifically in the formation of P - O bonds. Direct cofactor addition is very uneconomic and leads to an accumulation of inhibitory cofactor by-products and challenging recovery of end products. Enzymatic systems for ATP regeneration have been developed to overcome these problems (Resnick and Zehnder 2000). Four enzymatic regeneration systems have been most often applied for ATP regeneration from ADP: a) acetylphosphate/acetate kinase, b) phosphoenol-pyruvate (PEP)/ pyruvate kinase (PK), c) creatinphosphate/creatin kinase, d) polyphosphate/polyphosphate kinase. The PEP/PK system is considered as the most efficient ATP regeneration system. PEP is a stable phosphorylating agent and PK is commercially available on a large scale. Moreover, the PEP/PK have been successfully used in numerous preparative biocatalytic phosphorylations. (Andexer and Richter 2015). Therefore, the PEP/PK system for ATP regeneration was chosen in this thesis.

Cloning and expression of kinases in *E. coli*, their characterization by determination of activity, and applying in selective phosphorylation while using the phosphoenolpyruvate/pyruvate kinase system for ATP regeneration, is of great interest for fast and robust method development for selective production of metabolites and metabolite-like structures (Figure 8).

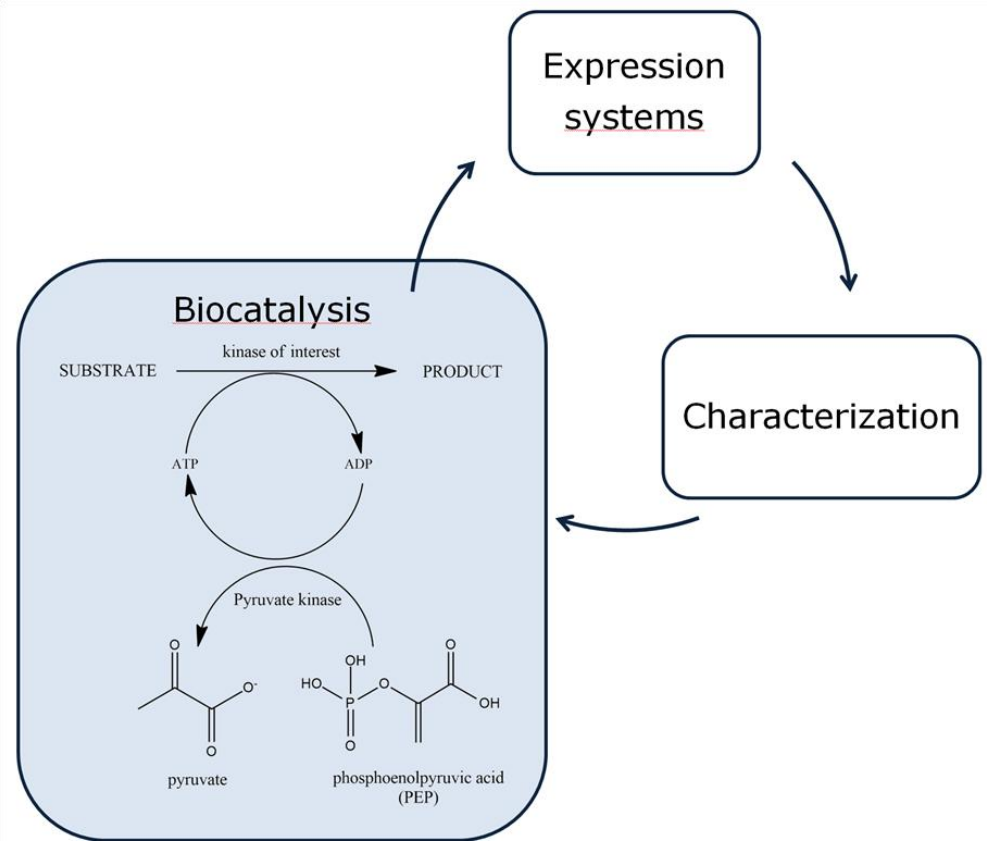

Figure 8: Expression of kinases, characterization by determination of activity, biocatalysis using the phosphoenolpyruvate/pyruvate kinase system for ATP regeneration.

1.3.1.1 Biocatalytic synthesis of N_ω-phospho-L-arginine by arginine kinase from *Limulus polyphemus*

Nω-phospho-L-arginine is an instable form of energy-rich phosphoarginine, which makes chemical synthesis of this compound complicated. The instability of phosphoarginine results from the fact that in phosphoarginine the phosphate is attached to a nitrogen atom (*N*-phosphorylation) forming an acid-labile phosphoramidate bond, unlike in the case of *O*-phosphorylation, where the phosphate group is attached to a hydroxyl group, yielding a bond of lower acid lability. This is due to the protonation of the bridging nitrogen, which induces considerable lengthening and thereby weakening of the N-P bond. Hence, the high energy N-P bond in phosphoarginine is extremely acid labile, unstable in hot alkali, and sensitive to heat (Figure 9).

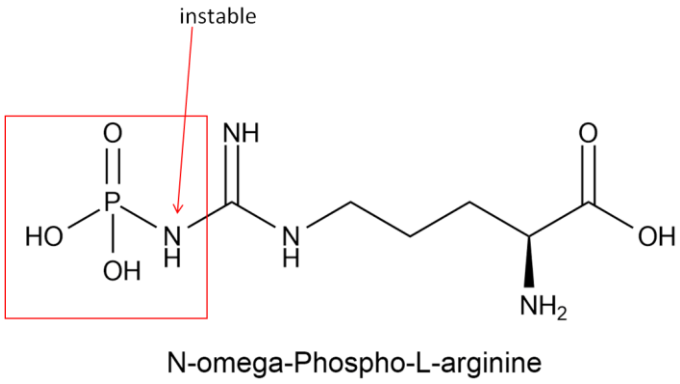

Figure 9: Instable form of N_ω-Phospho-L-arginine

Several multistep chemical synthesis routes have been employed for the preparation of phosphoarginine. A few entirely chemical syntheses involving several reaction steps have been published, but each route has bottlenecks and challenges (Schoenenberger et al. 2017a). In contrast, arginine kineses are designed by nature to site-selective phosphorylation of arginine.

Arginine kinase is found in a wide variety of invertebrates where it maintains ATP homeostasis during muscle contraction, ATP regeneration and energy transportation in cellular energy metabolism (Strong and Ellington 1993). N_ω-phospho-L-arginine has been found in biosynthetic pathways of parasites that are different from those pathways found in mammalian host tissues. Phosphoarginine plays a critical role as an energy reserve because it can be transferred to ATP when energy is needed. It is also a central reserve of high energy phosphate compounds in a wide variety of invertebrates and certain parasitic protozoa such as *Trypanosoma brucei*, *Trypanosoma cruzi*, and *Leishmania major*, which cause some of the most debilitating diseases in humans including leishmaniasis, African

sleeping sickness, and Chagas disease (Li et al. 2006). This makes the metabolic pathway of phosphoarginine an attractive therapeutic target against parasitic diseases (Pereira 2014).

Arginine kinase, like the other phosphagen kinases, contain a signature peptide in the binding sites of substrates of five arginine residues interacting with ATP, two carboxylate amino acids, and one cysteine residue interacting with the guanidino acceptor group (Strong and Ellington 1995; Zhou et al. 1998a; Pereira 2014). Arginine kinase from *Limulus polyphemus* (Uni-prot P51541, KARG_LIMPO) is one of the best-characterized. Additionally, different crystal structures of this enzyme are available (Figure 10).

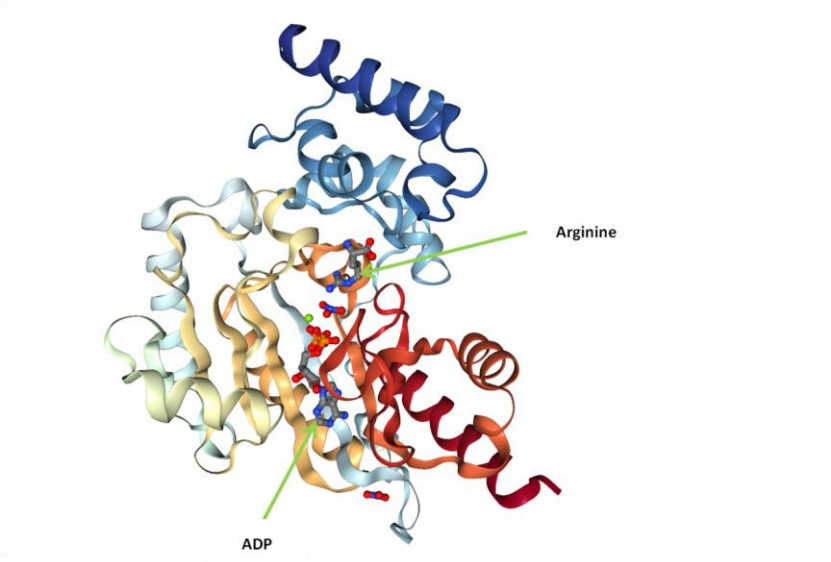

Figure 10: Transition state structure of arginine kinase from *Limulus polyphemus* (Uniprot P51541, KARG_LIMPO)(Zhou et al. 1998b)

Since arginine kinase from *Limulus polyphemus* is one of the best-characterized arginine kinase, it can be successfully applied for selective, biocatalytic phosphorylations in straightforward syntheses of phosphorylated metabolites like N_{ω}-phospho-L-arginine using the phosphoenolpyruvate/pyruvate kinase system for ATP regeneration (Figure 11).

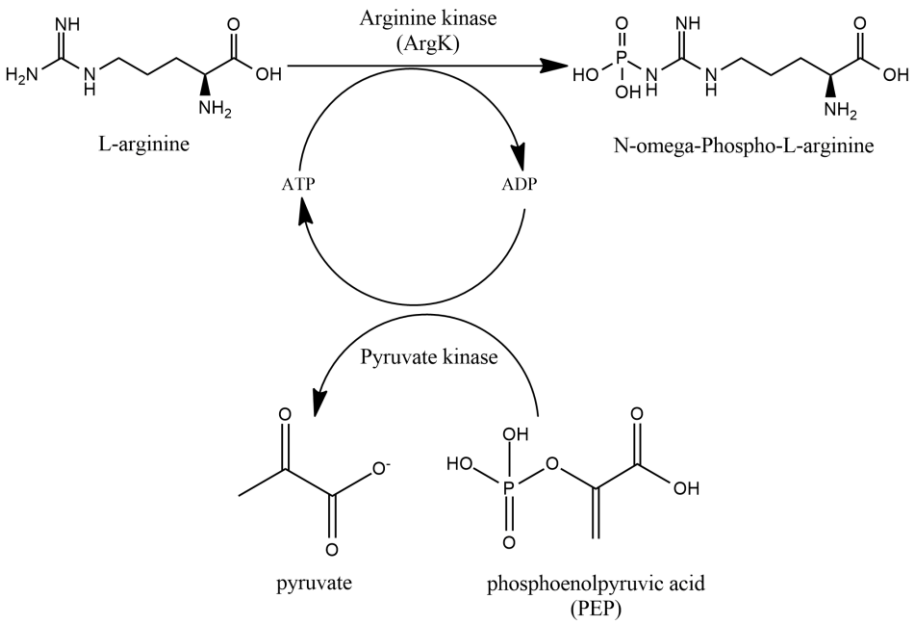

Figure 11: N-phosphorylation of L –arginine (Schoenenberger et al. 2017c).

1.3.1.2 Biocatalytic synthesis of shikimic-3-phosphate by shikimate kinase from *E. coli*

Shikimic acid 3-phosphate is a central parasite, microbial and plant metabolite. It is found in a number of microbial pathogens such as *Mycobacterium tuberculosis*, *Francisella novicida*, *Pseudomonas aeruginosa* and *Helicobacter pylori*. Therefore, shikimic acid 3-phosphate is also crucial for developing shikimic acid kinase inhibitors to obtain new antimicrobials. Moreover, shikimic acid 3-phosphate is important as a substrate for 5-enolpyruvoyl-shikimate 3-phosphate synthase, which is of interest as a drug target in infectious diseases as well as in herbicides (Figure 12) (Oliveira et al. 2001; Dias et al. 2007; Schoenenberger et al. 2018).

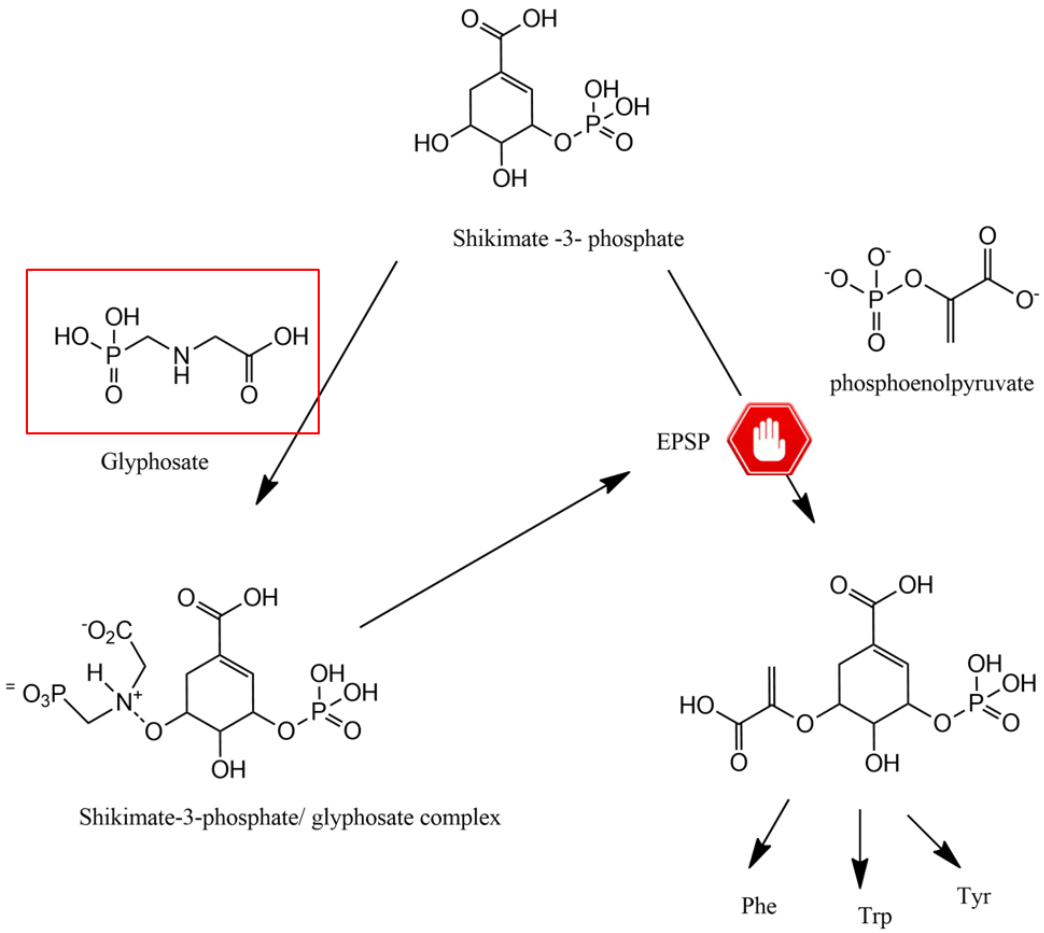

Figure 12: Biochemical mechanism for the herbicidal action of glyphosate through the inhibition of 5-enolpyruvylshikimate 3-phosphate synthase (EPSPS) by the herbicide.

The chemical synthesis of shikimate-3-phosphate is challenging due to the number of reaction steps, reaction times, hazardous/toxic chemicals. Since this key metabolite is still not available commercially, a selective one-step enzymatic phosphorylation of shikimic acid is necessary (Schoenenberger et al. 2018) (Shih and Wu 2000).

The shikimate pathway is essential in algae, higher plants, bacteria, fungi and parasites but is absent from mammals. Therefore, the shikimate pathway is an attractive target for the development of herbicides and antibiotic agents as well. Shikimate kinase (SK; EC 2.7.1.71), the fifth enzyme of this pathway, catalyzes the ATP dependent phosphorylation of shikimate to yield shikimate-3-phosphate. The shikimate kinase belongs to the NMP (nucleoside-phosphate kinase) structural kinase family, which consists of three domains: the core, having a highly conserved phosphate-binding loop (P-loop); the nucleotide-binding domains, which upon binding shikimate and ATP (Figure 13) undergo substantial conformational changes and require a divalent cation like magnesium or manganese for its activity; and the lid domain, which undergoes substantial conformational changes upon substrate binding (Dias et al. 2007; Schoenenberger et al. 2018).

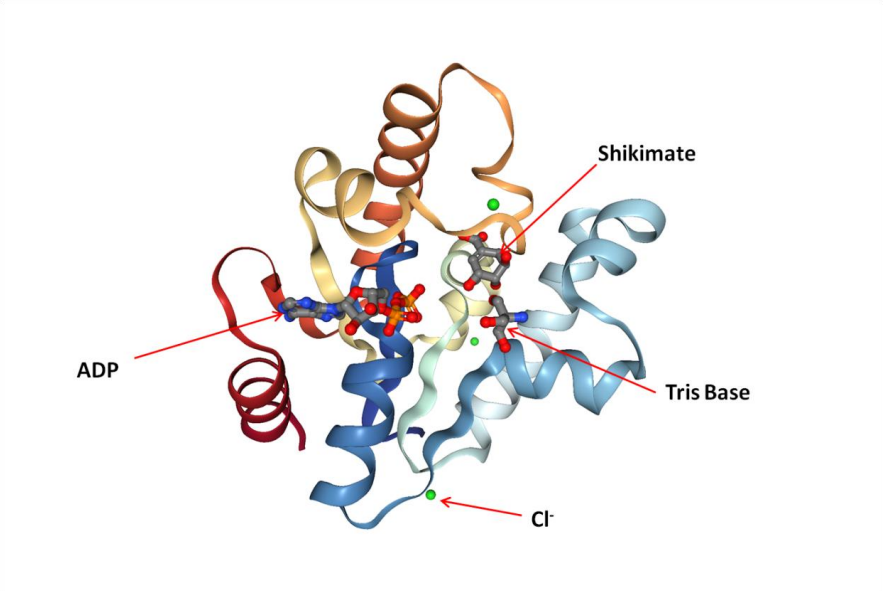

Figure 13: Structure of shikimate kinase from *Mycobacterium tuberculosis* in complex with ADP, shikimate and Cl (Dias et al. 2007).

Depending on the origin, the number of isoenzymes present varies. In *Escherichia coli*, the phosphorylation of shikimic acid is catalyzed by two isoenzymes, shikimate kinase I and II, which differ by their K_m. The catalytically more active shikimate kinase II, corresponding to the *aroL*-encoded enzyme AroL, has a K_m of about 200 µM for shikimate, whereas shikimate kinase I, corresponding to the *aroK*-encoded enzyme AroK, has a low affinity for shikimate with a K_m of more than 20 mM (Schoenenberger et al. 2018).

Therefore, application of shikimate kinase AroL from *E. coli*, as a route for selective biocatalytic phosphorylations in straightforward syntheses of shikimate-3-phosphate using the phosphoenolpyruvate/pyruvate kinase system for ATP regeneration, is desired (Figure 14).

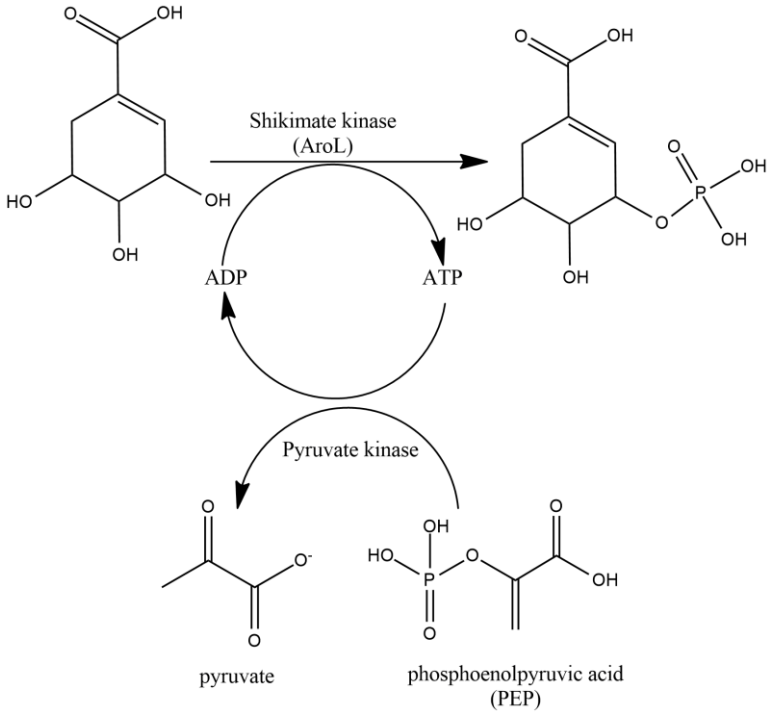

Figure 14: Shikimate kinase-catalyzed phosphorylation of shikimic acid (Schoenenberger et al. 2018)

1.4 Lyases

Lyases catalyze the cleavage or formation of C-C, C-N, C-O and other bonds to yield double bonds. Conversely, lyases can also catalyse the addition of groups to double bonds. The direction of the reaction will primarily depend on the equilibrium, constant for the reaction concerned. However, it may also be driven in a particular direction by the applied reaction conditions. Lyases differ from other enzymes in terms of two substrates involved in one direction of reaction and only one substrate involved in the reverse reaction. The elimination and addition reactions catalysed by lyases are described below (Figure 15).

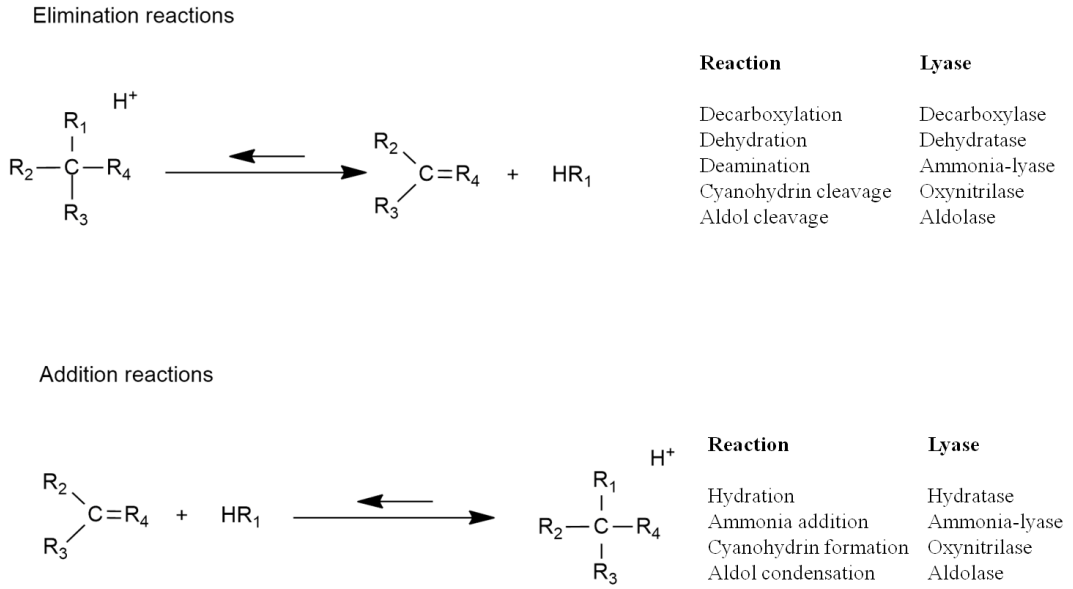

Figure 15: The elimination and addition reactions catalysed by lyases (van der Werf et al. 1994).

In the EC number classification of enzymes, EC 4 represents lyases, which can be further classified into the following seven subclasses. Hydroxynitrile lyases, aldolases, ketolases, and a certain type of thiamine-diphosphate-dependent lyases play important roles in industrial biotransformations. Moreover, halohydrin dehalogenases are useful biocatalysts for the production of enantiopure epoxides as well as they exhibit epoxide ring-opening activity with a range of small anionic nucleophiles such as azide, cyanide, nitrite, cyanate or thiocyanate, which is even more attractive as it enables the regio- and stereoselective formation of novel C−N, C−C, C−O and C−S bonds (Figure 16) (Calderini et al. 2019)

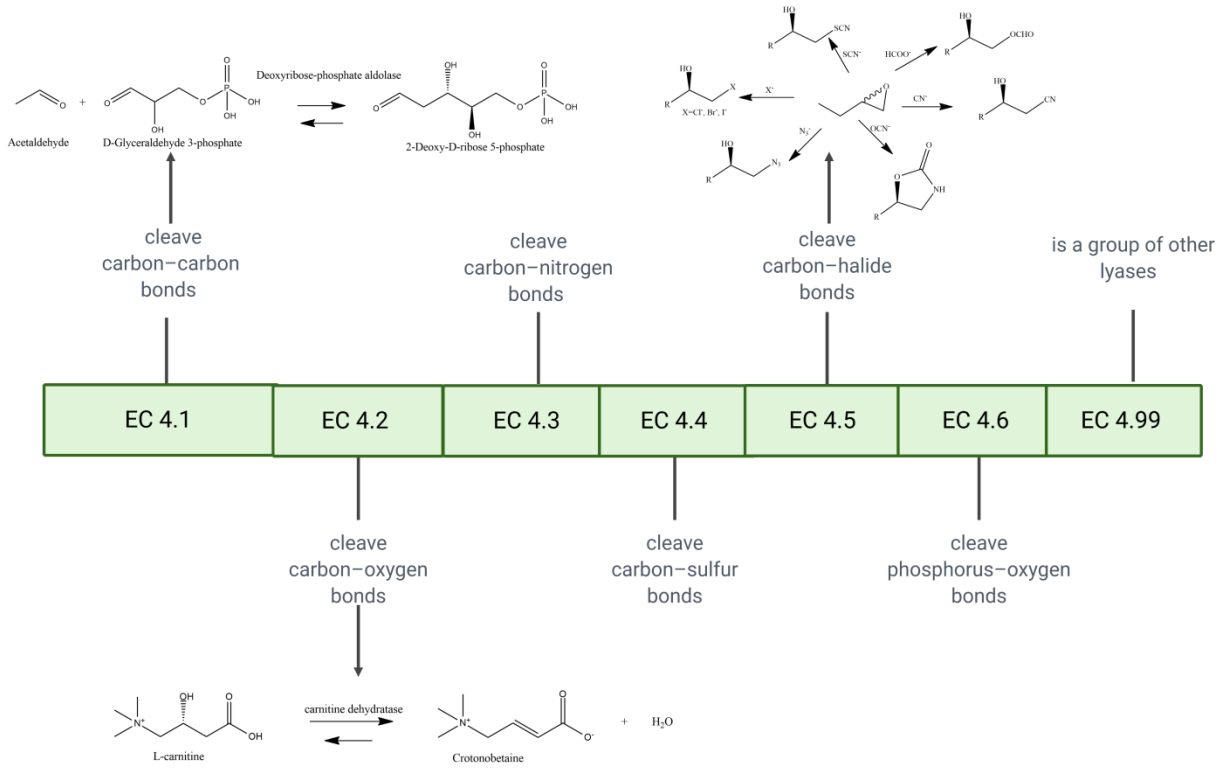

Figure 16: Classification of lyases and representative examples of lyase catalyzed reactions
Lyases in EC 4.1 cleave carbon-carbon bonds and include decarboxylases (EC 4.1.1 pyruvate decarboxylase) and aldolases (EC 4.1.2.4 2-deoxy-D-ribose 5-phosphate aldolase) (Jennewein et al. 2006). EC 4.2 contains a group of lyases that break carbon-oxygen bonds, such as dehydratases (carnitine dehydratase EC 4.2.1.89, nitrile hydratase EC 4.2.1.84) (Jung et al. 1989; Cánovas et al. 2005; Martinez et al. 2014; Lan et al. 2017). Lyases cleaving carbon-nitrogen bonds are sorted into EC 4.3 (phenylalanine ammonia lyase EC 4.3.1.24) (Bartsch and Bornscheuer 2010). Lyases in EC 4.4 cleaves carbon–sulfur bonds. Lyases cleaving carbon-halide bonds belong to EC 4.5 (halohydrin dehalogenases (EC 4.5.1.-)). (Calderini et al. 2019). EC 4.6 comprises lyases fracturing phosphorus-oxygen bonds, like adenylyl cyclase and guanylyl cyclase. EC 4.99 is a group of other lyases (Mahdi and Kelly 2008).

1.4.1 Biocatalytic synthesis of L-argininosuccinate using argininosuccinate lyase from *Saccharomyces cerevisiae*

Arginine metabolism has been recognized as a process of increasingly high importance for the study of tumour development and progression, since many tumour cells have lost the ability to produce L-arginine de novo. As an expression of the urea cycle, argininosuccinate synthetase enzyme decrease can be observed in melanoma, mesothelioma and cancers of the liver, kidney, pancreas, prostate and ovary. As a result, argininosuccinate formation is reduced, and aspartate is accumulated, enhancing the proliferation of cancer cells. Nitric oxide (NO), generated through L-arginine metabolism, has been linked to cardio-vascular diseases. L-Arginine and its metabolic pathways also affect the immune system by its impact on human T cells and T cell receptors. Additionally, it has a key role in the inflammatory function of macrophages, where the nitric oxide synthesis pathway is associated with the inflammatory M1 phenotype, while the arginase pathway is associated with the tolerant M2 cell phenotype (Schoenenberger et al. 2017b).

In the urea cycle, L-argininosuccinate is the product of the ATP dependent and rate-limiting reaction of citrulline and aspartate, catalysed by the argininosuccinate synthase enzyme (ASS). Subsequently, L-argininosuccinate is cleaved into fumarate and arginine by the argininosuccinate lyase enzyme (ASL) (Figure 17).

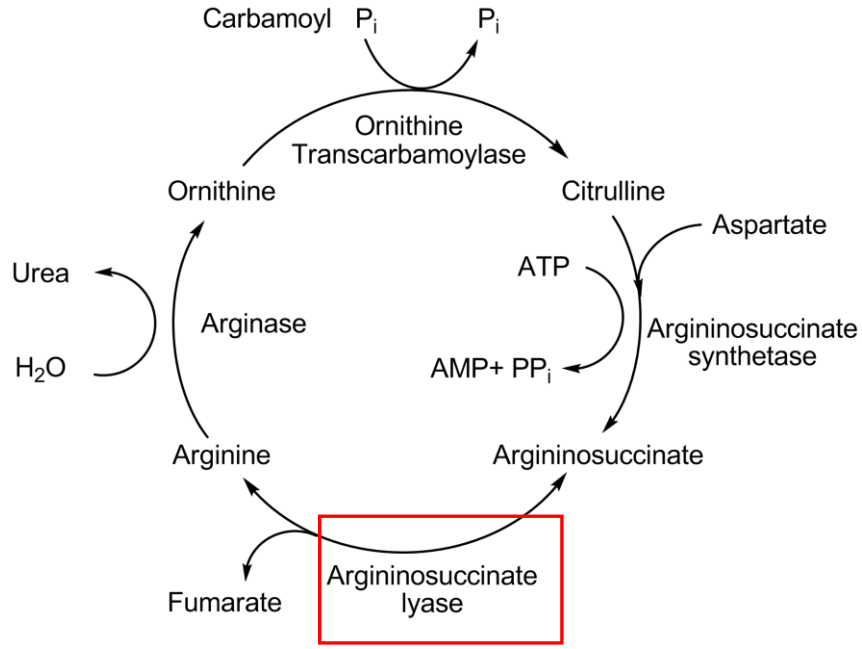

Figure 17: ASL is indicated in the red box as the fourth enzyme of the urea cycle (Schoenenberger et al. 2017b).

The highly conserved ASL enzyme has been studied in a wide range of organisms including rat, human, *Escherichia*, algae, saccharomyces and amphibian. It has been found to be active as a tetramer of identical monomers (Figure 18), where each subunit has a single polypeptide between 49–52 kDa (Yu and Howell 2000).

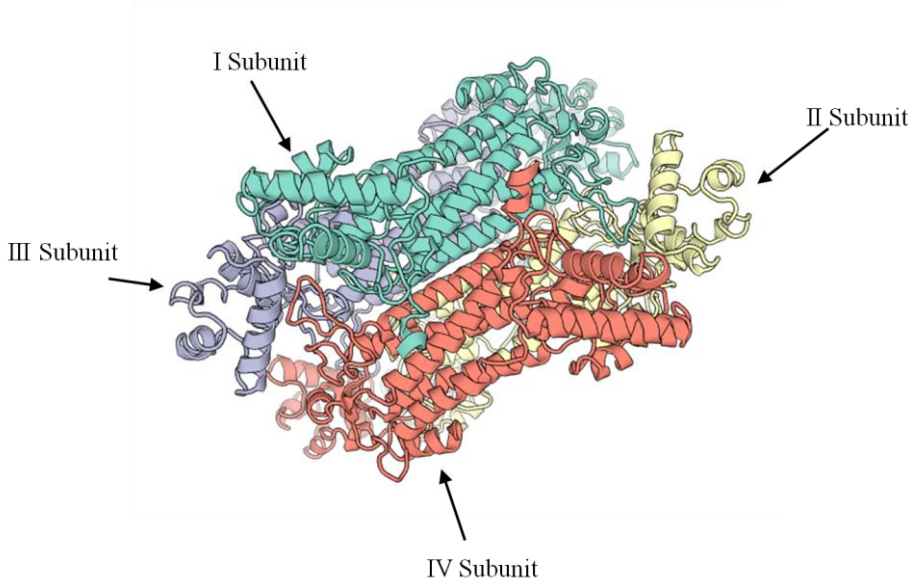

Figure 18: Structure of ASL from *Saccharomyces cerevisiae* **(**P04076 (ARLY_strain ATCC 204508 / S288c) (Baker's yeast))

Interestingly, ASL can also catalyse the reverse reaction to form L-argininosuccinate from arginine and fumarate in an ATP-independent manner as shown by Ratner et al., when fumarate and arginine have been used in excess to shift the equilibrium of the reaction (Figure 19) (Murakami-Murofushi and Ratner 1979).

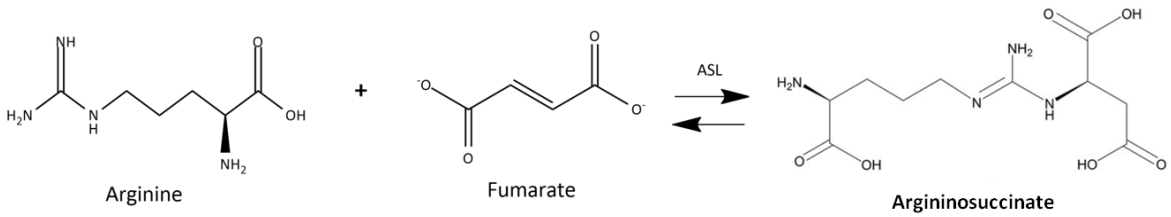

Figure 19: Argininosuccinate lyase-catalyzed reaction between arginine and fumarate argininosuccinate as part of the urea cycle running in reverse.

Since ASL can also catalyse the reverse reaction to form L-argininosuccinate from L-arginine and fumarate, a recombinant overexpression strategy for argininosuccinate lyase (ASL) employing the ARG4 gene from *Saccharomyces cerevisiae* (Uniprot P04076, ARLY_YEAST) was used in this thesis to develop a simple biocatalytic procedure for the synthesis of L-argininosuccinate.

2 Aim of this thesis

The pharmaceutical industry requires novel synthetic routes that are environmentally friendly. Biocatalysis that uses either isolated enzymes or whole-cell catalysts is becoming essential. Moreover, enzymes are excellent tools for chemical biology research and the analysis of complex, biological mechanisms. Therefore, the aim of this thesis was the enzymatic synthesis of bioactive molecules such as hydroxy fatty acids, phosphorylated compounds and bile acids.

2.1 Biosynthesis of bile acids using P450 monooxygenase

Bile acids can take over various roles in the human body, e.g. they can act as emulsifiers of lipid aggregates, transporters of lipids, function as hormones in cholesterol biosynthesis or promote liver regeneration. Since P450 monooxygenases are involved in the cholesterol catabolic pathway, they are the crucial biocatalysts for the formation of different bile acids, vitamin D derivatives and steroid hormones. Nevertheless, knowledge of bacterial P450s, which can convert bile acids selectively, is scarce. Therefore, the aim of this thesis was to develop a straightforward biocatalytic hydroxylation of certain 5β-cholanoic acid derivatives with high regio- and stereoselectivity employing the P450 monooxygenase OleP from *Streptomyces antibioticus* together with the heterologous redox partner system Pdx/PdR.

2.2 Biosynthesis of hydroxy fatty acids using P450 monooxygenase

Hydroxy fatty acids are essential chemicals for versatile applications, but their commercial availability is limited because they are difficult to be synthesized via chemical routes. Cytochrome P450 monooxygenases (P450s) are interesting catalysts due to their ability to selectively hydroxylate non-activated hydrocarbons. However, only a few P450-catalyzed processes have been industrially implemented due to the difficulty of developing economically feasible processes with such enzymes. Self-sufficient monooxygenases, in which the heme domain and the flavin reductase domain are fused, offer high potential to overcome this challenge. The fungal kingdom is a high source of still unexplored P450s, including many self-sufficient ones. The plant pathogenic fungi *Fusarium graminarium* possesses large numbers of P450s, which are involved in diverse biological processes, including production of primary and secondary metabolites and denitrification. Until now, only few fungal P450s have been functionally characterized. Therefore, investigation of

fungal P450s may offer opportunities to exploit their catalytic functions to produce hydroxylated fatty acids.

2.3 Biosynthesis of N_{ω}-phospho-L-arginine by arginine kinase

The lack of availability of N_{ω}-phospho-L-arginine, which is present in invertebrates to regulate energy requirements when it is highly needed, was due to a tedious chemical procedure, during which the N_{ω}-phospho-L-arginine, was prepared in over five reaction steps in a low yield. The medically important protozoa, which causes some of the most debilitating diseases in humans, including leishmaniasis, African sleeping sickness, and Chagas disease, can serve as an example of such invertebrate. Taking the above into consideration, the objective of this study was to develop a straightforward biocatalytic procedure for the phosphorylation of L-arginine, to N_{ω}-phospho-L-arginine, on the gram scale, employing site- and enantioselective arginine kinase.

2.4 Biosynthesis of shikimic-3-phosphate by Shikimate kinase

Since shikimic acid-3-phosphate is of high interest as an enzyme-substrate for 5-enolpyruvoyl-shikimate 3-phosphate synthase, a drug target in infectious diseases and a prime enzyme target for the herbicide glyphosate, industrial environmentally friendly production of this molecule isof high interest. Biocatalysis has the potential to deliver such 'greener' chemical syntheses. For this reason, Shikimate kinase (AroL) from *E. coli* was chosen as a tool for the biosynthesis of a central metabolite of the shikimate pathway, Shikimic acid-3-phosphate, at multi-gram scale.

2.5 Biosynthesis of L-argininosuccinate by argininosuccinate lyase

The primary natural amino acid L-argininosuccinate containing two chiral centres occurs in the L-alanine, L-arginine, L-aspartate, L-glutamate and L-proline metabolic pathways and plays a role in the biosynthesis of secondary metabolites and other amino acids. The aim of this work was to develop a simple and straightforward biocatalytic procedure for the synthesis of *N*-(([(4S)-4-Amino-4-carboxybutyl]amino)iminomethyl)-L-aspartic acid lithium salt (L-argininosuccinate). It was proposed to achieve this goal by running part of the urea cycle in reverse. Argininosuccinate lyase (ASL) from *Saccharomyces cerevisiae* was chosen

as the catalyst for this addition reaction. Using this argininosuccinate lyase, a novel, green synthesis route for this important metabolite can be developed.

3 Results and discussion

3.1 Cytochrome P450 monooxygenase CYP107D1 OleP from *Streptomyces antibiotics*

Bacterial P450 systems usually require the presence of FDR and FDX in order to couple electron flow from NAD(P)H to the terminal P450 component. Most of the bacterial P450s are class I, P450s, receiving electrons from a two-component reductase system, FDX and NADH FDR, such as in P450cam. Several redox systems (putidaredoxin reductase (PdR) – putidaredoxin (Pdx) from *Pseudomonas putida*, ferredoxin reductase (FdR) – ferredoxin (Fdx) from *Escherichia coli*, adrenodoxin reductase (AdR) – adrenodoxin (Adx) from bovine) have been used in different ratios to reconstitute the activity of various P450s. The most commonly employed redox system is the P450cam system from *Pseudomonas putida*. The P450cam monooxygenase system consists of three separate proteins. The PdR (putidaredoxin reductase- CamA) is a FAD-containing, strictly NADH-dependent protein, while PdX (putidaredoxin-CamB) is an iron sulfur protein that belongs to the group of [2Fe–2S] FDX and plays the role of an electron shuttle transferring the two electrons, one at a time, from CamA to P450cam (Sevrioukova and Poulos 2011; Urlacher and Girhard 2011).

Since the most widely used redox system is the P450cam and no physiological redox partners of CYP107D1 have been identified yet, the biotransformation system was designed to co-express CYP107D1 cytochrome P450, from *Streptomyces antibiotics*, along with PdR (putidaredoxin reductase) and PdX (putidaredoxin) from *Pseudomonas putida*. This was carried out using two plasmids with different selection markers and compatible origins of replication. The PdX/PdR was cloned into the pACYC vector and CYP107D1 was cloned into pET28a (+) vector.

The aim of this study was to investigate a whole-cell biocatalyst based on *Escherichia coli* expressing CYP107D1 together with corresponding redox partners to develop a straightforward biocatalytic procedure for the selective hydroxylation of bile acids.

3.1.1 Recombinant coexpression of CYP107D1 together with redox partners and purification of P450_CYP107D1.

E. coli C43(DE3) was chosen as host strain for the efficient expression of all three proteins (CYP107D1, PdX and PdR). *E. coli* naturally does not contain any endogenous heme proteins like P450 enzymes, the presence of which could result in undesired background activity (Bracco et al. 2013b). Since *E. coli* lacks P450s, the addition of δ-aminolevulinic acid, a precursor for the heme synthesis, is necessary (Lundemo and Woodley 2015). The expression factors such as temperature, length of growth and media supplementation affect the yield of protein expression. In general, *E. coli* transformed with a P450 plasmid are grown in supplemented Terrific Broth media for an extended period at low temperatures with aeration. Moreover, lower expression temperature has been reported to yield stable expression of proteins without aggregation. However, the low temperature can also lead to low expression (Zelasko et al. 2013). Therefore, different strategies were applied in order to increase the amount and activity of soluble P450 CYP107D1 and its redox partners' genes expressed in *E. coli*. The influence of different media (TB, Power Broth, LB), temperature, aeration during expression (baffled and non-baffled shake flasks), as well as duration of expression and the supplementation with a heme precursor (δ-aminolevulinic acid, $FeSO_4$, hemin) was tested. It is recommended by the manufacturer of the pET system to lower the temperature during expression to achieve more soluble, active enzyme. However, an expression temperature of 30°C turned out to be more efficient than lower temperature of 20°C. Expression of CYP107D1, and PdR/PdX was confirmed by SDS-PAGE (Figure 20 A). The size of the expressed CYP107D1 was approximately 46 kDa, whilet the redox partner proteins were 45 kDa (PdR) and 11 kDa (PdX) as determined by SDS-PAGE analysis (Figure 20A). Since the recombinant OleP carried an N-terminal His-tag, it could successfully be purified by IMAC (Figure 20 B).

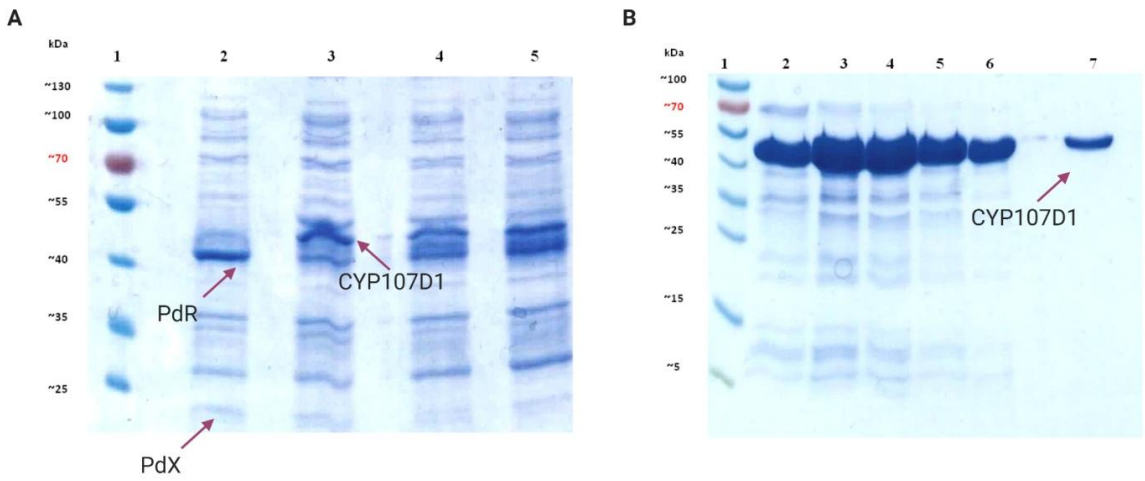

Figure 20: (A) Recombinant expression of P450 CYP107D1 and PdX/PdR. (B) SDS-PAGE analysis showing His-tag purification of the recombinant CYP107D1.

(A) Lane 1: marker, lane 2: soluble fraction of the cell crude extract from *E. coli* (PdX/PdR), lanes 3-5: soluble fraction of the cell crude extract from *E. coli* (CYP107D1+PdX/PdR) MW of CYP107D1: ~ 46 kDa, PdX: ~11 kDa, PdR: ~45 kDa. (B) SDS-PAGE analysis showing His-tag purification of the recombinant CYP107D1. (B) Lane 1: marker, lanes 2-7: elution of purified CYP107D1, MW of CYP107D1: ~ 45 kDa.

Moreover, highest biomass production was achieved in TB medium respectively, in comparison to LB and Power Broth. Beside higher biomass production, TB medium also sustained the higher expression of CYP107D1, measured as volumetric productivity (data not shown).

Since it is well recognized that conventional electrophoresis conditions result in the nearly complete dissociation of heme from P450 holoprotein, to provide an independent evaluation of the nature of the heme-P450 interaction in CYP107D1, SDS-PAGE analysis with TMBZ/hydrogen peroxide staining was conducted specifically for detection of the heme group (Figure 21). Intense staining in the 46 kDa region is evident for the CYP107D1 preparation.

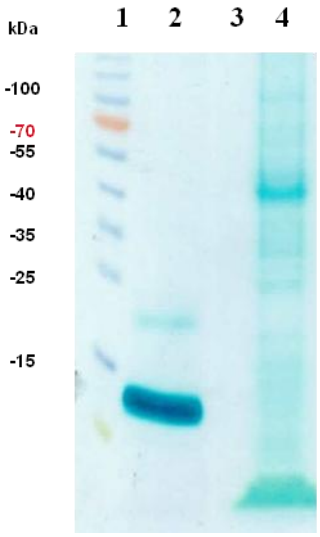

Figure 21: SDS-PAGE developed with TMBZ/hydrogen peroxide stain specific for heme.
Lanes: 1, molecular weight markers; 2, Cytochrome C; 4, CYP107D1

3.1.2 Spectral features of the CYP107D1 enzyme and NADPH–P450 reductase activity

Reduced heme iron of the CYP forms an adduct with CO and the resulting CYP-CO complex gives a characteristic peak near 450 nm. This technique has been extensively used for the quantification of active CYPs from the absorbance difference of A450–490 using the molar extinction coefficient of 91 $mM^{-1}cm^{-1}$ (Lamb and Waterman). To determine the concentration of active CYP107D1, CO-difference spectra were measured. Correct insertion of the heme prosthetic group is indicated in these spectra by a typical absorption maximum at 450 nm. In contrast, inactive P450 enzymes show a peak at 420 nm (Luthra et al. 2011).

Moreover, baffles are often used in shake flasks to increase oxygen transfer into the flask (Gupta and Rao 2003). Therefore, the impact of baffled flasks on the biomass measurement and P450 concentration was investigated. The effect of baffles and different sterile closures in a shake flask have been tested on the cell growth during *E. coli* fermentation (50 mL scale). An experiment performed with three non-baffled flasks covered with different plugs (cotton, sponge, and milk filter) and a baffled flask covered with filter showed that the difference in the oxygen transfer rate in a shake flask under varying conditions led to different oxygen level during fermentation. If the dissolved oxygen concentration falls below the critical level, then the cells may be metabolically disturbed. The impact of oxygen transfer was not limited only to the biomass growth rate, but it also affected the expression level of P450. As shown in Figure 22, the P450 concentration of P450 in baffled flask (0.129 nmol mL^{-1}) was 40% higher than in non-baffled flask (0.086 nmol mL^{-1}).

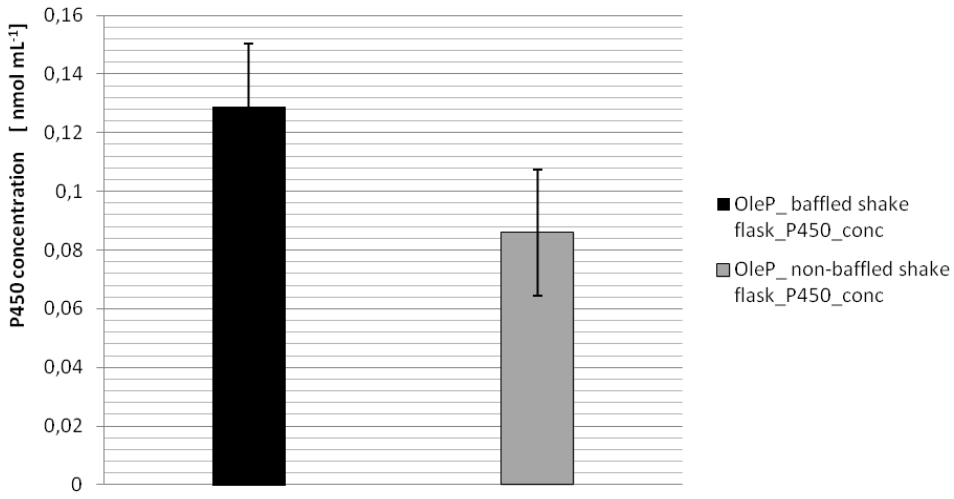

Figure 22: Examination of the influence of aeration with baffled and non-baffled shake flask on the CYP107D1 concentration. Concentration of the recombinant P450 CYP 107D1 expressed in *E. coli* in cultures in baffled (black column) and non-baffled (gray column) flasks. The reduced CO-difference spectral analysis carried out, here, for the purified CYP107D1.

Hence, for larger scale (400 mL) expression baffled shake flask was chosen. The reduced CO-difference spectral analysis carried out, here, for the purified CYP107D1 resulted in a maximum absorption at 450 nm. This confirms the active nature of the purified CYP107D1 (Figure 23). Based on the CO-difference spectra, the concentration of purified CYP107D1 was estimated to be 16.92 nmol mL^{-1}.

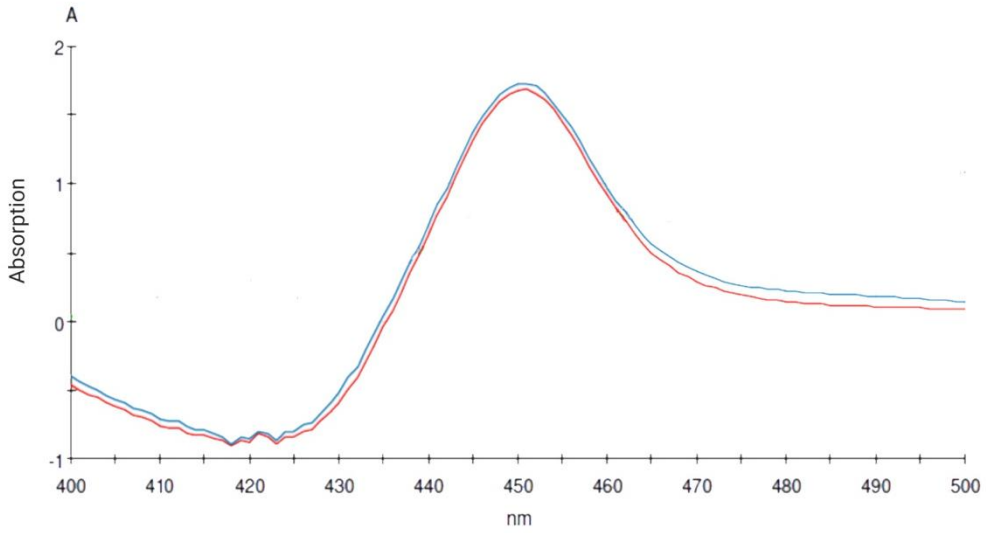

Figure 23.: CO binding analysis of purified CYP107D1 expressed in *E. coli*.

Earlier, Rodriguez et al. has already described the expression of OleP in *E. coli* as a fusion protein to a maltose-binding protein but in their work the enzyme was inactive (Rodriguez et al. 1995). In contrast, obtained results indicate that the recombinant OleP with N-terminal His-tag was overexpressed in *E. coli* as a soluble and what is more important an active cytochrome P450.

The catalytic activity of P450s requires one or more redox partners to transfer two electrons from NAD(P)H to the heme iron. The efficiency of electron transfer directly affects the overall rate of P450-catalyzed reactions. Therefore, determining the activity of the PdX/PdR redox system was essential. The cytochrome P450 reductase is capable of transferring electrons not just to P450, but to artificial acceptors, such as cytochrome c (cyt c) and 2,6-dichlorophenolindophenol (DCIP), as well. These molecules serve as model substrates for the reductase to assess how alterations in structure or reaction conditions affect enzyme catalysis. Spectrophotometric assays were used reduction of cytochrome c, and DCPIP and NADPH utilization (Gray et al. 2010). The activity of PdX and PdR from *Pseudomonas putida* was investigated by adding NADPH and DCPIP. Here, a fast NADPH depletion was observed along with the conversion of dark blue DCPIP to its colorless reduced

form. Based on the DCPIP assay, the obtained specific activity of the electron transfer components was in the range of 1.0 to 1.1 U mL^{-1}. Therefore, PdX and PdR from *Pseudomonas putida* can be applied as surrogate electron transfer partners required for CYP107D1 activity.

3.1.3 OleP -Substrate screening

Information on substrate selectivity is key to the understanding of the P450's function. In addition, once the CYP107D1 crystal structure is known, a comprehensive understanding of changes in substrate selectivity enables the design and creation of a CYP107D1 mutant with the desired selectivity. Since CYP107D1 is able to hydroxylate testosterone, this P450 is an excellent candidate as catalysts for the synthesis of high-value hydroxylated steroid molecules, such as hydroxylated bile acids.

In this research an integrated P450 substrate screening system to select "sample" substrates for the P450 of interest was developed. Because of the limitations of P450s as biocatalysts on industrial scale such as cofactor dependency, low stability and catalytic activities in isolated form, it is often favored to use them as whole cells rather than isolated enzymes. Biotransformations using whole cells show advantages since this is the most efficient solution for cofactor regeneration. The cofactor recycling step is carried out within the intact cell, driven by the reduction equivalents introduced via the external carbon and energy source (glucose). What is more, whole cells allow biotransformation on larger scale, especially when the microorganisms applied as expression host can be cultivated in high cell density (Rasor and Voss 2001; Ghisalba, O., Meyer, H. P., & Wohlgemuth 2010; Hernández-Martín et al. 2014; Lundemo et al. 2016). In order to set up optimal biotransformation conditions for the resting cells of *E. coli* C43(DE3) (pET28a(+)CYP107D1) (pACYCcamAB), and to enable NADH regeneration within the *E. coli* metabolism, the buffer was supplemented with glucose and glycerol (Glazyrina et al. 2010). A library of 22 steroid compounds and 4 fatty acids were screened as a potential substrate for CYP107D1 using the whole-cell biotransformation (steroids and fatty acids tested in this study as substrates for CYP107D1 can be found in the Appendix: Table A 1). For biotransformation, the substrate was added to a final concentration of 2 mg mL^{-1} from a 100 mg mL^{-1} stock solution in DMSO. Reactions were incubated at 28°C with shaking at 160rpm. Samples (1 mL) were taken over a period of 24 h extracted twice with 1 mL ethyl acetate and centrifuged (13300 g, 5 min) to remove cells. The supernatants were used for products quantification. The biotransformation reactions were initially followed by thin layer chromatography (Figure 24). Three of the tested substrates has shown conversion: testoserone (Figure 24a), LCA (Figure 24b), and DCA (Figure 24c). TLC analysis showed that OleP accepted testosterone as a substrate resulting in several reaction products, in agreement with the preliminary findings of

Agematu et al.(Agematu et al. 2006). The identity of the diverse hydroxylated testosterone derivatives hasn't been confirmed, since testosterone was not in the focus of this study.

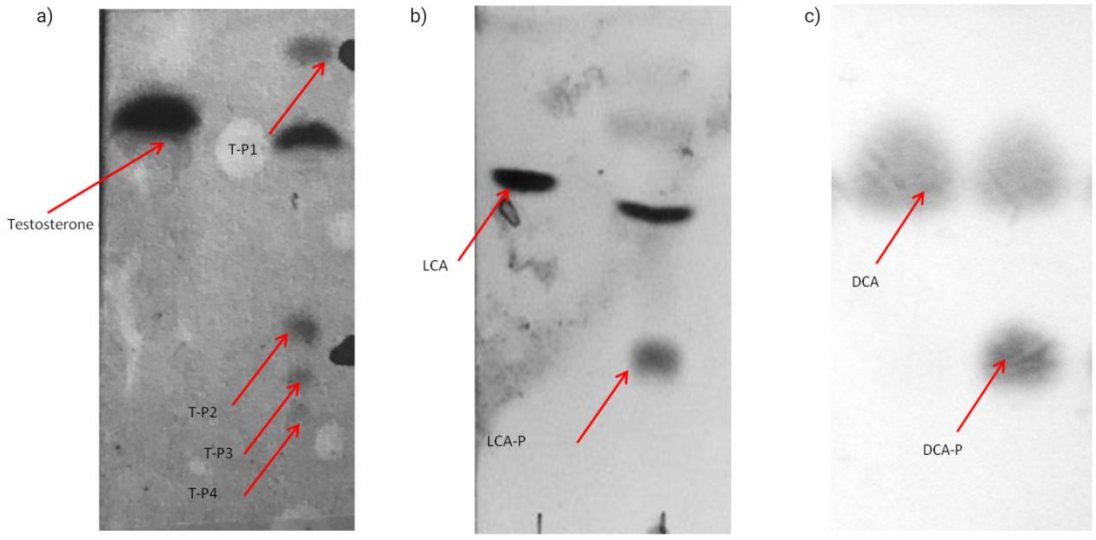

Figure 24.:a) Conversion of testosterone; b) conversion of LCA; c) conversion of DCA detected on TLC; LCA-P- product of conversion of LCA by OleP with PdX/PdR; T-P1-4 - product of conversion of testosterone by OleP with PdX/PdR; DCA-P - product of conversion of DCA by OleP with PdX/PdR.

In addition, CYP107D1 also accepted LCA and DCA bile acids as substrates, in both cases giving only one product selectively. To the best of current knowledge, CYP107D1 is the first reported P450 that can catalyze the hydroxylation of LCA and DCA with high selectivity. Moreover, such selective reactions performed by CYPs are extremely hard to achieve via conventional chemical routes. Therefore, this promising reaction was further studied.

Both isolated enzymes and whole cells have been used as catalysts. However, the application of the whole cells for bile acids biotransformation resulted in higher conversions than cell-free extract (based on TLC). Enzymes in cells are protected from the external environment, thus, they are generally more stable in the long-term than free enzymes. Moreover, in vivo catalysis mostly solves the problem of cofactor regeneration. Furthermore, the best conversion of LCA and DCA was obtained with enzymes expressed at 30°C. In the control reactions with *E. coli* C43(DE3) (PdR/PdX) not expressing CYP107D1, no product formation was observed (Figure 25).

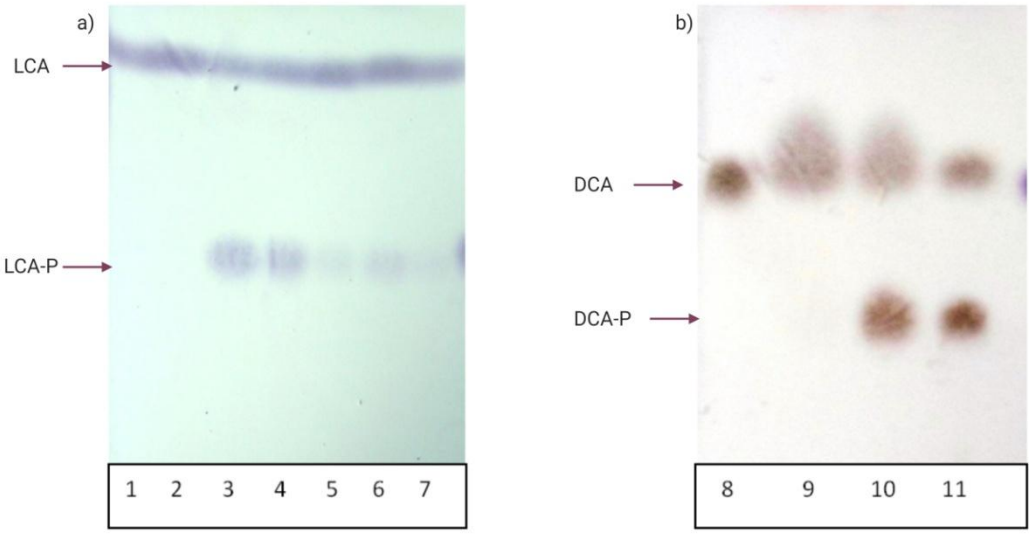

Figure 25: TLC results on biotransformation of LCA (25a) and DCA (25b) OleP and PdR/PdX as redox partner From left to right: 1 spot: LCA-control; 2 spot: LCA- PdR/PdX control; 3 spot: LCA CYP107D1+PdR/PdX expressed at 30°C (expression 1); 4 spot LCA CYP107D1+PdR/PdX expressed at 30°C (expression 2); 5 spot: LCA CYP107D1+PdR/PdX expressed at 20°C (expression 1); 6 spot: LCA CYP107D1+PdR/PdX expressed at 20°C (expression 2); 7 spot: LCA CYP107D1+PdR/PdX expressed at 20°C (expression 3); 8 spot: DCA - control; 9 spot: DCA CYP107D1+PdR/PdX expressed at 30ºC (t0); 10 spot: DCA CYP107D1+PdR/PdX expressed at 30°C (t1(12h));11 spot CYP107D1+PdR/PdX expressed at 30°C (t1(24h)).

3.1.4 Identification of products

The biotransformation products were isolated by column chromatography. Their structure was verified by 2D-NMR experiments (2D NMR analysis can be found in the Appendix: Figure A 1 and Figure A 3) and mass spectrometry (MS) (MS analysis can be found in the Appendix: Figure A 2 and Figure A 4). The structure elucidation revealed that in both cases the hydroxylation occurred stereoselectively, resulting in a new hydroxyl group in the 6β position. The product obtained from DCA was 3α,6β,12α-trihydroxy-5β-cholan-24-oic acid. This hydroxylated derivative of DCA has been synthesized before by a tedious time-consuming chemical method (Iida et al. 1986). The product obtained from LCA was murideoxycholic acid, which is a known metabolite in humans and house mice (Figure 26).

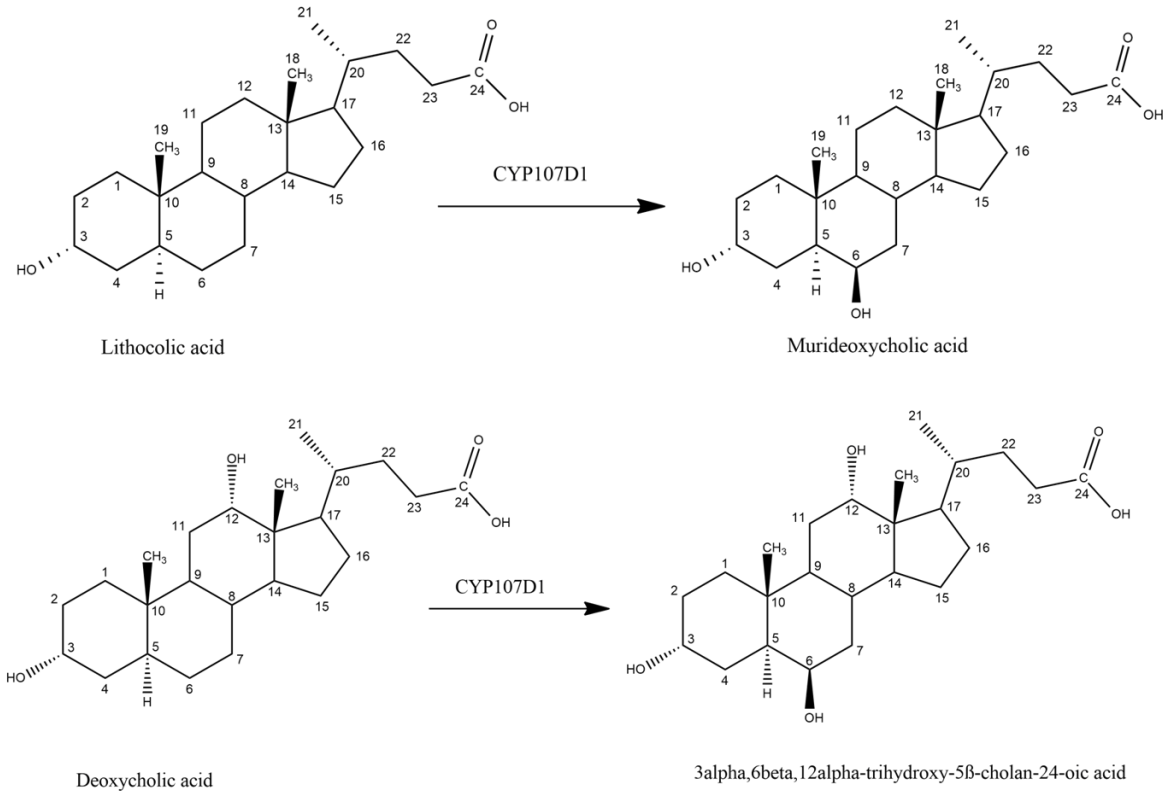

Figure 26: OleP (CYP107D1) catalyses the conversion of LCA or DCA into the corresponding 6-hydroxylated products.

DCA is a component of human bile acid, which plays an important role in emulsifying and digesting fat in the intestine (Virtanen and Kolehmainen 2004). Moreover, DCA and its sodium salt are globally approved drug products for decades; they have diverse applications in the pharma and beauty industry such as treatment of lipomas as an alternative to surgical excision, or the disruption of Influenza viruses during vaccine production (Rotunda et al.

2004, 2005; Arnold and Linke 2008; Ascher et al. 2016). Therefore, since DCA is widely used in medicine, more knowledge about its possible metabolites becomes essential.

In this study DCA was used in whole-cell biotransformation at 200 mL scale with 200 mg DCA. Starting from the DCA material (2 mg mL^{-1} 5.51 mM or 5.51 µM mL^{-1})), 0.7 mg mL^{-1} (1.7 mM) 6β_DCA was produced within 24 h, resulting in a yield of 35 %. This led to 1.7 mmol L^{-1} of 6β_DCA in the culture and a space-time yield of 0.071 mM h^{-1}. Calculations were based on the dry cell weight of *E. coli* and the cell density of the culture (OD600 = 18): one liter of culture yields 7.02g of dry cells, which consequently leads to 0.26 mmol/gCDW.

The structural difference between LCA and DCA is the additional 12α-hydroxyl group in the DCA which changes the hydrophilic-hydrophobic balance of the bile acid leading to overall higher hydrophilicity of the compound (Monte et al. 2009). Based on the results of TLC, which is a qualitative and straightforward method, HPLC analysis was performed. For further characterization, the time course of product formation during whole-cell conversions of LCA showed that the product distribution changed over time. Samples were taken every 2 h over 24 h with a break after 12 h (Figure 27).

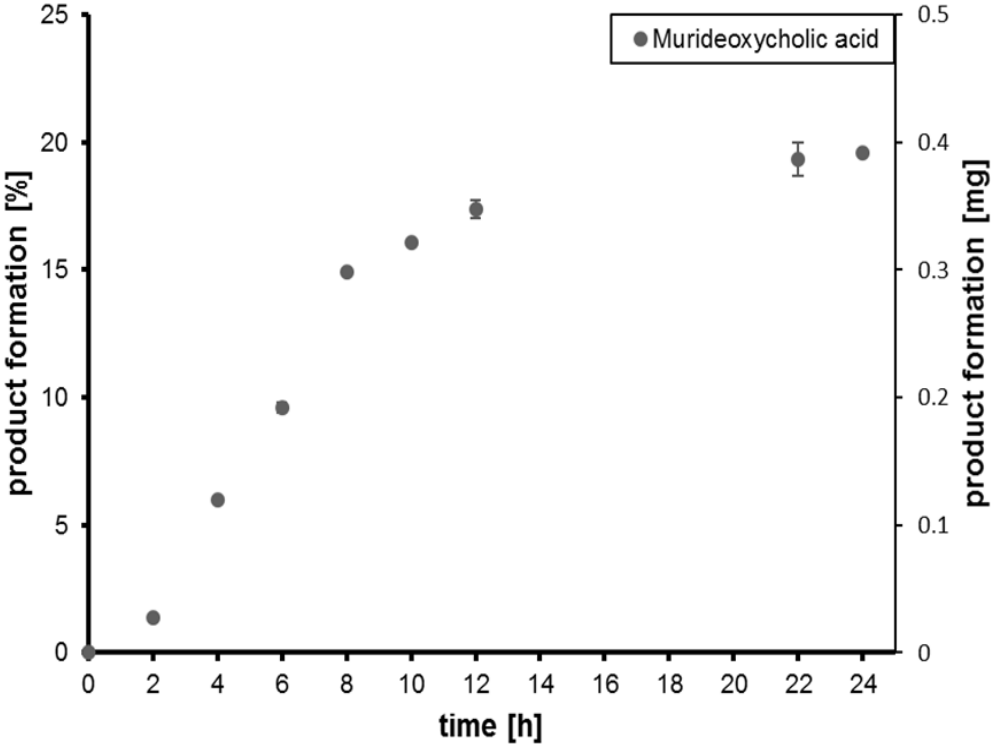

Figure 27: Whole-cell biotransformation of 5.31 mM LCA using *E.coli* C43 (DE3) co-expressing OleP and PdR/PdX. The percentage and amount (in mg) of LCA converted to MDCA at each time point is plotted as mean with standard deviation (n=3) (Grobe et al. 2020).

As indicated in Figure 27, MCA was found to be the main product in the first 8-12 hours of the reaction, and it is dependent on the activity of CYP107D1. The error bar indicates that only a small amount of MCA is produced between 12 and 24 hours of the reaction. Based on the time course and a standard curve for MCA, the yield can be determined. Starting from the LCA material (2 mg mL^{-1} (5.31 mM or 5.31 μM mL^{-1})), 0.39 $mg \cdot mL^{-1}$ (0.99 mM) MCA was produced within 24h, resulting in a yield of 19.5 % MCA. This led to 0.998 mmol L^{-1} of MCA in the culture and a space-time yield of 0.042 $mM \cdot h^{-1}$. Calculations were based on the dry cell weight of *E. coli* and the cell density of the culture (OD600 = 18): one liter of culture yields 7.02 g of dry cells, which consequently leads to 0.14 mmol/gCDW.

3.1.5 Discussion

Applying a heterologous three-component system (CYP107D1+PdR/PdX) in the bioconversion of LCA, we have shown that CYP107D1 is not only involved in oleandomycin biosynthesis as described by Montemiglio et al., but also exhibits excellent regio- and stereoselectivity for LCA and DCA, producing 6β-hydroxylated bile acids exclusively (Montemiglio et al. 2015; Parisi et al. 2019). Agematu et al. expressed a CYP107D1 with PdR/PdX as a redox partner in *E. coli* and reported OleP hydroxylated testosterone at the 6β-, 7β-,12β and 15β- positions, indicating that OleP was a multifunctional P450 (Agematu et al. 2006). The different selectivity of OleP, observed in this study, can be explained by the differences in the steroidal structure. While testosterone contains a double bond between C4 and C5 and the A/B ring fusion has a trans conformation, the A/B ring in the bile acids is *cis*, creating a significant spatial difference between the molecules (Li and Chiang 2014). Hydroxylation of LCA in 6β-position was also described in the literature for eukaryotic P450 monooxygenase from *Golden hamster* CYP3A10, which has only 20% similarity to OleP (Teixeiras and Gilg 1991; Chang et al. 1993). In humans, by contrast, P450 CYP3A4 hydroxylate steroid hormones on position 6β can also metabolize lithocholic acid, but in this case the bile acid is hydroxylated at the 6α position. Since DCA is widely used in medicine and the possibility of producing its metabolites has become important. The synthesis of 6β-hydroxylated DCA starting from DCA was previously described in 11 steps with an overall yield below 20% which is time-consuming and a complicated procedure compared to one-step biotransformation using CYP107D1 (Iida et al. 1986). OleP is the first bacterial P450, which selectively hydroxylates bile acids on the 6β position and thus provides the opportunity to use it as an alternative drug target for metabolic disorders, cancer, and also as antimicrobial agent.

In summary, CYP107D1 from *Streptomyces antibioticus* represents a promising new biocatalyst for hydroxylation reactions. The enzyme can be easily expressed with the redox partners PdX/PdR in *E. coli.* OleP has been found to hydroxylate certain bile acids in a regio- and stereoselective manner. The multifunctionality of OleP opens up new horizons for the commercial production of physiologically active steroids, which are difficult to obtain from alternative steroid raw materials.

Moreover, since the CYP107D1 crystal structure has been known, it is a good starting point for protein engineering to modify the selectivity of the enzyme. The organic synthesis of the API bile acid UDCA is a long process. Nowadays organic synthesis of UDCA is complicated and risky due to the nature and toxicity of the reagents used, the costs of disposal

of large amounts of sodium hydroxide, chromium salts and organic solvents, and the purification processes necessary to eliminate byproducts formed at each step of reaction involved (Tonin and Arends 2018). Therefore, research nowadays is geared towards more economical synthesis methods that are waste-free and safe to operate. An approach that bears great promise is the biotransformation with non-pathogenic, easy-to-manage microorganisms as *E. coli*. The one-pot or one-flow reaction, involving highly selective enzymatic steps would be preferred. Therefore, designing a CYP107D1 mutant with 7β-hydroxylation activity towards LCA can lead to the discovery of a new commercial path to the production of the UDCA.

3.2 P450 monooxygenases from *Fusarium graminarium*

To explore the diversity of fungal P450 systems, a search through the Fungal Cytochrome P450 Database was performed (Park et al. 2008). The genome of *F. graminarium* is predicted to contain 119 putative CYP genes and only nine CYPs have been functionally characterized three of those are paralogs of CYP51, which encodes an ergosterol biosynthetic enzyme (Shin et al. 2018). Out of 119 P450s from *F. graminarium*, only three have been recognized as self-sufficient: (P450_FG07 (UniProt-I1RTT0_GIBZE), P450_FG060 (Uni-Prot- A0A098D0P1_GIBZE), P450_FG067 (UniProt-I1RE90_GIBZE). Self-sufficient P450s from *F. graminarium* are grouped into two classes according to their topology (Figure 4), which differ in the arrangement of the P450 redox partners and associated fusion proteins. The P450_FG07 (UniProt-I1RTT0_GIBZE) and P450_FG067 (UniProt-I1RE90_GIBZE) are in the class VIII topology, the heme-monooxygenase domain is fused to a FAD- and FMN-containing NADPH-cytochrome P450 reductase (Fig. 4-I). In contrast, the heme-monooxygenase domain of P450_FG060 (UniProt-A0A098D0P1 _GIBZE) is fused to a FMN and iron-sulfur cluster-containing reductase (Class VII) (Fig. 4-H). Interestingly, BLAST analysis showed that the amino acid sequence of P450_FG067 from *F. graminarium* showed shared 86% identity with P450foxy from *F. oxysporum*. The P450foxy (CYP505A1) is already characterized as a self-sufficient ω-1, ω-2, ω-3 fatty acid hydroxylase (Nakayama et al. 1996; Kitazume et al. 2002, 2008). The prediction of function only from protein structure similarity is however challenging as combined information about sequence, structure, and function is often still missing. This makes an activity screening inevitable. Therefore, P450_FG067 was chosen for further investigation as novel self-sufficient P450 for fatty acid hydroxylation. Moreover, use of microorganisms, such as *E. coli* or *P. pastoris*, as a whole-cell biocatalyst protects the enzymes from destabilization and degradation and appears to be a useful alternative to the enzymatic approach for the bioconversion of fatty acids (Kelly et al.; Bernhardt 2006; Hernández-Martín et al. 2014).For expression of the eukaryotic P450-FG067 (UniProt: I1RE90_GIBZE), the two host systems *P. pastoris* and *E. coli* were compared. Both hosts have been widely used the for expression of P450s. Synthetic gene for *P. pastoris* was codon-optimised and equipped with a C-terminal 6x-His-tag. For an expression in *E. coli*, an expression plasmid harbouring P450_FG0067 was constructed. The gene was amplified and subcloned to the pET24a vector. Plasmid pET24a was considered to be the most suitable over expression vector, providing kanamycin resistance, the T7 promoter and encodes a C-terminal hexa-histidine tag for the affinity purification. The strategy of subcloning of P450_FG0067

into pET24 vector can be found in the Appendix: Figure A 8. A DNA insert encoding the P450_FG0067, using the pUC_P450_FG0067 plasmid as a template, was prepared by PCR using the primers containing an HindIII and BamHI restriction site. Specific PCR products of the approximate expected size (3330 bp) were obtained (PCR amplification of P450-FG067 can be found in the Appendix: Figure A 9). The resulting PCR product containing P450_FG0067 gene was placed under the control of a tac promoter by digesting the amplicon with HindIII and BamHI, and ligating into a HindIII and BamHI-digested pET24a, yielding plasmids P450_FG067_pET24a (PCR control to monitor the integrity of P450-FG067 amplicons in PET24a vector can be found in the Appendix: Figure A 10).

3.2.1 Expression and activity determination in *E. coli*

While many proteins can be successfully expressed to very high levels in *E. coli* BL21(DE3), in some cases, significant over-production cannot be achieved because of the toxicity of the target protein, which may even cause bacterial cell death. The P450s are heme proteins and over-expression of heme binding proteins in *E. coli* often results in sub-optimal heme incorporation into the recombinant proteins. Moreover, the target protein P450-FG067 is an eukaryotic protein with high molecular weight (120 kDa). It has been reported that proteins with molecular weights above 60 kDa are difficult to express. Since *E. coli* C43(DE3) strain is effective in overexpressing toxic and membrane proteins from all classes of organisms, including viruses, eubacteria, archaea, yeasts, plants, insects, and mammals, therefore, this strain was chosen for expression of eukaryotic P450-FG067 (Dumon-Seignovert et al. 2004). Supplementing the growth media with δ-amino levulinic acid (δ–ALA), a precursor of the heme biosynthesis pathway, increases levels of heme biosynthesis and thereby heme incorporation into the target protein (Delcarte et al. 2003). Hence, this necessitated an investigation of δ–ALA dependence on the production of P450_FG067 in *E. coli*. The recovered P450_FG067 was separated by gel electrophoresis to verify the expression of P450_FG067 with an expected size of 120 kDa. However, no signal for P450-FG067 was detected. Moreover, supplementation with δ-ALA did not enhance the production of P450_FG067 (Figure 28).

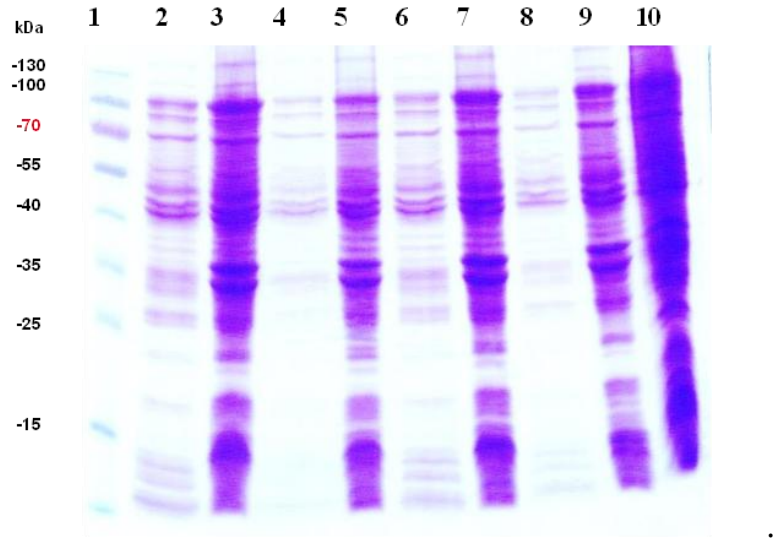

Figure 28: SDS-PAGE analysis of crude extract of *E. coli* DE3 cells after expression of P450-FG067(120 kDa) Lane 1: Marker, lane 6- P450_Fg0067_pET24a C43(DE3) *E. coli* – soluble protein after centrifugation without δ-ALA supplementation during cultivation, line 7 P450_Fg0067_pET24a C43(DE3) *E. coli* –insoluble protein fraction withut δ-ALA supplementation during cultivation, line 8- P450_Fg0067_pET24a C43(DE3) *E. coli* –

soluble protein after centrifugation with δ-ALA supplementation during cultivation, line 9 P450_Fg0067_pET24a C43(DE3) *E. coli* – insoluble protein fraction after centrifugation with δ-ALA supplementation during cultivation MW of FG067: ~ 120 kDa.

Additionally, a Western blot analysis was performed using anti-His-Tag. for P450_FG067 (120 kDa) no signal was detected in the soluble and insoluble fractions of *E. coli*. However, one signal was detected with a size of approximately 65 kDa (Figure 29).

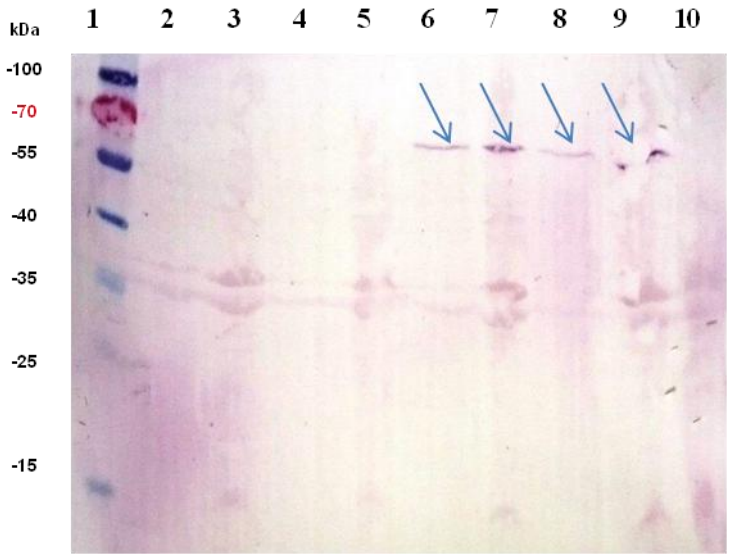

Figure 29: Western blot of recombinant FG067 in *E. coli*

Lane 1: Marker, lane 6- P450_FG0067_pET24a C43(DE3) *E. coli* –soluble proteins without δ-ALA supplementation during cultivation ,line 7 P450_FG0067_pET24a C43(DE3) *E. coli* –insoluble proteins without δ-ALA supplementation during cultivation, line 8- P450_FG0067_pET24a C43(DE3) *E. coli* –soluble proteins with δ-ALA supplementation during cultivation, line 9 P450_FG0067_pET24a C43(DE3) *E. coli* –insoluble proteins with δ-ALA supplementation during cultivation MW of FG067: ~ 120 kDa.

The structural relatives of P450-FG067 were determined using the BLAST program. P450_FG0067 belong to the self-sufficient class of P450 monoxygenases. The entire polypeptide spans over 1069 amino acids, having two structural domains: N-terminal P450 heme domain and the carboxyl-terminal half comprising 599 amino acid (~66 kDa), which is the FAD and FMN-NADPH-dependent reductase domain. The reductase domain allows the electrons to transfer from NADPH to the heme iron of the cytochrome P450 and is coded by the *cysJ* gene (Ostrowski et al. 1989) (Figure 30).

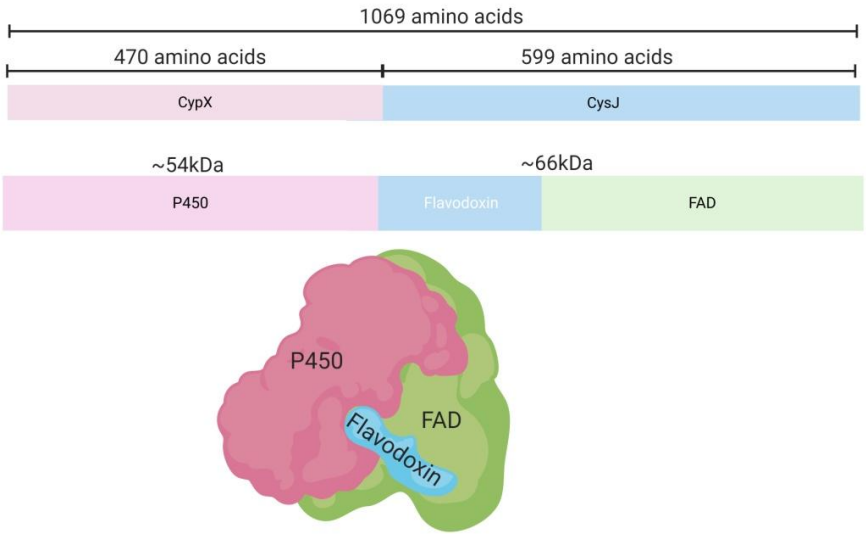

Figure 30: Conserved domains found by BLASTP suite for P450_FG067.

The use of *E. coli* for the production of recombinant proteins can provide many practical problems. It has been alerady reported that *E. coli* is not suitable for the production of many large, complex proteins containing disulfide bonds, or proteins that require post-translational modifications. Furthermore, the stability of foreign proteins produced in *E. coli* can be low due to proteolytic degradation, and overexpressed proteins are often produced in the form of inclusion bodies, which later require complicated and costly denaturation and refolding processes to make them functional (Rosano and Ceccarelli 2014). Protease-deficient bacterial strains (BL21 cells) did not decrease the proteolytic degradation of the recombinant enzyme. The P450-FG067 is 120 kDa and C-terminal His-tagged protein. The recombinant P450_FG067 was found to be partially degraded by the host-cell BL21(DE3). As shown by western immunoblot analysis, one major band of about 66 kDa was observed. It is possible that recombinant P450-FG067 expressed by *E. coli* was cleaved by a protease during the cultivation into two parts. The first one: FAD and FMN-NADPH-dependent reductase domain (~66 kDa), which is corresponding to the western-blot analysis shown in Figure 29 (C-terminal. The second: P450 heme domain (N-terminal). Moreover, P450 content in different fractions (soluble and insoluble) was checked by carbon monoxide (CO)-difference spectrum analysis using a ferrous-CO assay, but with the maximum typical shift of absorption from 420 nm to 450 nm was absent. That indicates that P450-FG067 was not successfully expressed in *E. coli*.

3.2.2 Expression and activity determination in *P. pastoris*

P. pastoris has the ability to produce foreign proteins at high levels and to provide advanced protein folding pathways for heterologous proteins, such as glycosylation, disulfide bond formation and proteolytic processing. (Macauley-Patrick et al. 2005). Moreover, recent studies have reported the heterologous synthesis of fatty acids using *P. pastoris* as a host (Kim et al. 2014; Meesapyodsuk et al. 2015). Therefore, as a second host for the heterologous expression of eukaryotic P450s, *P. pastoris* has been chosen. Expression of any foreign gene in *P. pastoris* requires three basic steps: the insertion of the gene of interest into an expression vector; introduction of the expression vector into the *P. pastoris* genome; and examination of potential expression strains for the foreign gene product (Cereghino and Cregg 2000). The choice of the proper expression vector and complementary host strain are the most important prerequisite for successful recombinant protein expression. Since P450_FG067 is a large protein (~120 kDa), a pPICZ A vector was chosen for intracellular expression. The pPICZ A contains the Zeocin resistance gene for the positive selection in *E. coli* and *P. pastoris.* . The following *P. pastoris* strains were transformed by electroporation with the linearized pPICZ A-FG067 and plated on YPDS-agar containing Zeocin: BG10 (wild type), BG11 (aox1Δ MutS) - slow methanol utilization derivative of PPS-9010 and protease deficient BG16 (pep4Δ, prb1Δ). The P450_FG067 was intracellularly expressed in all three *P. pastoris* strains, using batch cultivations with methanol pulses. The purified fractions were analyzed by SDS–PAGE as shown in Figure 31.

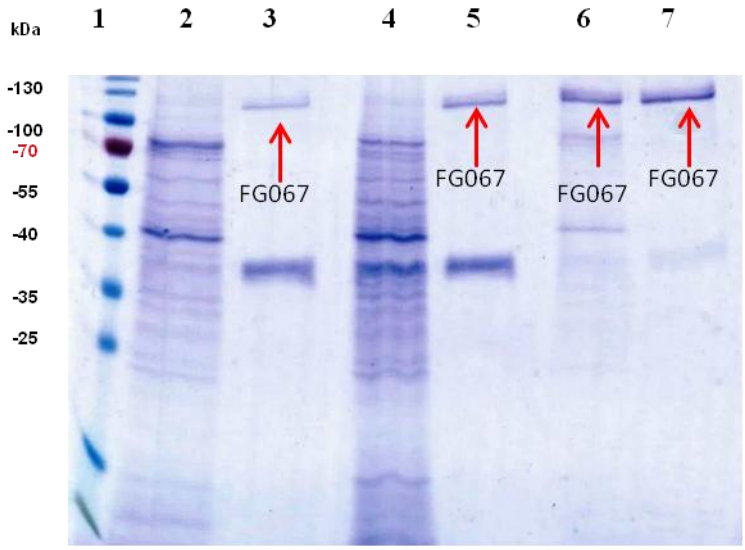

Figure 31: SDS-PAGE analysis of crude cell extract and the purified fraction of *P. pastoris* BG10, BG11, BG16 after expression of P450-FG067 (120 kDa).

Lane 1: Marker, lane 2- P450_Fg0067_pPICZ A BG10 *P. pastoris* – soluble protein after centrifugation ,lane 3 P450_Fg0067_pPICZ A BG10 *P. pastoris* – purified fraction, lane 4- P450_Fg0067_pPICZ A BG11 *P. pastoris* – soluble protein after centrifugation, lane 5 P450_Fg0067_pPICZ A BG11 *P. pastoris* – purified fraction, lane 6 P450_Fg0067_pPICZ A BG16 *P. pastoris* – soluble protein after centrifugation, lane 7 P450_Fg0067_pPICZ A BG16 *P. pastoris* – purified fraction MW of FG067: ~ 120 kDa.

As shown in Figure 31, P450_FG067 was expressed in all *P. pastoris* strains. In contrast to *E. coli*, *P. pastoris* contains endogenous CYPs. This is not considered as a complication, since endogenous P450s appear in non-significant levels and are hardly detectable by CO-difference spectroscopy (Lee et al. 2010). However, determination of P450 concentration in crude extract of *P. pastoris* was challenging. Therefore, only purified fractions were determined by the carbon monoxide (CO) difference spectrum assay. The typical shift of the maximum absorption from 420 nm to 450 nm was detected was observed only in the purified fraction of P450_FG0067_pPICZ_A *P. pastoris* BG10 strain. As shown in Figure 32, the reduced CO difference spectra, showed two distinct peaks at 420. Formation of the peak at 420 is related to the denatured forms of P450, and the peak at 450 is specific to the active form of the cytochrome P450. This instability of the expressed P450 could be the result of improper extraction and purification. Based on the CO-difference spectra, the concentration of purified FG0067 was estimated to be equal to 0.16 μmol mL^{-1}.

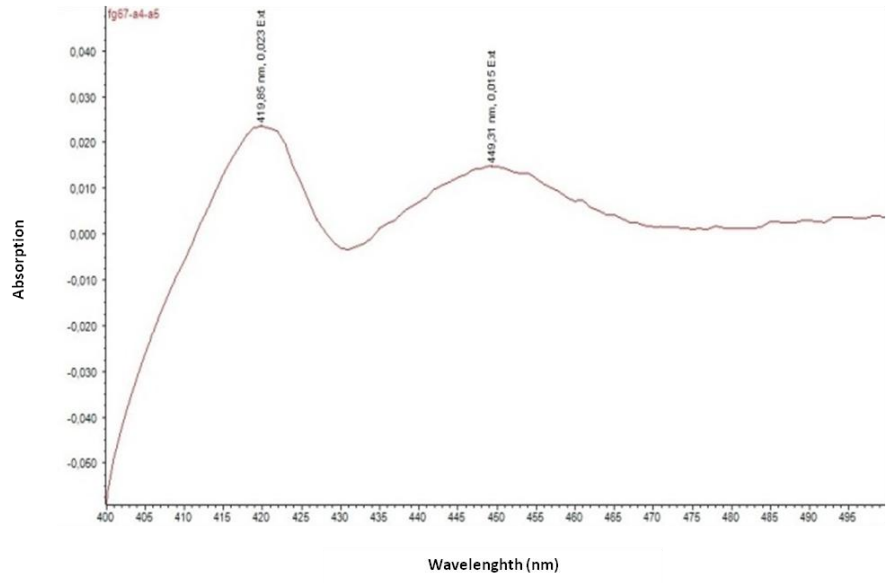

Figure 32: CO binding analysis of purified P450-FG067 expressed in *P. pastoris*.

The efficiency of the electron transfer directly affects the overall rate of P450-catalyzed reactions. Therefore, possibilities for the activity determination of the redox system has been investigated. Like the cytochrome P450 reductase, it is capable of transferring electrons not just to P450, but to artificial acceptors, such as cytochrome c (cyt c) and 2,6-dichlorophenolindophenol (DCIP) as well. These molecules serve as model substrates for the reductase activity determination. Here, a fast NADPH depletion was observed along with the conversion of dark blue DCPIP to its colorless reduced form. Based on the DCPIP assay, the activity of the electron transfer components was qualitatively measured, showing an active form of the reductase domain of cytochrome P450_FG067. After the concentration of P450_FG067 as well as the activity of the reductase domain were measured, *P. pastoris* BG10 (wild type) strain was selected as the best expression strain for P450-FG067 for larger scale expression. Moreover, P450_FG0067 was successfully purified by IMAC from *P. pastoris* crude extract (Figure 33).

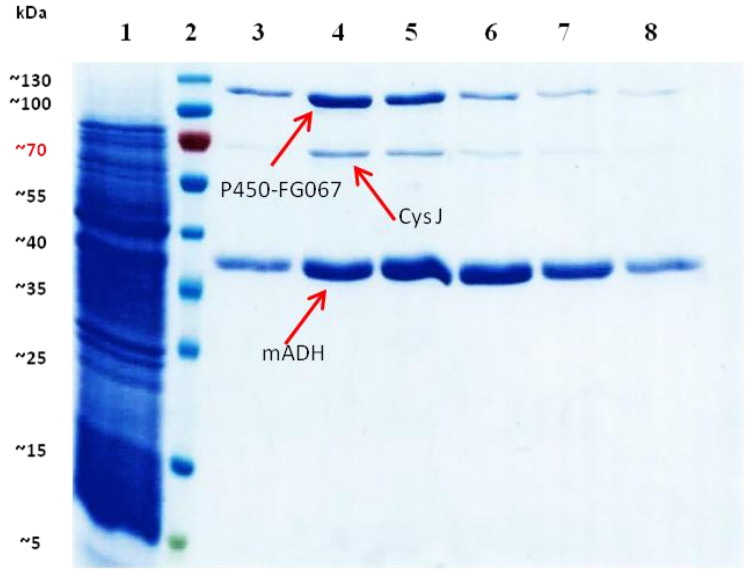

Figure 33: SDS-PAGE of His-tag purification of recombinant FG067

Lane1: Soluble fraction of cell crude extract from *P. pastoris*, lane 2: Marker, lanes 3-8: Elution of purified FG067, MW:FG067: ~ 120 kDa, CysJ~66 kDa, 35-40 kDa mADH.

Molecular mass of the expressed P450_FG067 was calculated to be equal to 120 kDa. As determined by SDS-PAGE analysis (Figure 33), the protein was in part degraded and visible as 66 kDa (CysJ- which is the FAD and FMN-NADPH-dependent reductase domain) protein, similar as in the *E. coli* expression earlier (Figure 29). Moreover, the co-purified protein of approximately 35-40 kDa was identified as a typical *P. pastoris* intracellular protein.

According to Chen et al. it is most probably the mitochondrial alcohol dehydrogenase isozyme III (mADH), which exhibits a high binding affinity for Ni-IMAC (Chen et al. 2014).

3.2.3 P450-FG067 as a fatty acid hydroxylase

The whole-cell conversion system with P450-FG067 in *P. pastoris* has been tested for the ability to hydroxylate fatty acids such as capric acid (C10), lauric acid (C12), myristic acid (C14), palmitic acid (C16) and stearic acid (C18). Resting and growing whole cells are commonly used as biotransformation catalysts. The use of growing cells is considered more beneficial than resting-cells, when expressing a protein with low stability, since they permit sustained protein expression during biotransformation. However, resting cells have the advantage that the desired reaction can be tested regardless of growth and at higher cell densities. Moreover, the conditions for the biotransformation can be selected independently of growth conditions, minimizing side reactions and at the same time the identification of potential limitations (Liu et al. 2018). Differences between growing and resting cells on fatty acid hydroxylation rates were investigated. However, no significant difference was noted. Substrate specificity of P450_FG067 against saturated fatty acids was determined using different thin layer chromatography methods (Figure 34). The pPICZ A, an empty vector expressed in *P. pastoris* was used as a negative control.

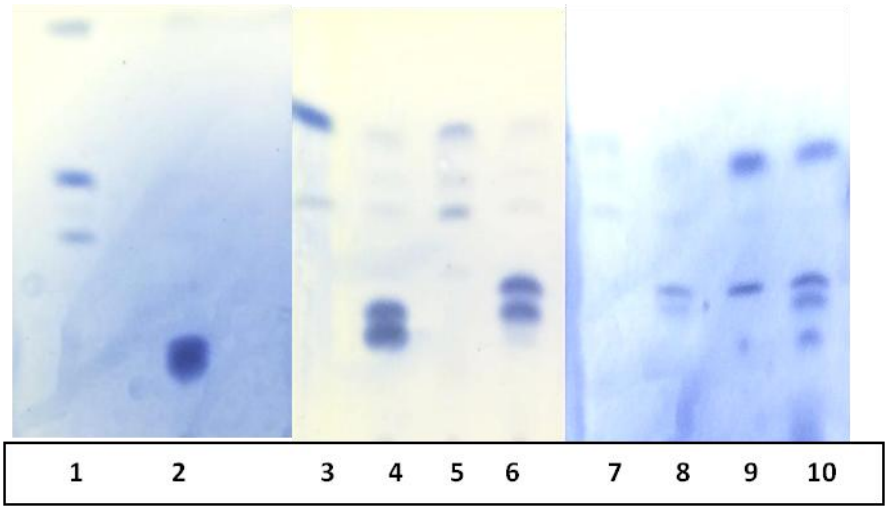

Figure 34: Fatty acid hydroxylation by whole-cell conversion system with P450-FG067 in *P. pastoris*.
From left to right: 1 spot: capric acid (C10) control *P. pastoris* ; 2 spot: capric acid (C10) control FG067 *P. pastoris*; 3 spot: lauric acid (C12) control *P. pastoris*; 4 spot: lauric acid (C12) control FG067 *P. pastoris*; 5 spot: myristic acid (C14) control *P. pastoris*; 6 spot: myristic acid (C14) FG067 *P. pastoris*; 7 spot: palmitic acid (C16) control *P. pastoris*; 8 spots: palmitic acid (C16) FG067 *P. pastoris*; 9 spot: stearic acid (C18) control *P. pastoris*; 10 spot: stearic acid (C18) FG067 *P. pastoris*.

The experimental results of TLC have indicated that the P450_FG067 was able to unspecifically hydroxylate fatty acids such as capric acid, lauric acid, myristic acid, palmitic acid and stearic acid into corresponding hydroxy fatty acids (Figuer 35). Based on the results of TLC, GC-MS and HPLC analysis was performed. The MS analysis data can be found in the Appendix (Figure A 11- Figure A 14).

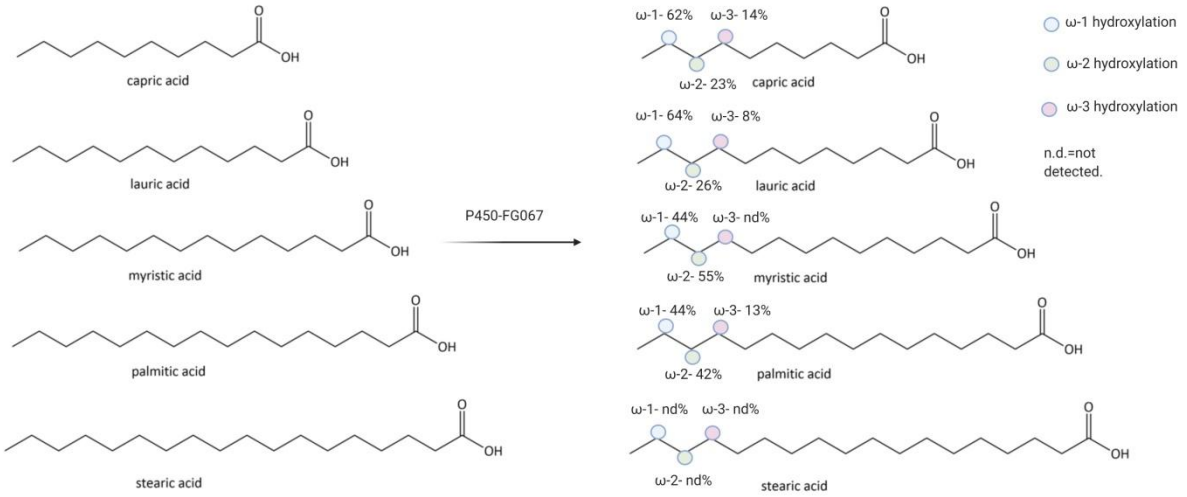

Figure 35: Reaction scheme of mono-hydroxylation of fatty acids by *Fusarium graminarium* cytochrome P450 monooxygenase. P450-FG067 can hydroxylate capric acid (C10), lauric acid (C12), myristic acid (C14) and palmitic acid (C16) into their respective ω-1, ω-2 and ω-3 hydroxy fatty acids derivatives

Analysis of the product profile and detailed characterization of hydroxylated fatty acid products were performed via gas chromatography–mass spectrometry (GC–MS). GC–MS analysis of the product mixtures resulting from FA conversions by P450-Fg067 revealed that the enzyme preferentially hydroxylated the inner carbon atoms of the FA chains and generated mono-hydroxylated products (Figure 35 and Table 1). The five FAs are unselectively hydroxylated at their inner chain carbon atoms, with the highest regioselectivity exhibited towards capric acid (62% hydroxylation in ω-1 position) and lauric acid (64% hydroxylation in ω-1 position). The conversion of fatty acids were estimated from the signal intensity on HPLC and shown in Table 1.

Table 1: The ratios of hydroxy fatty acids produced by P450 FG067 using capric acid (C10) lauric acid (C12) myristic acid (C14), palmitic acid (C16), stearic acid (C18) as substrates. The enzyme catalysis was allowed to proceed for 24 h.

Substrate	Products [%]				Conversion[%]
	ω	ω-1	ω-2	ω-3	
Capric acid (C10)	0	62.1	23.0	14.9	94.0
Lauric acid (C12)	0	64.9	26.9	8.2	88.0
Myristic acid (C14)	0	44.1	55.9	n.d.	38.0
Palmitic acid (C16)	0	44.0	42.0	13.7	8.0
Stearic acid (C18)	0	n.d	n.d	n.d.	n.d.

n.d.=not detected.

3.2.4 Discussion

Similarly to CYP505 (P450foxy), P450-FG067 catalyzes the subterminal (ω−1 to ω−3) hydroxylation of fatty acids (Nakayama et al. 1996). The product distribution for P450-FG067 was substrate dependent with respect to the chain length of fatty acid. Capric acid was the most efficiently converted to ω−1to ω−3 hydroxy decanoic acids in the order of ω−1> ω−2 > ω−3, with a total product yield of 94%. The hydroxylation of lauric acid (C12) occurred primarily at the ω-1 position (64.9%) to hydroxylate at the ω-2 position (26.9 %) over ω-3 (8.2%). The biotransformation of myristic acid (C14) by P450-FG67 is of particular interest to predominantly give the ω-2 hydroxyacid (55.9%) with the ω-1 (44.1 %), and ω-3 product was not detected. Moreover, P450-FG067 showed a slight preference of palmitic acid hydroxylation at the ω-1 position (44%) over ω-1 (42.4%) and ω-3 (13.7%) positions with a low total product yield of 8%.

This study demonstrated the use of a self-sufficient fungal P450 as a biocatalyst to convert fatty acids to ω−1to ω−3 hydroxyl FAs. A critical issue with P450 enzymatic conversion is the electron transfer. More specifically, for catalytic activity P450s must be associated with redox partner proteins that transfer electrons from NAD(P)H to the P450 heme center, which make P450 systems more complex (O'Reilly et al. 2011). By contrast, self-sufficient P450_FG067 overcomes these barriers because it does not require additional

redox partner. The P450-FG067 has a phylogenetically close relationship to P450foxy and P450BM3. The biotechnological importance of catalytically self-sufficient P450s, in particular the fatty acid hydroxylases, have already been well established (Kitazume et al. 2000, 2008; Munro et al. 2002). Development of novel self-sufficient P450s opens up new horizons in the field of the synthesis of new molecules. Furthermore, the recombinant cell-dependent system described herein does not require NADPH for bio-conversion. Recombinant P450foxy expressed in *P. pastoris* facilitates the hydroxylation of C10:0 to C16:0 fatty acids at the positions ω-1 to ω-3 (for C10:0 and C12:0 position ω-1 is most favored). The P450_FG067 can be applicable as biocatalysts in the production of hydroxy fatty acids in industry like other self-sufficient P450-BM3 or P450-foxy (Iliuta et al. 2015; Xiao et al. 2018).

3.3 Arginine kinase

ArgK-encoded arginine kinase (EC 2.7.3.3) was selected for developing a biocatalytic production of N_{ω}-phospho-L-arginine.

3.3.1 Recombinant Expression and Purification of ArgK in *E. coli*

The ArgK is one of the best-characterised arginine kinase and different crystal structures of the enzyme are available. Moreover, the isolation of ArgK-LP from biological sources such as horseshoe crab sperm or muscle would be both inefficient and uneconomic compared to the recombinant expression of this enzyme (Strong and Ellington 1993). The *E. coli* B strain is characterized protease deficiency, low acetate production at a high level of glucose. These properties make *E. coli* B a desirable host for the production of genetically engineered proteins. Moreover, *E. coli* BL21(DE3) carries a DE3 recombinant phage harboring the T7 RNA polymerase gene that can direct high-level expression of cloned genes under the control of the T7 promoter (Jeong et al. 2009). Since *E. coli* BL21(DE3) has been very widely used to express recombinant proteins, this strain of *E .coli* was chosen for expression of ArgK-LP. The 6xHis tag is small and does not usually interfere with protein function, for the production of pharmaceuticals and removal of the tag may be desired to obtain a protein with the native amino acid sequence. Several ways of removing N-terminal tags are available. The tag can be cleaved by an endoprotease, such as TEV (Booth et al. 2018). Therefore, the designed construct containing TEV recognition site and coding sequence of ArgK-LP and the presence of a His-tag in the fusion facilitates protein purification by affinity chromatography. The arginine kinase was overexpressed as recombinant protein in *E. coli* BL21 (DE3) and the amount of the ArgK was examined on SDS-PAGE. The size of the expressed cytoplasmatic monomer was approximately 40 kDa (Figure 36) This result is similar to the isolated sperm ArgK as determined by Strong and Ellington (Strong and Ellington 1995).

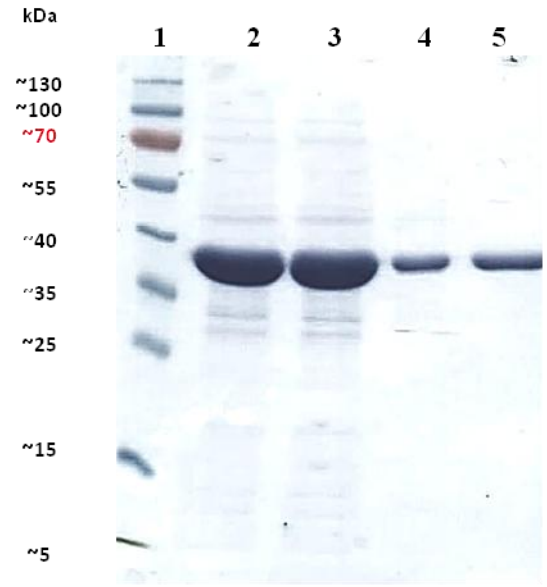

Figure 36: SDS-PAGE of His-tag purification of recombinant ArgK

Lane 1: Marker, lane 2: Soluble fraction of cell crude extract from *E. coli* BL21 (DE3), lane 3: Washing fraction, lane 4: Elution of purified ArgK, lane 5: desalted and purified protein fraction of ArgK, MW of ArgK: ~ 40 kDa.

As the recombinant protein carried an N-terminal His-tag, ArgK was successfully purified by IMAC purification (Figure 35). Moreover, ArgK-LP was overexpressed in *E. coli* BL21 (DE3) as a soluble protein in high yield. Around 30% of the protein was localized in the soluble protein fraction of *E. coli*. The obtained yield of the purified ArgK was 24 mg L^{-1} of *E. coli* culture. In contrast, in a previous study by Strong et al., in which no codon-optimised gene was expressed, the concentration of soluble ArgK-LP was much lower (~3 mg L^{-1} of culture) and most of the recombinant protein was aggregated as insoluble and inactive protein (Strong and Ellington 1996).

3.3.2 Arginine kinase activity determination and storage stability

The activity of arginine kinase was determined by the pyruvate kinase/LDH assay following the procedures devised by Oliveira et al. using L-arginine as a substrate (Oliveira et al. 2001). The specific activity of purified protein was about 80 U mg^{-1} and the activity in the crude extract 834 U mL^{-1}(Table 2). In addition, the specific activity of the recombinant ArgK-LP in this study was also approximately 28 times higher than that reported by Strong and Ellington (Strong and Ellington 1996).

Table 2: Protein content and photometric activity determination of Arginine kinase

Protein content:	1.68 mg mL^{-1}
Activity of cell crude extract (soluble fraction):	834 U mL^{-1}
The specific activity of purifiedArg4:	80 U mL^{-1}

The use of enzymes in industry is widely recognized because of their substrate specificity and green chemistry instead of harmful chemicals. However, their application has been hampered owing to their associated high costs and lack of stability under process conditions and storage (Martins et al. 2019). Knowledge of arginine kinase properties and behavior would allow optimizing conditions of its storage as well as formulating strategy towards its stabilization. The aim of this work was to study the enzyme activity and stability under different conditions and elaborate effective approaches towards its stabilization to verify the applicability of this enzyme for industrial use. Therefore, the stability of arginine kinase under storage conditions was investigated. Further, the influence of glycerol as a stabilizer was assayed. The activity of arginine kinase over one month in different formulations and storage temperatures (4ºC and -20ºC) was investigated. The storage temperature and the addition of 30% glycerol had a positive influence on the enzyme activity. Without any precautions, a maximum loss of 40% was observed when ArgK-LP was stored at 4ºC. In a case where the crude extract of ArgK was freeze-dried, a maximum loss of 50% was determined. When glycerol was added, and Arg-LP was stored at -20ºC, only 13% loss of activity was detected (Figure 37).

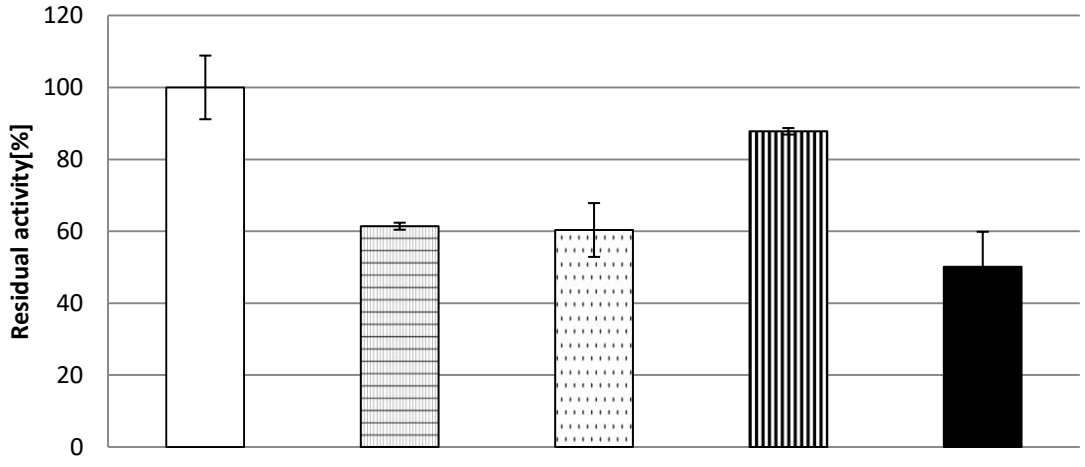

Figure 37: Storage stability investigation of recombinant arginine kinase in different formulation.
Arginine kinase activity measured in different enzyme formulations are shown as relative activities compared with the highest activity measured for fresh prepared soluble enzyme with 100% activity (white columns), respectively to activity of soluble enzyme stored over one month at 4°C (squared columns), soluble enzyme stored over one month at 4°C with additional of 30% glycerol (dotted columns), soluble enzyme stored over one month at -20°C with additional of 30% glycerol (striped columns), freeze-dried arginine kinase (filled columns). The results ± standard deviations are means of three independent experiments, each set in triplicate.

3.3.3 Biocatalytic phosphorylation of L-arginine

Since recombinant arginine kinase has been prepared in *E. coli* as a highly active and stabile enzyme, teodius five-step chemical synthesis reactions of N_{ω}-phospho-L-arginine can be replaced by a straightforward one-step biocatalytic phosphorylation. The development of biocatalytic phosphorylations is strongly facilitated by direct ^{31}P-NMR analysis of product formation in the reaction mixture. The simultaneous consumption of the phosphoenolpyruvate and the formation of the correct product is thereby an advantage and suitable reaction conditions can be easily developed. The time course of a biocatalytic Nω-phosphorylation of L-arginine was, therefore, followed by ^{31}P-NMR spectroscopy as shown in Figure 37. The reaction was carried out at pH 8.0 and with ATP recycling by using the PEP/pyruvate kinase system with a slightly sub-equimolar amount of PEP. A slight excess of L-arginine compared with PEP was chosen to avoid incomplete transformation of the latter, which turned out to be challenging to separate from the arginine-phosphate. In contrast to^{1}H-NMR spectra, the ^{31}P-NMR spectra are very clear and in time the signal increases (from bottom lane 1 to the top lane 7 in Figure 38A) at-3.65 ppm. This demonstrates the formation of the desired product -Nω-phospho-L-arginine- whereas the decreasing signal at 0.80 ppm shows the consumption of PEP, in line with ATP turnover. The time required for complete conversion can be optimised by selecting the total activity of the arginine kinase utilised for the reaction. It is shown in Figure 38 B for phosphorylation completed within 24 h. The method turned out to be suitable for the synthesis of preparative quantities of N_{ω}-phospho-L-arginine, whereby the use of crude extract of ArgK and purified ArgK gave similar results.

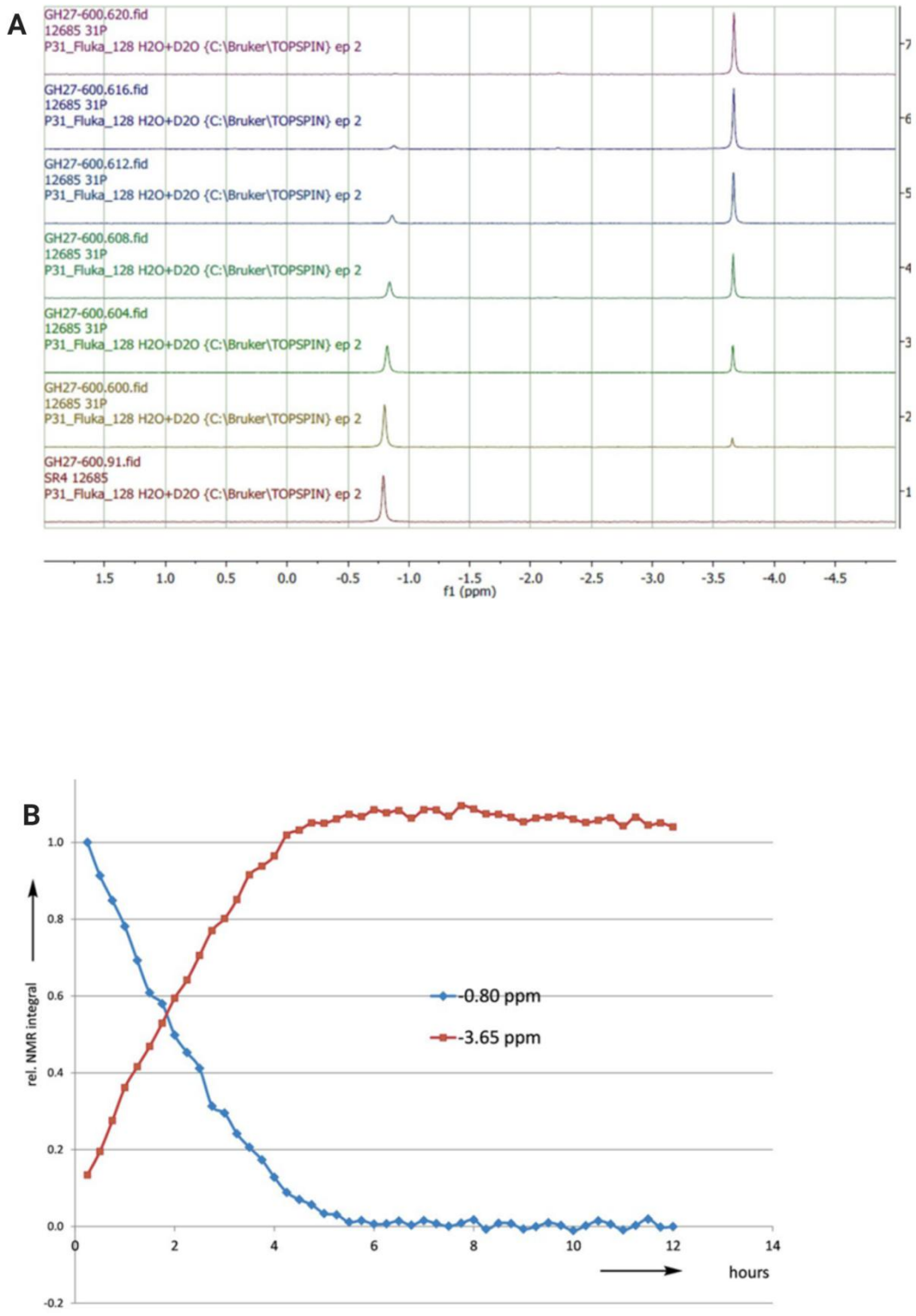

Figure 38. A) Reaction kinetics of biocatalytic phosphorylation of L-arginine; ^{31}P-NMR spectra of a reaction mixture from t=0 (lane1) to t=5h (lane7); signal at 0.80 ppm: PEP; signal at -3.65 ppm: N_{ω}-phospho-L-arginine. B) Time course of N_{ω}-phospho-L-arginine product formation and PEP consumption during biocatalytic phosphorylation of L-arginine.

The biocatalytic procedure and the subsequent work-up to the pure product, which is N_{ω}-phospho-L-arginine, have been successfully demonstrated and open up new opportunities for the selective biocatalytic N-phosphorylation of interesting low molecular weight's compounds and metabolites. Moreover, biocatalytically produced N_{ω}-phospho-L-arginine is already implemented in industry by the Merck company.

3.4 Shikimate kinase

AroL-encoded type II shikimate kinase (EC 2.7.1.71) was selected for the development of a biocatalytic shikimic-3- phosphate production.

3.4.1 Recombinant Expression and Purification of AroL in *E. coli*

K12 is the most studied *E. coli* strain (K strain), *E. coli* BL21 (B strain) is the most used for recombinant protein production. The *E. coli* BL21 strain lack some proteases (e.g. Lon protease, key to eliminating unfolded proteins), achieve higher biomass yields and produces much less acetate than *E. coli* K12 (Pinske et al. 2011). Moreover, using *E. coli* as a host system for an expression of gene which origin from *E. coli* is a good choice. Herein, designed constructs to express shikimate kinase in *E .coli* BL21 harboring a N-terminal His-tag fusion, which can be efficiently removed using the TEV protease is described. Employing the *aroL* gene from *E. coli* K12 (Uniprot P0A6E1, AROL_ECOLI), the shikimate kinase was recombinantly overexpressed in *E. coli* BL21(DE3) in a significant amount as a soluble protein, consisting of around 30% of total protein. The solubility of recombinant AroL from *E. coli* was similar to the solubility of recombinant shikimate kinase from *Mycobacterium tuberculosis* expressed in *E. coli* BL21(DE3) by Oliviera et al. (Oliveira et al. 2001). The recombinant His6-tagged AroL protein was purified on a Ni-IDA column. On the SDS-gel, a major band with a molecular weight of 20 kDa was observed and matched with the predicted mass of shikimate kinase (Figure 39).

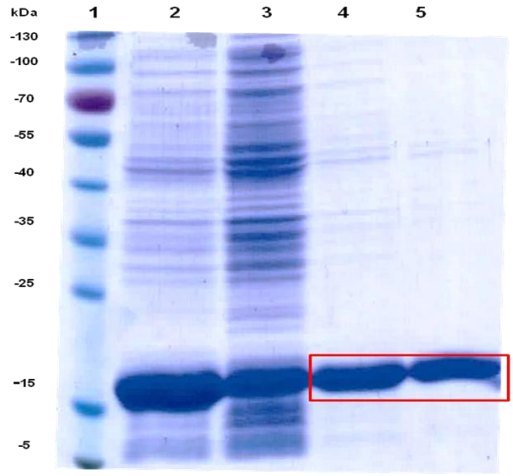

Figure 39.:SDS–PAGE of His-tag purification of recombinant AroL.

Lane 1: marker; lane 2: soluble fraction of cell crude extract from *E. coli* BL21 (DE3); lane 3: washing fraction; lane 4: elution of purified AroL; and lane 5: desalted and purified protein fraction of AroL, MW of AroL: 20 kDa.

3.4.2 Shikimate kinase activity determination and storage stability

The protein content (determined with the BCA assay) of the purified AroL was 1.47 mg mL^{-1} and the obtained yield of the purified AroL was 40 mg L^{-1} of *E. coli* culture. Shikimate kinase enzyme activity was determined at 25ºC and pH 7.5 spectrophotometrically by measuring the oxidation of NADH at 340 nm, based on ADP release by a coupled assay with pyruvate kinase and lactate dehydrogenase (LDH), according to Millar et al. (Millar et al. 1986). The specific activity of the purified recombinant AroL 41 U mg^{-1} with a total yield of 39 400 U L^{-1}. The activity of shikimate kinase obtained in the crude extract was 788 U mL^{-1} (Table 3).

Table 3: Shikimate kinase activity of cell crude extract (soluble fraction), AroL protein content, and shikimate kinase activity of the purified protein. Activity of cell crude extract (soluble fraction) 788 U mL^{-1} Activity a) of purified AroL 41 U mg^{-1} Protein content of purified AroL 1.47 mg mL^{-1}

Activity of cell crude extract (soluble fraction)	788 U mL^{-1}
Activity of purified AroL:	41 U mg^{-1}
Protein content of purified AroL	1.47 U mL^{-1}

Interestingly, the activity and the yield of recombinantly produced shikimate kinase is higher than that of shikimate kinases isolated from *E. coli*, *Bacillus subtilis*, *Spinacia oleracea, Oryza sativa or Sorghum bicolor*. It has been concluded that the stability of an enzyme is essential for its application in industry. Therefore, the activity of the recombinant shikimate kinase AroL has been measured in different formulations and at the storage temperatures of 4ºC and 20ºC over the period of 1 month. Glycerol when used as a cryoprotectant gives good results (Iyer and Ananthanarayan 2008). Addition of 30% glycerol and the storage temperature had only a slight influence on the enzyme activity. Moreover, AroL can also be stored as a powder without any precautions, as we observed only 30% loss of starting activity during lyophilisation (Figure 40).

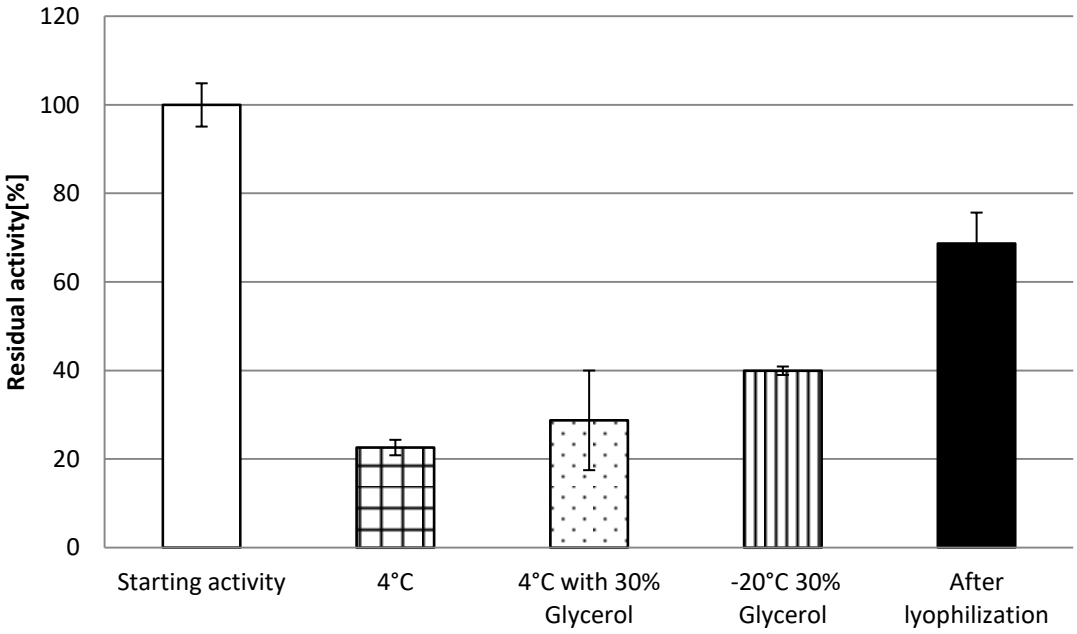

Figure 40: Shikimate kinase activity measured in different crude enzyme formulations are shown as relative activities as compared to the activity of the freshly prepared soluble enzyme fraction, which was set to 100% activity (white columns): relative activity of soluble AroL stored for over 1 month at 4ºC with no addition (squared columns), soluble enzyme AroL with addition of 30% glycerol stored for over 1 month at 4 C (dotted columns), soluble enzyme stored for over 1 month at 20ºC with addition of 30% glycerol (striped columns), freeze-dried shikimate kinase (filled columns). The results standard deviations are means of three independent experiments, each measured in triplicate.

3.4.3 Biocatalytic phosphorylation of Shikimic acid

In contrast to the tremendous chemical efforts involved in the proof of the right shikimate-3-phosphate structure, formation of shikimate 3-phosphate can now be easily identified by NMR spectroscopy. As shown below by the NMR-spectra of the selective shikimate kinase-catalyzed monophosphorylation of shikimic acid in the 3- position (Figure 41).

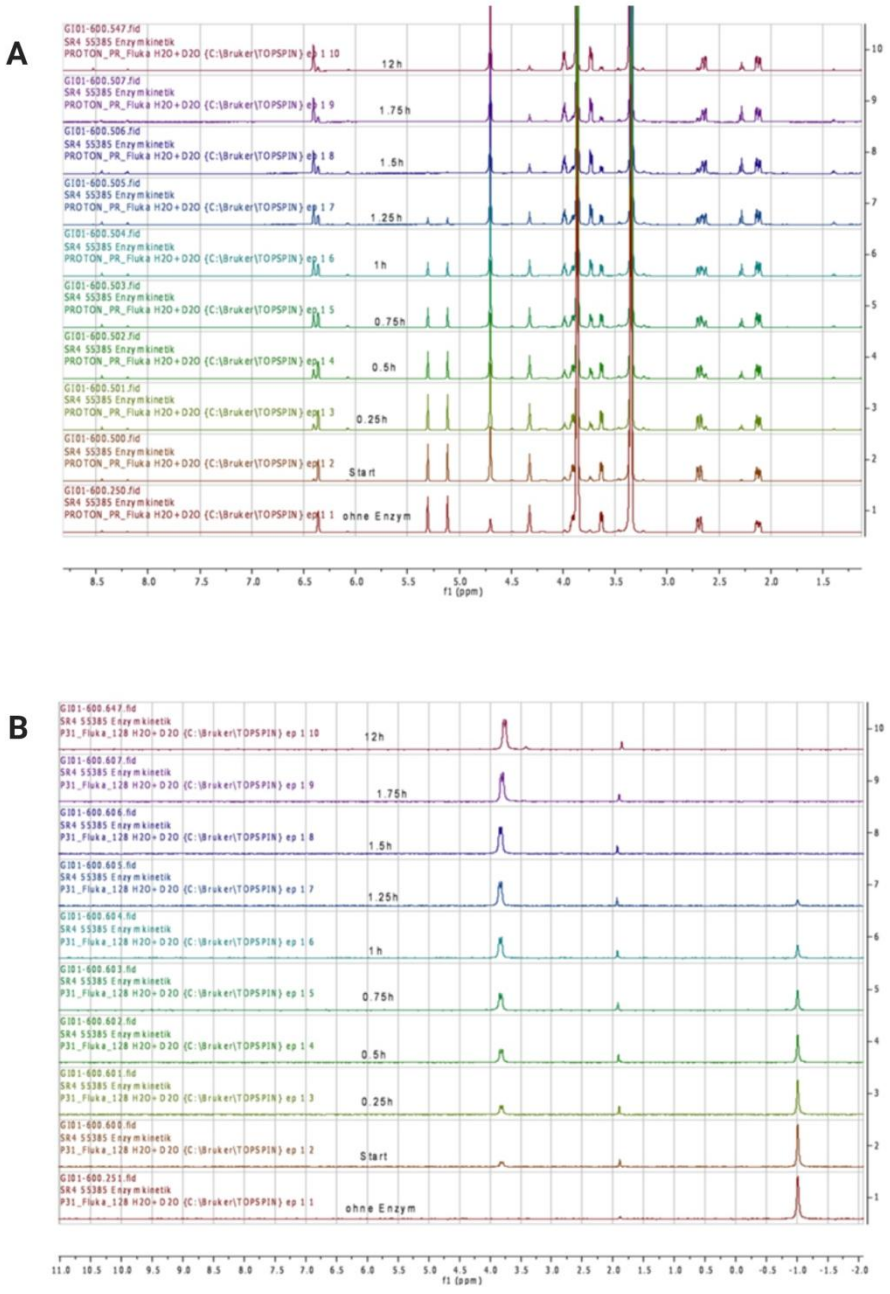

Figure 41: Typical time course of shikimate kinase-catalyzed phosphorylation of shikimic acid from a series of seven experiments under different reaction conditions (n¼1) measured by A) ^{1}H-NMR, signals at 6.40 and 6.36 ppm: H-C(2) ofproduct and substrate, respectively; signals at 5.30 and 5.11 ppm: PEP; B) ^{31}P-NMR, signal at 3.84 ppm (d): shikimic acid 3-phosphate; signal at -1.01 ppm (s): PEP

The ^{1}H-NMR spectra thereby show that with the time course of the phosphorylation (from the start at the bottom lane 1 to the time point t ¼ 12 h at the top lane 10 in Figure 40A), the signal at 6.36 ppm of H-C(2) of the substrate decreases and the signal at 6.40 ppm of H-C(2) of the product increases. If the same reaction was analyzed by ^{31}P-NMR, the increase of the doublet signal with increasing time (from the start at the bottom lane 1 to the time point t ¼ 12 h at the top lane 10 in Figure 44B) at 3.84 ppm would show the desired product shikimate 3-phosphate, while the signal decrease at 1.01 ppm would show the concomitant phosphoenolpyruvate consumption for the ATP cofactor regeneration.

Moreover, reaction conditions for shikimic acid phosphorylation can be developed rapidly, as demonstrated by the time course of the conversion to shikimic acid 3-phosphate within less than 100 min in Figure 42. The AroL catalyzed synthesis was carried out at pH 7 using the phosphoenolpyruvate (PEP)/ pyruvate kinase(PK)-system for ATP recycling. As demonstrated in Figure 42, the phosphoryl-donor PEP is thereby completely consumed, which is relevant for facilitating product purification.

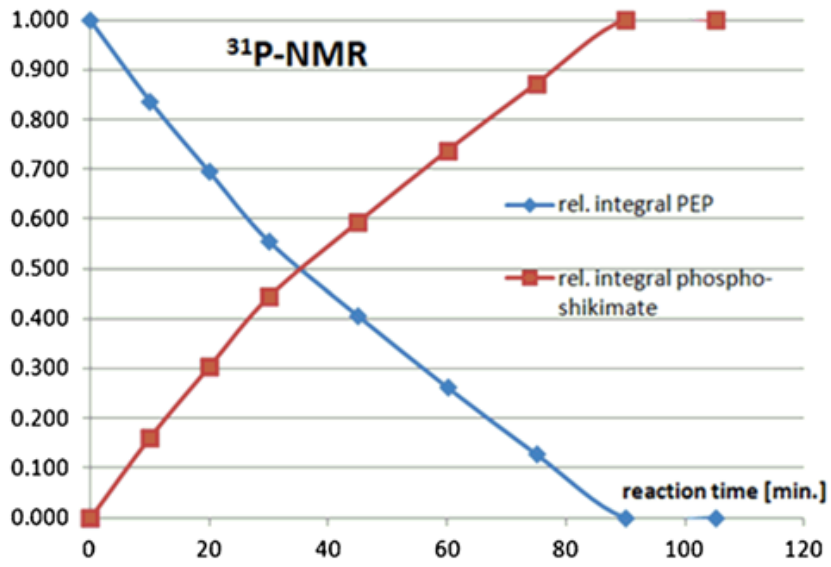

Figure 42: Typical reaction, monitoring of the AroL-catalyzed phosphorylation of shikimic acid by ^{31}P-NMR showing the increase of shikimic acid-3-phosphate (red curve) and the decrease of phosphoenolpyruvate (blue curve).

3.4.4 Discussion

The chemical synthesis of shikimic acid-3-phosphate has been described as the tedious multi-step procedure, which require the introduction and removal of protecting groups and involve reagents/solvents with safety, health, and environment issues (Bartlett and Mcquaid 1984). Biocatalytic phosphorylation of shikimate in the 3-position overcomes the problems associated with the chemical processes for the synthesis of this commercial valuable metabolite. The production of the highly active and stable recombinant *E. coli* K12 shikimate kinase AroL has been achieved by synthesizing the codon-optimized aroL gene and expressing it in high yield in *E. coli* BL21. The recombinantly expressed shikimate kinase has been applied in the ATP-dependent phosphorylation of shikimic acid, which was coupled with the pyruvate kinase-catalyzed ATP regeneration to avoid inhibition by ADP. The time course of the highly selective phosphorylation of shikimate in the 3-position was investigated by ^{1}H- and ^{31}P-NMR. This has facilitated the development of an efficient biocatalytic one-step synthesis at multi-gram scale of shikimic acid-3-phosphate, which after a standard workup procedure could be prepared in >97% purity and with a yield of the isolated pure lithium salt of 53%. Additionally, the highly active and stable shikimate kinase enables rapid access to other, various phosphorylated shikimate analogues and expands the platform for the biocatalytic phosphorylation of metabolites (Wohlgemuth et al. 2017). Moreover, the enzymatic phosphorylation of shikimic acid in the 3-position and the subsequent workup has been scaled up to multi-gram scale and it is already implemented in industry by Merck company.

3.5 Argininosuccinate lyase (ASL)

Arg4-encoded argininosuccinate lyase (EC 4.3.2.1) was selected for developing a biocatalytic procedure for the synthesis of L-argininosuccinate.

3.5.1 Recombinant Expression and Purification of ASL in *E. coli*

Since *E. coli* BL21 is the most used for recombinant protein production, herein, designed construct to express argininosuccinate lyase in *E. coli* BL21 harboring a N-terminal His-tag fusion, which can be efficiently removed using the TEV protease was used. Employing the *arg4* gene from *Saccharomyces cerevisiae* (Uniprot P04076, ARLY_YEAST), argininosuccinate lyase was recombinantly overexpressed in *E. coli* BL21 (DE3). The argininosuccinate lyase was overexpressed in *E. coli* as a soluble protein in high yield, i.e. around 50% of the protein was localized in the soluble protein fraction of *E. coli*. As an active enzyme, ASL is a tetramer, composed of four active sites. The size of one monomer is approximately 52 kDa, as determined by SDS-PAGE analysis (Figure 43). Since the recombinant protein carried an N-terminal His-tag, ARG4 was successfully purified by IMAC purification (Figure 43). The obtained yield of the purified ARG4 was 20 mg L^{-1} of *E. coli* culture.

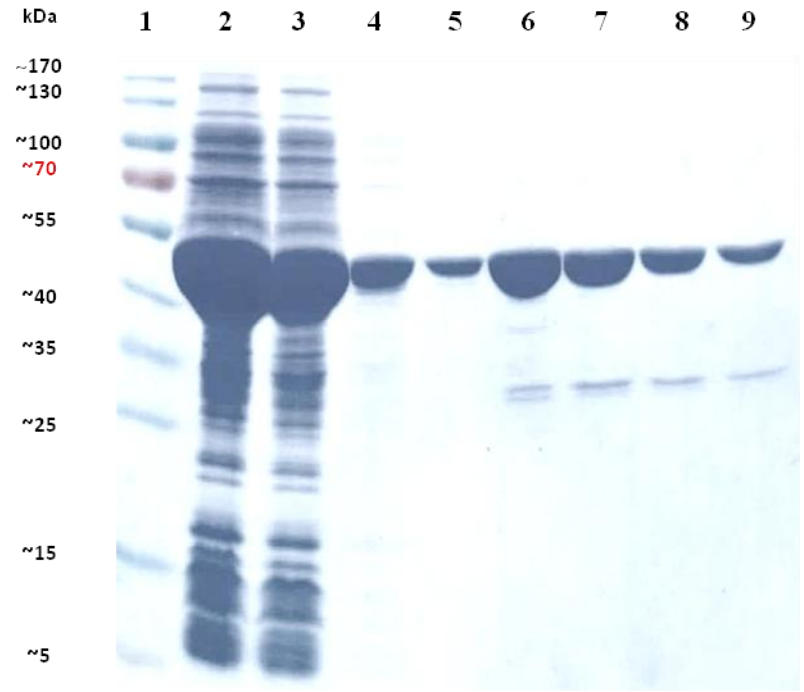

Figure 43: SDS-PAGE of His-tag purification of recombinant ARG4.

Lane 1: Marker, lane 2: Soluble fraction of cell crude extract from *E. coli* BL21(DE3), lane 3: Flow-through, lane 4: Washing fraction, lane 5-9: Elution of purified ASL, MW of ASL: ~ 52 kDa

3.5.2 Argininosuccinate lyase activity determination and storage stability

The activity determination of argininosuccinate lyase was based on the production of fumarate by to Kuchel et al. (Kuchel et al.1975). The specific activity was about 20 U mg^{-1} of purified protein and 206 U mL^{-1} in the crude extract (Table 4). In contrast to this, the specific activity of argininosuccinate lyase purified from *Saccharomyces cerevisiae* crude extract was much lower, only 0.081 U mg^{-1}.

Table 4. :Arg4 protein content, the activity of cell crude extract (soluble fraction) and activity of purified protein

Protein content:	0.92 mg mL^{-1}
Activity of cell crude extract (soluble fraction):	206 U mL^{-1}
Activity of purified ASL:	20 U mg^{-1}

Commercial enzyme products are usually formulated in aqueous solutions or dry products. Both liquid and dry preparations must be formulated with the final application in mind. It is important for both the producer and customer to take into account storage stability requirements such as stability of enzyme activity. Therefore, employing argininosuccinate lyaseas as a biocatalyst in industry, the stability of the enzyme over one month in different formulations and storage temperatures (4°C and -20°C) was studied. The storage temperature and the addition of 30% glycerol had no influence on the enzyme activity. Hence, the argininosuccinate lyase, ARG4, can be stored as powder as well as crude extract (at 4°C) without any precautions (Figure 44).

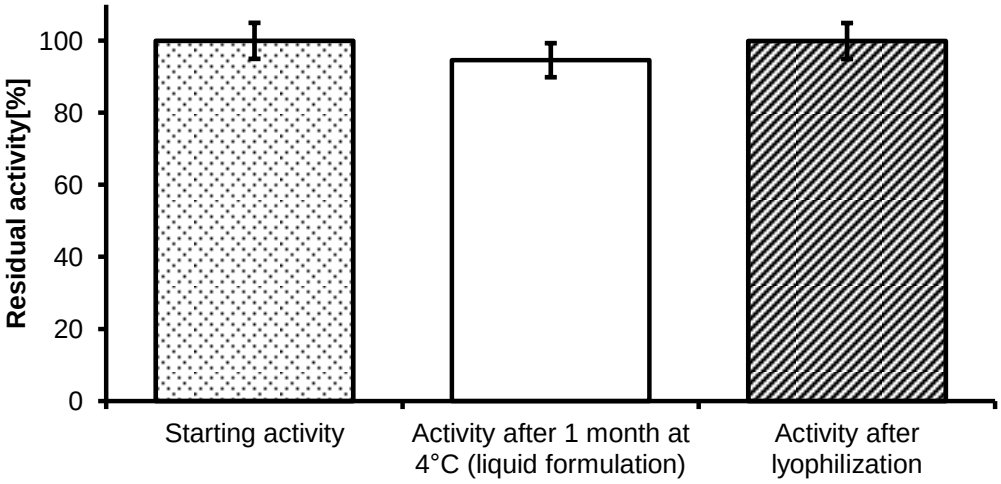

Figure 44:Activity of different formulations of argininosuccinate lyase.

3.5.3 Biocatalytic synthesis of the pure metabolite N-(([(4S)-4-amino-4-carboxybutyl] amino)iminomethyl)- L-aspartic acid as its lithium salt

To evaluate the enzyme activity under reaction conditions, the biocatalytic Michael addition reaction was analyzed as a function of time directly in the NMR tube. ^{1}H-NMR signals at 4.17 ppm (proton at the newly formed asymmetric carbon atom on the succinate portion) and 6.44 ppm (fumarate protons) were used for diagnosis of the reaction progress Figure (45A).

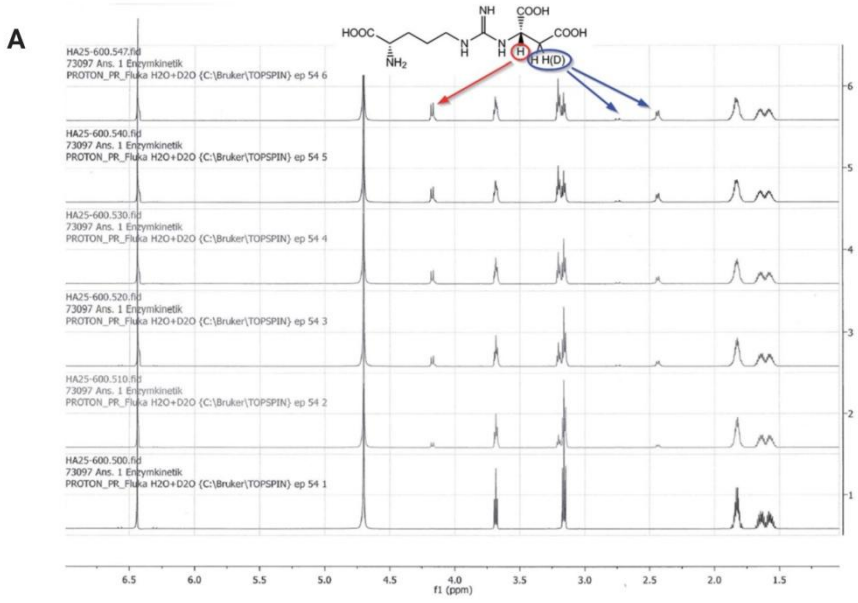

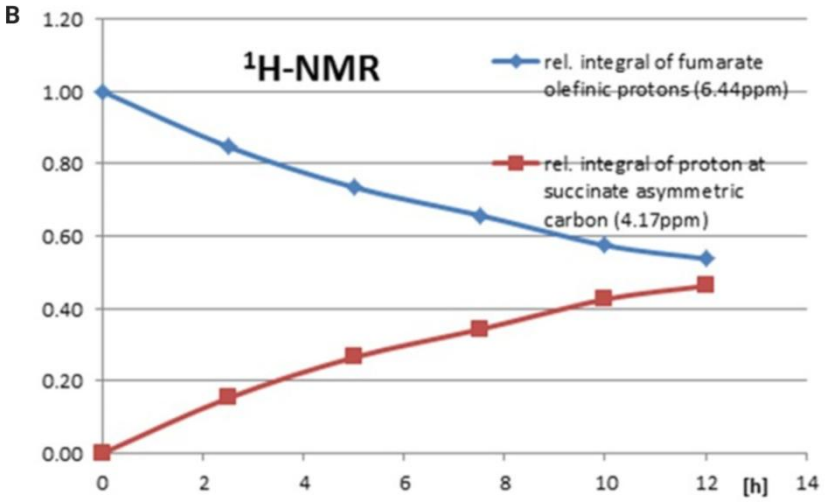

Figure 45:A: NMR of the biocatalytic Michael addition reaction of L -arginine to fumarate in D_2O. ^{1}H-NMR signals at 2.75 and 2.43 ppm show a too small integral due to insertion of deuterium from the solvent (D_2O). B Time course of a biocatalytic Michael addition reaction using a solution of 50 µmol fumarate, 100 µmol L-arginine in 1 mL D_2O, adjusted to pH 7.5 with NaOH and 20 µl argininosuccinate lyase (ASL) solution (soluble fraction).

Enzyme activity of roughly 4 U mL^{-1} was calculated for the cell crude extract (soluble fraction) from the fumarate turnover rate during the first 5 hours of the reaction. The time course of the biocatalytic Michael addition reaction could be seen from the increase of the ^{1}H-NMR-signal for the proton at the asymmetric succinate carbon and the decrease in the ^{1}H-NMR-signal for the olefinic protons of fumarate (Figure 45B).

3.5.4 Discussion

For the first time, a simple and straightforward biocatalytic asymmetric Michael addition reaction was established for the synthesis of the key metabolite *N*-(([[(4S)-4-amino-4-carboxybutyl] amino)iminomethyl)-L-aspartic acid due to its lithium salt (L-argininosuccinic acid lithium salt), with 70% yield (based on the isolated pure product) and excellent purity. This one-step addition reaction was developed by running part of the urea cycle in reverse. Moreover, lyases are still unexplored class of enzymes, therefore, the use of the argininosuccinate lyase and reaction monitoring by NMR has enabled the development of a biocatalytic asymmetric Michael addition reaction as a novel green chemistry route with high molecular economy for the synthesis of this important metabolite at gram scale. This not only provides a straightforward one-step route to L-argininosuccinic acid lithium salt without side-products, but also opens excellent future opportunities for utilising biocatalytic asymmetric Michael addition reactions for simple synthetic routes with high molecular economy to complex metabolites by the use of simple building blocks.

4 Summary and conclusions

The definition of Green Chemistry was first formulated at the beginning of the 1990s – 30 years ago and states as follows: "design of chemical products and processes to reduce or eliminate the use and generation of hazardous substances" (Poliakoff et al. 2002). Biocatalysis is one of the examples of "green" chemistry as it is relying on natural or modified enzymes. Today, biocatalysis is a standard technology for the production of chemicals (Straathof et al. 2002).

In this PhD thesis, the implications of biocatalysis using different class of enzymes are discussed: two cytochrome P450 monoxygenases, two kinases and one lyase are shown as tools for the production of bioactive compounds.

The P450 enzymes have a central role in the oxidative metabolism of a wide variety of compounds including the synthesis of endogenous substrates such as steroids and fatty acids. Moreover, P450s catalyze the hydroxylation of non-activated carbon atoms in a regio- and stereospecific fashion avoiding use of protecting groups and several, time-consuming chemical steps.

Here, the recombinant expression and biocatalytic characterization of bacterial CYP107D1 for the regio- and stereoselective hydroxylation of two steroid compounds is reported. Since the natural electron transfer partners of these P450s are unknown, PdX and PdR from *P. putida* were employed to supply CYP107D1 with the necessary electrons for catalysis. This three-component system was used in bioconversions of two bile acids: LCA and DCA. P450 CYP107D1 exhibits high regio- and stereoselectivity for the tested steroids, giving 6β-hydroxylated products. The properties of the CYP107D1 make this multifaceted P450 monooxygenase an attractive enzyme for the production of novel drug metabolites. Moreover, the crystal structure of the enzyme is known, which provides the basis for developing a protein-engineering strategy aimed at catalytic properties of the CYP107D1

The second enzyme described in the thesis is the self-sufficient cytochrome P450 monooxygenase from *Fusarium graminarium* (FG067). From the overall structure, it resembles the well investigated CYP102 from *Bacillus megaterium* (CYP BM3) and the P450 from *Fusarium oxysporum* (CYPfoxy). In this study, two different strategies to recombinantly produce the fungal P450 monooxygenase P450-FG067, namely (a) producing in *E. coli* and (b) producing in *P. pastoris* were investigated. The P450 FG_067 from *Fusarium graminarium* was successfully overexpressed in *P. pastoris*. The enzyme was functionally active, converted fatty acid substrates of carbon chain length C10-16 with regiospecificity of the hydroxylating position ω -1, ω - 2 and ω-3, with the highest affinity for capric acid. The

hydroxylation at different positions of the fatty acid chain is needed for different chemical industries. For example, ω-HFAs can be used as starting materials for the synthesis of polymers, with high resistance to heat or chemicals (Xiao et al. 2018). Therefore, the application of recombinant enzyme such as self-sufficient P450 FG_067 for a commercial production of HFAs is in high industrial demand.

In this thesis, two kinases were used for the producton of phosphorylated metabolites. Kinases catalyzing *N*-phosphorylation, which are of synthetic interest because of tedious chemical procedures in selective chemical *N*-phosphorylations. A highly active and stabile arginine kinase, obtained by cloning and expressing the argK gene from *Limulus polyphemus* in *E. coli*, was used in the one-step synthesis of N_{ω}-phospho-L-arginine using the phosphoenolpyruvate/pyruvate kinase system for ATP regeneration. Applying arginine kinase in biocatalysis opens up new opportunities for the selective biocatalytic *N*-phosphorylation of interesting low-molecular-weight compounds and metabolites.

Another kinase investigated in this thesis was shikimate kinase. The highly active and stable shikimate kinase AroL was achieved by synthesizing the codon-optimized aroL gene and expressing it in high yield in *E. coli*. Next, shikimate kinase was used in an one-step synthesis of shikimate-3-phosphate using the phosphoenolpyruvate/pyruvate kinase system for ATP regeneration. Development of the described biocatalytic preparation of shikimate-3-phosphate is a superior route incomparison to a tedious multi-step and low yield classical synthesis of this compound. The biocatalytic phosphorylation is of great interest for a commercial production of metabolites and metabolite-like structures.

The last investigeted enzyme in this PhD thesis was argininosuccinate lyase from *Saccharomyces cerevisiae*. The argininosuccinate lyase was cloned and overexpressed in *E. coli* as a highly active and stable biocatalyst. A simple and straightforward biocatalytic asymmetric Michael addition reaction has been established for the synthesis of the key metabolite *N*-(([(4S)-4-amino-4-carboxybutyl]amino)imino methyl)-L-aspartic acid, commonly referred to as L-argininosuccinate. This one-step addition reaction was developed by running part of the urea cycle in reverse. The use of this argininosuccinate lyase and reaction monitoring by NMR enabled the development of a biocatalytic asymmetric Michael addition reaction as a novel green chemistry route with high molecular economy for the synthesis of this important metabolite at gram scale.

Recent advances in the field of scientific research have helped to understand the structure and functional activities of enzymes, which has in turn led to an increase in their stability, activity and substrate specificity. Nowadays, biocatalysis provide more sustainable,

efficient, and less polluting methods for the production of fine chemicals and advanced pharmaceutical intermediates. The biocatalysts used in this thesis are introduced as a technology for the efficient synthesis of biologically active compounds, which is greener, reduces pollution and costs compared to chemical synthesis. In summary, the pharmaceutical industry should use the advantage of the progress of biochemistry to obtain biocatalysts in the production of fine chemicals on an industrial scale, improving the quality of end products and saving costs.

5 Materials

5.1 Chemicals and consumables

Unless stated differently, all chemicals and consumables were purchased from the commercial suppliers ABCR (Karlsruhe), Fischer Scientific (Schwerte), Greiner (Solingen), Roth GmbH (Karlsruhe), Sarstedt (Nümbrecht), Sigma-Aldrich (Taufkirchen), StarLab (Ahrensburg) and VWR (Darmstadt) and used without further purification.

5.2 Enzymes

Table 5: List of used enzymes

Enzyme	**Supplier**
SacI	New England BioLabs® Inc. (Ipswich, USA)
BamHI	New England BioLabs® Inc. (Ipswich, USA)
HindIII	New England BioLabs® Inc. (Ipswich, USA)
OptiTaq	Roboklon (Berlin, Germany)
Taq	Roboklon (Berlin, Germany)
Lyticase from *Arthrobacter luteus*	Sigma-Aldrich (Steinheim, Germany)

5.3 Oligonucleotides

All used oligonucleotides were synthesized by Thermo Fisher Scientific (Waltham, USA).

Table 6: List of primer used for sequencing

Primer	**Sequence (from 5' to 3')**	**Purpose**
5´ AOX1	GACTGGTTCCAATTGACAAGC	Sequencing recombinant *P. pastoris* clones
3´ AOX1	GCAAATGGCATTCTGACATCC	

Table 7: List of primer used for subcloning (fw – forward, rev – reverse).

Primer	**Sequence (from 5' to 3')**	**Purpose**
E15_FW	CGCGGATCCATGGCTGAGAG TGTCCCTATC	Primers used for the cloning approach to construct the pET24a_P450_FG067 plasmid
E16_RV	CCCAAGCTTGTCAAAAACGTC AGTGGCAA	

5.4 Strains

For recombinant expression of proteins, *E. coli* and *P. pastoris* strains of different species were used (Table 10).

Table 8: Strains

Species	Strain	Genotype	Supplier
Escherichia coli	DH5α	supE44 _lacU169(F80lacZ_M15) hsdR17 recA1 endA1 gyrA96 thi-1 relA1	Clontech
Escherichia coli -	BL21 (DE3)	F⁻ompT gal dcm lon hsdSB(rB-mB-) λ(DE3 [lacI lacUV5-T7 gene 1 ind1 sam7 nin5])	Novagen
Escherichia coli	TOP10	F⁻mcrA Δ(mrr-hsdRMS-mcrBC) Φ80dlacZΔM15 ΔlacX74 nupG recA1 araD139 Δ(ara-leu)7697 galE15 galK16 rpsL(StrR) endA1 fhuA2 λ-	Invitrogen
Escherichia coli	NEB 5-alpha	F⁻φ80dlacZΔM15 Δ(lacZYA-argF) U169 end A1 recA1 hsdR17 (rk^-, mk^+)supE44λ- thi-1gyrA96relA1 phoA	New England Biolabs
Escherichia coli	C41(DE3)	F –ompT hsdSB (rB- mB-) gal dcm(DE3)	Lucigen
Pichia pastoris	BG10	wild type	atum.bio
Pichia pastoris	BG11	BG11, aox1Δ (MutS)	atum.bio

5.5 Genes and plasmids

5.5.1 Monooxygenase P450 (Olep) and putidaredoxin reductase (CamA) and putidaredoxin (CamB)

E. coli C43(DE3) (Lucigen) was used for expressions. Plasmid pACYCcamAB for coexpression of putidaredoxin reductase (CamA) and putidaredoxin (CamB) from *Pseudomonas putida* were kindly provided by Anett Schallmey (Braunschweig University of Technology Department of Bioinformatics and Biochemistry). For gene synthesis of CYP107D1 (OleP), the nucleotide sequence of CYP107D1(OleP) was derived from the amino acid sequence published by Rodriguez (Rodriguez et al. 1995). This gene (GenBank: Q59819) was purchased from GenScript and already cloned into the final expression vector (pET28a (+) CYP107D1- Figure 46).

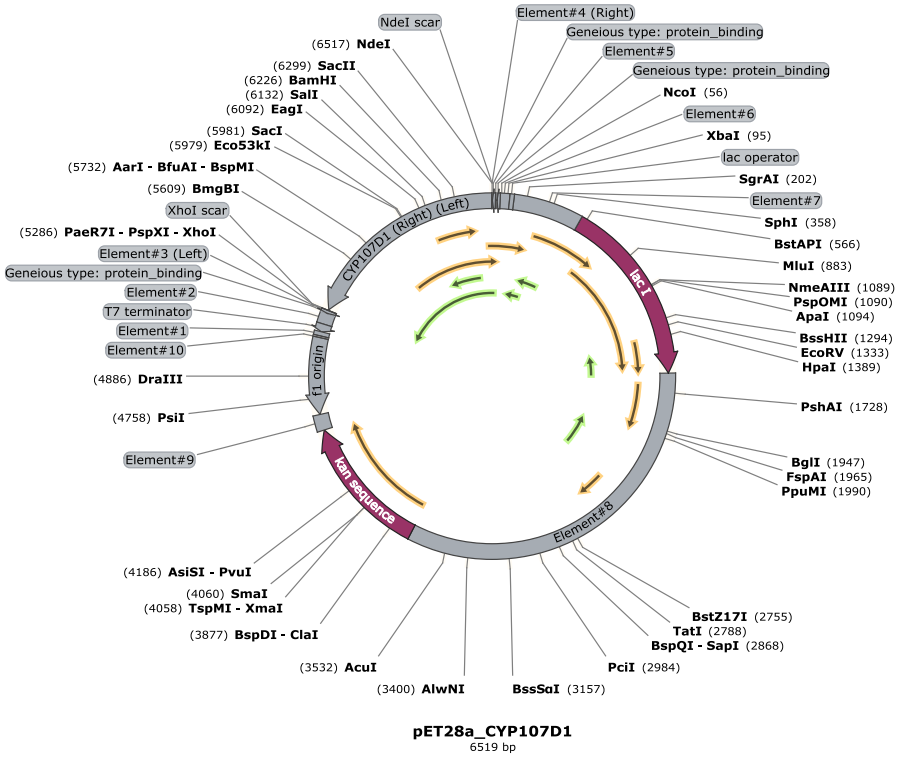

Figure 46: Vector card of pET28_CYP107D1

5.5.2 Monooxygenase P450_FG067

The putative cytochrome P450 gene sequence of *Fusarium graminarium* was obtained from the Fungal Cytochrome P450 Database. One of the synthetic genes was codon-optimised for *E. coli* and equipped with a C-terminal 6x-his-tag. The gene was synthesised and subcloned into pET24a(+) via NotI and XhoI by Genscript XhoI (USA), giving vector pET24a(+) _P450-FG067 (Figure 47). The second synthetic gene was codon-optimised for *P. pastoris* and equipped with a C-terminal 6x-His-tag. The gene was synthesised and subcloned into pPICZ A via EcoRI and NotI by Genscript (USA), giving vector pPICZ(A)_P450-FG067(Figure 48).

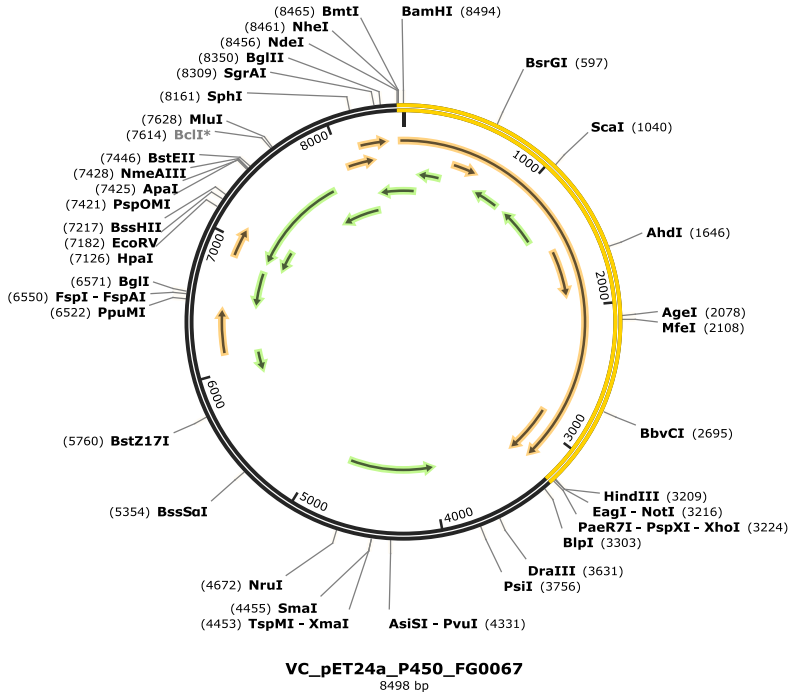

Figure 47: Vector card of pET24a_FG67

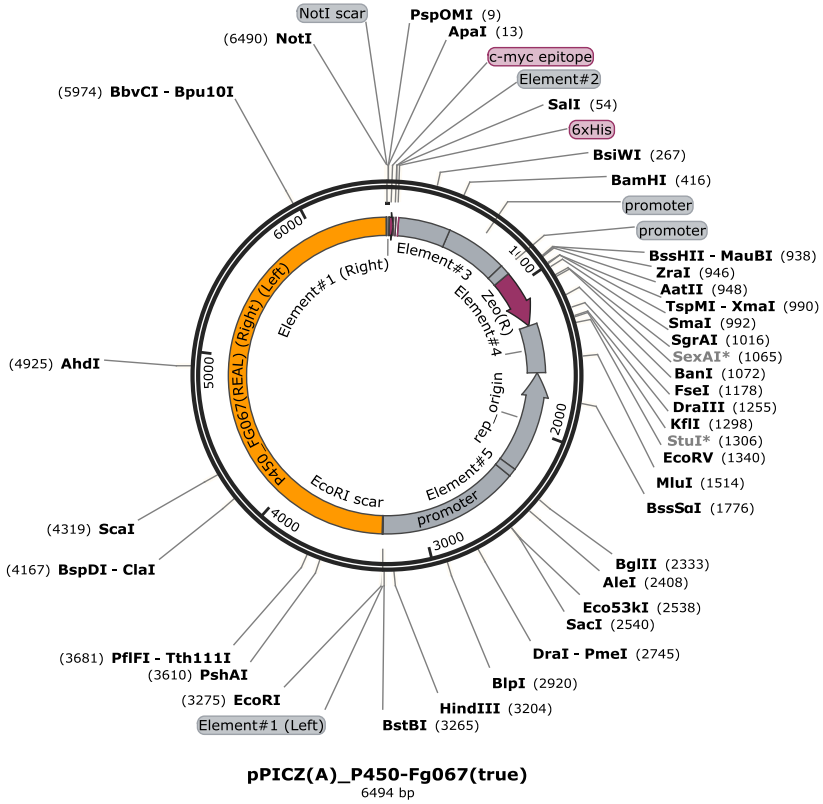

Figure 48: Vector card of pPICZ(A)_P450_FG067

5.5.3 Arginine kinase

The arginine kinase gene ArgK was derived from *Limulus polyphemus* (ArgK-LP;UniProtKB:P51541) as described by Strong and Ellington (Strong and Ellington 1995). The synthetic gene was codon-optimized for *E. coli* and equipped with an N-terminal 6-His-tag and aTEV (tobacco etch virus) protease cleavage site for optional removal of the affinity tag. The gene was synthesised and subcloned into pET24a(+)via NdeI and NotI by Genscript (USA), giving vector pET24His(TV)-Karg-LimPo(op) (Figure 49).

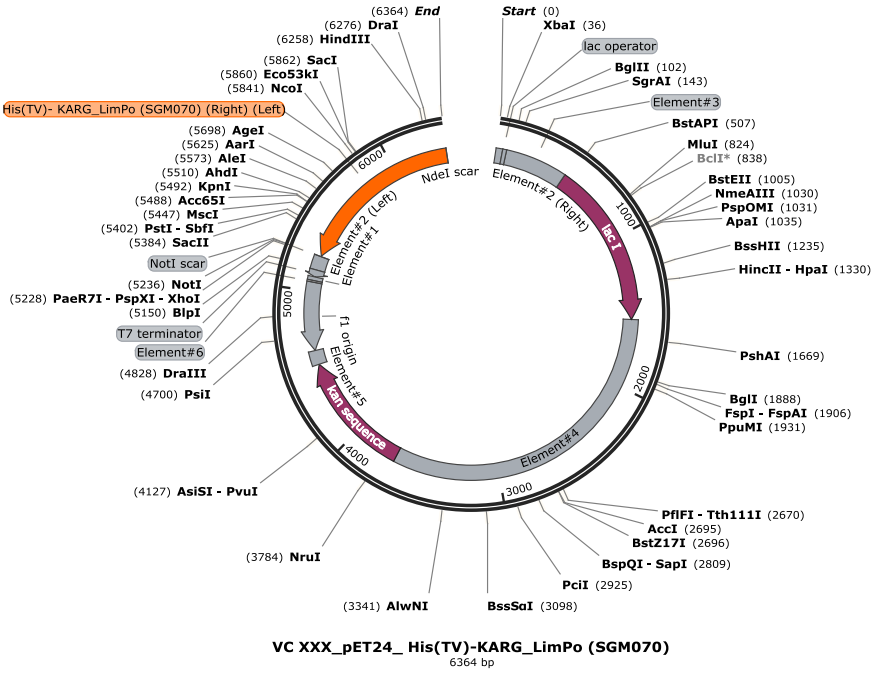

Figure 49: Vector card of pET24His(TV)-Karg-LimPo(op)

5.5.4 Shikimate kinase

The shikimate kinase gene aroL was derived from *E. coli* K12 (UniProtKB: P0A6E1) as described by Millar et al. (Millar et al. 1986). The synthetic gene was codon-optimised for *E. coli* and equipped with an N-terminal 6-His-tag and a TEV protease cleavage site for optional removal of the affinity tag. The gene was synthesised and subcloned into pET24a(+) via NdeI and NotI by Genscript (USA), giving vector pET24-His(TV)-AroL-*E.coli*(op) (Figure 50).

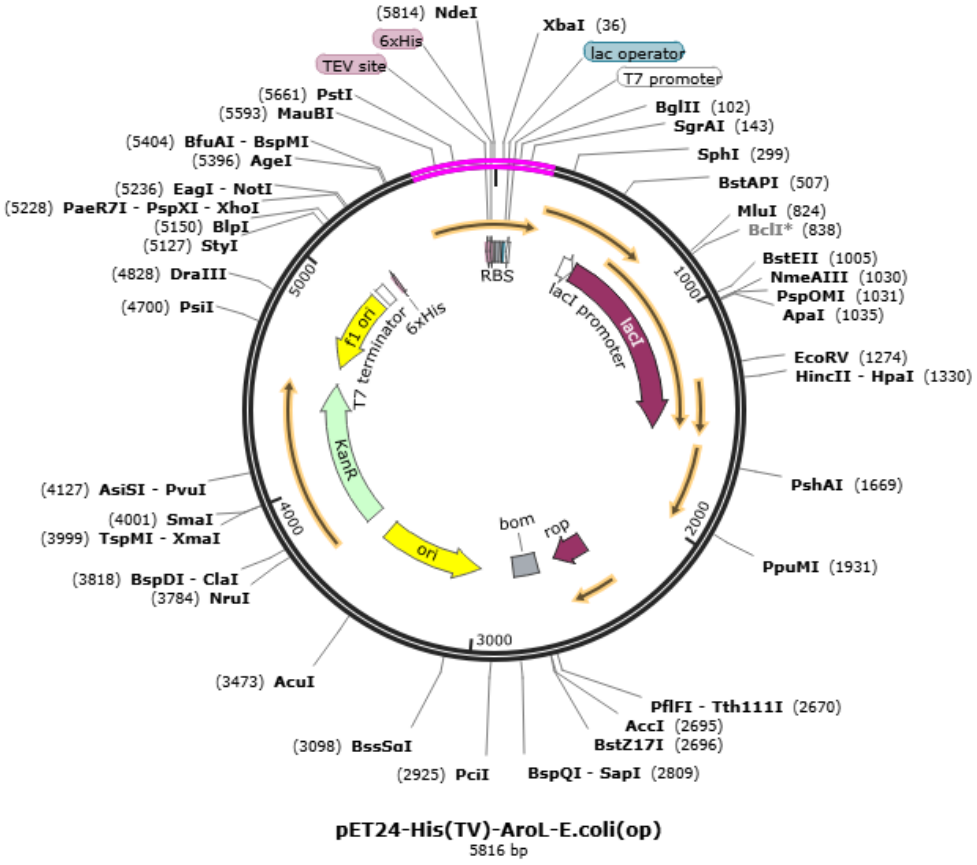

Figure 50: Vector card of pET24-His(TV)-AroL-*E.coli*

5.5.5 Argininosuccinate lyase

The argininosuccinate lyase gene Arg4 was derived from *Saccharomyces cerevisiae* (strain ATCC 204508 / S288c) (UniProtKB: P04076) as described by Beacham and coworkers. The synthetic gene was codon-optimised for *E. coli* and equipped with an N-terminal 6x-His-tag and a cleavage site TEV protease for optional removal of the affinity tag. The gene was synthesised and subcloned into pET24a(+) via NdeI and NotI by Genscript (USA), giving vector pET24-His(TV)-Arg4-Ecoli(op)(Figure 51).

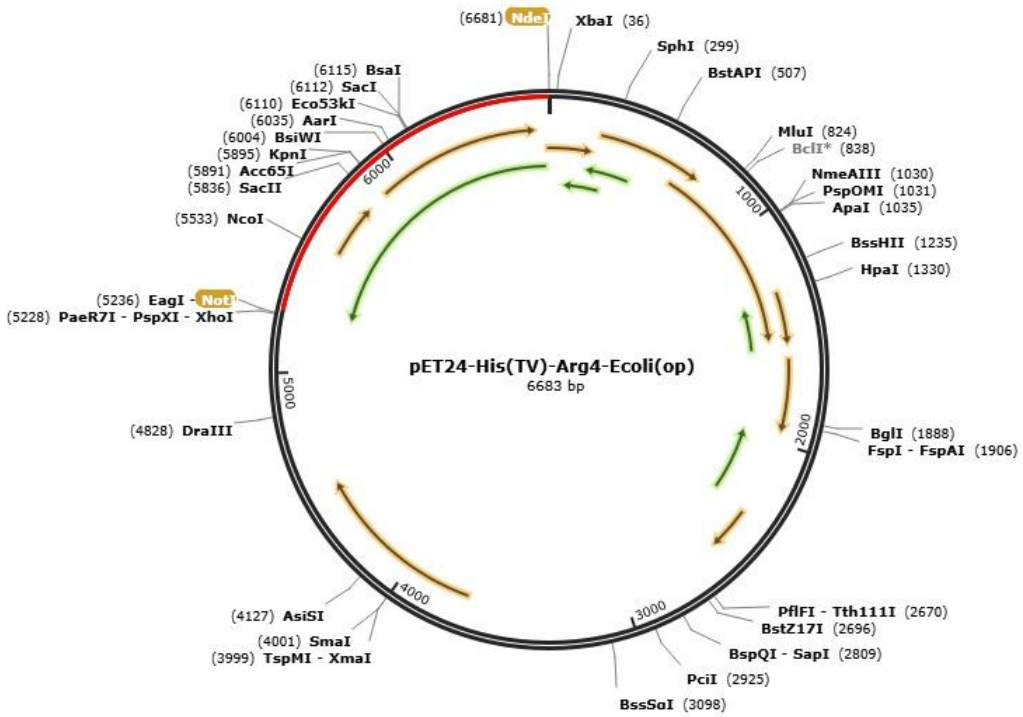

Figure 51: Vector card of pET24-His(TV)-Arg4-Ecoli(op)

5.6 Media, additives and inducers

Table 9: Media recipes used for liquid cultures.

Medium, buffer or solution	Components and preparation
Lysogeny Broth medium/LB medium	1% (w/v) NaCl 1% (w/v) tryptone 0.5% (w/v) yeast extract Filled with dest. water and sterilized in autoclave at 121°C for 21 min
LB-SOC medium	Addition of 10% (v/v) of 10 x SOC solution to sterile LB medium
10X SOC solution	0.2% (w/v) KCl 2.0% (w/v) $MgCl_2$ 2.0% (w/v) $MgSO_4$ 4.0% (w/v) glucose
Terrific Broth medium/TB medium	12% Casein, enzymatically digested 24% Yeast extract 12.54 g L^{-1} K_2HPO_4 2.31 g L^{-1} KH_2PO_4
YPD-Medium	1% (w/v) Yeast extract 2% (w/v) Peptone Filled with dest. water and sterilized in autoclave at 121°C for 21 min. 10% (v/v) 10x D solution added
10x D Solution	20% (w/v) Glucose, sterile filtered
YPDS-Medium	1% (w/v) Yeast extract 2% (w/v) Peptone 1 M Sorbitol sterilized in autoclave at 121°C for 21 min 10% (v/v) 10x D Solution added
BMGY-Medium	1% (w/v) Yeast extract 2% (w/v) Peptone 1% (v/v) Glycerine sterilized in autoclave at 121°C for 21 min 10% (v/v) Phosphate Buffer (1 M, pH 6.0), sterile filtered 0,2% (v/v) 500x B-Solution added
500x B-Solution	0,02% (w/v) Biotin, sterile filtered

BMMY-Medium	1% (w/v) Yeast extract 2% (w/v) Pepton sterilized in autoclave at 121°C for 21 min 10% (v/v) Phosphate Buffer (1 M, pH 6,0), sterile filtered 0,2% (v/v) 500x B-Solution 0,5% (v/v) Methanol added

In order to create agar plates, the above mentioned liquid media recipes were used and 15% (w/v) agar-agar was added to the solution before autoclaving. When agar plates with antibiotics were prepared, the corresponding antibiotic was added to the adequate concentration after the LB-agar solution had cooled down to 40°C.

Table 10: Recipes for concentrated used antibiotic and inductor stock solutions.

Antibiotic/inductor/Additives	**Components and preparation**
Ampicillin (Amp)	Standard solution: 100 mg mL^{-1} in water, sterile filtered
Kanamycin (Kan)	Standard solution: 50 mg mL^{-1} in water, sterile filtered
Chloramphenicol	Standard solution: 50mg mL^{-1} in 95% EtOH, sterile filtered
Zeocin (Zeo)	Standard solution: 100 mg mL^{-1} in H_2O , sterile filtered
IPTG	Standard solution: 0.1 M in water, sterile filtered
δ-Ala	Standard solution: 0.1 M in water, sterile filtered
Methanol	100%

5.7 Buffers and solutions

5.7.1 General buffers

Table 11: Genereal buffers and solution recipes

Buffer / solution	**Components and preparation**
50 mM sodium phosphate buffer pH 7.5	14,99 g/l NaH_2PO_4 x 12 H_2O 1,13 g/l Na_2HPO_4 x 7 H_2O
100 mM Phosphate buffer pH 6.0	13.2 mL 1M K_2HPO_4 86,8 mL 1 M KH_2PO_4 The combined 1 M stock solutions are diluted to 1000 mL with dest. water and pH is adjusted to 7.4 if necessary. The buffer was sterilized if needed. Phosphate buffer of lower strength was prepared to dilute this concentration with dest. water and adjusting the pH
100 mM Phosphate buffer pH 7.4	80.2 mL 1M K_2HPO_4 19,8 mL 1 M KH_2PO_4 The combined 1 M stock solutions are diluted to 1000 mL with dest. water and pH is adjusted to 7.4 if necessary. The buffer was sterilized if needed. Phosphate buffer of lower strength was prepared to dilute this concentration with dest. water and adjusting the pH

5.7.2 Chemical Competent *E. coli* cells

Table 12: Buffers and solution recipes needed for the preparation of chemical competent *E. coli* cells

Buffer /solution	**Components and preparation**
Buffer RF1	100 mM RbCl 50 mM $MnCl_2$ 30 mM CH_3COOK 10 mM $CaCl_2$ 15% (v/v) glycerol pH is adjusted to 5.8 with 0.2 M acetic acid, and the solution is sterilised by filtration (0.2μm diameter).
Buffer RF2	10mM RbCl 75 mM $CaCl_2$ 10 mM 3-(N-morpholino) propane sulfonic acid 15% (v/v) glycerol The pH is adjusted to 6.8-7.0, and the solution is sterilized by filtration (0.2 μm diameter).

5.7.3 Electrocompetent *P. pastoris* cells

Table 13: Buffers and solution recipes needed for the preparation of electrocompetent *P. pastoris* cells.

Buffer / solution	**Components and preparation**
Sorbitol solution	1M Sorbitol in water, filter sterile 2M Sorbitol in water, filter sterile

5.7.4 Agarose gel electrophorese

Table 14: Buffers and solution recipes needed for agarose gel electrophorese.

Buffer / solution	**Components and preparation**
Agarose gel solution	1 g agarose in 100 mL 1x TAE buffer, dissolved by heating in microwave oven, per 50 mL gel 3 µL RotiStain (Carl Roth, Karlsruhe) were added for visualization under UV light
Agarose gel loading Buffer	30% (v/v) Glycerol 25 mM EDTA 0,25% (w/v) Bromophenol
TAE-buffer (1x)	40 mM Tris 20 mM Acetic acid 2 mM EDTA (pH adjusted to 8.3)

5.7.5 Protein purification

Table 15: Buffers used for purification with IMAC using hand columns

Buffer	**Components and preparation**
Equilibration/Wash buffer	50 mM sodium phosphate buffer pH 7.5 500 mM NaCl
Elution buffer	50 mM sodium phosphate buffer pH 7.5500 mM NaCl 300 mM Imidazole
Column cleaning and storage solution	20% ethanol

Table 16: Buffers used for purification with IMAC using AKTA

Buffer	**Components and preparation**
Equilibration/Wash buffer	50 mM sodium phosphate buffer pH 7.5 500 mM NaCl 30 mM Imidazole
Elution buffer	50 mM sodium phosphate buffer pH 7.5 500 mM NaCl 500 mM Imidazole
Column cleaning and storage solution	20% ethanol

5.7.6 SDS-PAGE

Table 17: Buffers and solution recipes needed for SDS-PAGE.

Buffer	Components and preparation
4 x Upper Tris	0.5 M Tris-HCl pH 6.8 0.4% (w/v) SDS
4 x Lower Tris	1.5 M Tris-HCl pH 8.0 0.4% (w/v) SDS
Acrylamide solution	30% (w/v) acrylamide-, bisacrylamide solution (37.5:1)
APS solution	10% (w/v) ammonium persulfate solution in dest. Water
Coomassie blue -staining solution	0.1% (w/v) Coomassie Brilliant Blue G250 30% (v/v) ethanol 10% (v/v) acetic acid Filled with dest. water
Coomassie blue- destaining solution	30% (v/v) methanol 10% (v/v) acetic acid Filled with dest. Water
10 x SDS-Running buffer	30.3 g Tris 144 g glycerol 10 g SDS Filled with dest. water, pH adjusted to 8.4
SDS- Sample buffer	20% (w/v) glycerol 6% (w/v) 2-mercaptoethanol 0.0025% (w/v) bromophenol blue Filled with 1 x Upper Tris
Resolving gel	2 mL 4 x Lower Tris 3.33 mL acrylamide solution 2.67 mL dest. water 40 µL APS 4µL TEMED
Stacking gel	1 mL 4 x Upper Tris 520 µL acrylamide solution 2.47 mL dest. water 40 µL APS 4 µL TEMED

5.7.7 Western blot

Table 18: Buffers and solution recipes needed for western blot.

Buffer	Components and preparation
Laemmli 2X buffer/loading buffer	4% SDS 10% 2-mercaptoethanol 20% glycerol 0.004% bromophenol blue 0.125 M Tris-HCl pH and adjusted to 6.8
Running buffer	25 mM Tris base 190 mM glycine 0.1% SDS pH and adjusted to 8.3
Transfer buffer (wet)	25 mM Tris base 190 mM glycine 20% methanol pH and adjusted to 8.3
Blocking buffer	1x TBST 5% BSA (bovine serum albumin)
1X TBST	20 mM Tris base 150 mM NaCl 0.1% Tween 20
Substrat buffer for alkaline phosphatase	5mM $MgCl_2$ 100mM Tris-HCl, pH 9.5 100 mM NaCl
BCIP	20mg mL^{-1} 5-bromo-4-chloro-3-indolyl phosphate in 100% DMF
NBT	50mg mL^{-1} p-nitroblue tetrazolium chloride in 70% DMF

5.7.8 Protein quantification

Table 19: Buffers and solutions used for the protein quantification

Buffer	Components and preparation
BCA Protein Assay Kit	PierceTM
BSA stock solution	10mg mL^{-1} bovine serum albumin

5.7.9 Activity assays

Table 20: Buffers and solutions used for the activity assays.

Buffer	Components and preparation
Arginine kinase assay	100 mM Tris-HCl buffer pH 7.5 1mM phosphoenolpyruvate 5mM $MgCl_2$ 50mM KCl 0.15 mM NADH 4U of pyruvate kinase 8U of lactate dehydrogenase 2.5 mm ATP 10 mM L-arginine enzyme solution
Shikimate kinase assay	100 mM Tris–HCl buffer pH 7.5 1 mM phosphoenolpyruvate 5 mM $MgCl_2$ 50 mM KCl 0.15 mM NADH 4U of pyruvate kinase 8U of lactate dehydrogenase 2.5 mM ATP 1.6 mM of Shikimic acid enzyme solution
Argininosuccinate lyase assay	50 mM KPP buffer pH 7.5 1 mM of potassium Argininesuccinate enzyme solution

5.7.10 TLC Visualization Reagents

Table 21.: Reagents used for TLC detection

Solution	Components and preparation
Cer-reagent	2.5% (w/v) $H_3[P(Mo_3O_{10})^4]$ x H_2O 1% (w/v) Cer(SO4)2 8% (v/v) conc. H_2SO_4 Filled with dest. water and filtered
Vanilin-reagent	0.5g vanillin in 100ml sulfuric acid/ethanol (40:10).
Running solution	DCM/Acetone/Acetic acid 60/15/1

5.8 Equipment

Table 22: Used equipment.

Equipment	Name	Producer
Agarose electrophoresis	Mini-Sub Cell	Bio-Rad (Munich, Germany)
	GT Compact XS/S	Biometra GmbH (Göttingen, Germany)
Balances	PCB350-3 PCB2500-2	Kern & Sohn GmbH (Belingen, Germany
	Explorer E14130	Ohaus (Parsippany, USA)
	MC1 Analytic AC 120S	Sartorius (Göttingen, Germany)
Centrifuges Biofuge	Biofuge pico	Thermo Fisher Scientific (Waltham, USA)
	Biofuge 400R	Thermo Fisher Scientific (Waltham, USA)
	Multifuge 3S-R	Thermo Fisher Scientific (Waltham, USA)
	Fresco 17	Thermo Fisher Scientific (Waltham, USA)
	Sprout-Minizentrifuge	Biozym Scientific (Oldendorf, Germany)
Cell lysis	Sonoplus HD/UW 2070	Bandelin (Berlin, Germany)

	Equipped with: Ultrasonic horn MS72 Ultrasonic horn KE76	
	Hielscher sonicator UP200St. Equipped with: Glass beads (Ø 0.25-0.5 µm)	Hielscher (Berlin, Germany)
Cleanbench	HeraSafe KS15	Thermo Fisher Scientific (Waltham, USA)
FPLC	ÄKTApurifier	GE Healthcare (Buckinghamshire, United Kingdom)
Gas chromatography	GC-2010(plus) incl. AOC-20i-s	Shimadzu (Duisburg, Germany)
	GCMS-QP2010	Shimadzu (Duisburg, Germany)
Heating-/stirring plate	RCT basic	IKA Labortechnik (Staufen, Germany
Homogenization	FastPrep-24	MP Biomedicals, Inc. (Eschwege, Germany)
HPLC	LaChrom L7100 Equipped with L7100 pump, L7420 UV-Detector, L7200	Merck Hitachi (Darmstadt, Germany)
	Autosampler, D7000 Interface	Merck Hitachi (Darmstadt, Germany)
Incubation	Incucell	MMM Medcenter Einrichtungen GmbH(Gräfelfing, Germany)
	Multitron Standard	Infors AG (Bottmingen, Switzerland)
	Minitron	Infors AG (Bottmingen, Switzerland) pH
Lyophilisator	Alpha 1-2,	Christ GmbH (Osterode am Harz)
pH-meter	PH211	Hanna Instruments (Vöhringen, Germany)
Photometer	Jasco V-550 with PSC-498T Temperature controller	Jasco Analytical Instruments (Easton USA)
	NanoDropTM 1000 UV	Peqlab (Erlangen, Germany)
	Mini-1240	Shimadzu (Duisburg, Germany)
Power supply for electrophoresis	EPS EV231 Standard Power Pack 25	Consort (Turnhout, Belgium) Biometra (Göttingen, Germany)
Protein electrophoresis	Minigel-Twin	Biometra (Göttingen, Germany)
Sterilization	V-120 autoclave	Systec (Bergheim-Glessen,

		Germany)
	Laboklav ECO	SHP Steriltechnik AG (Detzel, Germany)
	Dry-Line oven	VWR International (Darmstadt, Germany)
TLC	Färbekasten nach Hellendahl (85x35x95 mm)	Roth(Karlsruhe,Germany)
Thermocycler	Thermocycler	Analytic Jena (Jena, Germany)
Thermoshaker	Thermomixer comfort	Eppendorf (Hamburg, Germany)
UV table	Benchtop UV Transiluminator	UVP (Upland, USA)
Vortex	Vortex Genie 2	Scientific Industries (Bohemia, USA)
96-well plate reader	Infinite® M200PRO	Tecan Trading AG (Männedorf, Switzerland)

6 Methods

6.1 Microbiological methods

6.1.1 Strain maintenance

Transformants and strains were kept on agar plates (LB for *E. coli* and YPD for *P. pastoris*) and stored at 4°C. For more extended storage at 4°C, fresh plates were prepared every 6–8 weeks. For long-term storage, glycerol stocks were made for each strain/transformant. Here, 1 mL overnight culture was mixed 1:1 with a 60% glycerol solution. The vials with the mixture were stored at -80°C.

6.1.2 Overnight cultures

For the preparation of overnight cultures, 5 of medium containing an appropriate selection of marker(s) (LB for *E. coli* and YPD for *P. pastoris*) were inoculated with single colonies picked from agar plates. These cultures of *E.coli* and *P. pastoris* were grown overnight at 37°C, 200 rpm and 30°C, 250 rpm respectively for 24 hours.

6.1.3 Preparation of competent cells

6.1.3.1 Preparation of chemically competent *E. coli* cells

Rubidium chloride method was used for the preparation of chemically competent *E. coli* cells. LB medium (100 mL) was inoculated with an overnight culture and incubated at 37°C and 200 rpm until the culture reached OD_{600}=0.3-0.4. Afterwards, the cells were harvested, chilled on ice for 15 min, and centrifuged at 4°C for 25 min at 4000 x g. The pellet created in the process was then resuspended in 20 mL ice-cold RF1 buffer, incubated at 4°C for 15 min and centrifugated at 4°C for 25 min at 4000 x g. The pellet was resuspended again, but this time in 4 mL RF2 buffer, incubated at 4°C for 15 min and distributed in 50 µL aliquots. These aliquots were immediately frozen in liquid nitrogen and stored at -80°C.

6.1.3.2 Preparation of electrocompetent *P. pastoris* cells

YPD medium (5 mL) was inoculated with a single colony of *Pichia pastoris* strain and grown overnight at 30°C in an incubator with shaking (200 rpm). YPD medium (500 mL) was inoculated with 0.5 mL of overnight culture and grown overnight at 30°C and 200 rpm to an OD600=1.3-1.5. Cells were then harvested and centrifuged at 1500x g for 5 minutes at 4°C. Pellet was resuspended with 500 mL of ice-cold (0°C), sterile water. The cells were

centrifuged again at 1500x g for 5 minutes at 4°C; then the pellet was resuspended with 250 mL of ice-cold (0°C), sterile water. Cells were centrifuged for the third time at 1500x g for 5 minutes at 4°C, and the pellet was resuspended with 20 mL of ice-cold (0°C), 1M sorbitol. Afterwards, the cells were centrifuged at 1500x g for 5 minutes at 4°C, and the pellet was resuspended in 1 mL of ice-cold (0°C), 2M sorbitol for a final volume of approximately 1.5 mL and distributed in 100 µL aliquots. These aliquots were immediately frozen in liquid nitrogen and stored at -80°C.

6.1.4 Transformation

6.1.4.1 Transformation of chemically competent *E. coli* cells

To a 50 µL aliquot of *E. coli* cells, 1-10 µL of DNA solution was added, and the mixture was incubated for 30 min on ice. The cells were permeabilised by heat shock (30 sec at 42°C) and chilled on ice for 5-10 min. Next, 300 µL of LB-SOC medium was added to the cells and incubated for 1-3 hours at 37°C with 200rpm shaking. Different volumes of the culture were plated on agar, supplemented with an adequate antibiotic and incubated overnight at 37°C.

6.1.4.2 Transformation of electrocompetent *P. pastoris* cells

To a 100 µL aliquot of *P. pastoris* cells, 10µL of DNA (5-10µg) solution with low salt concentration was added. The mixture was gently mixed and immediately transferred to an ice-cold electroporation cuvette and incubated on ice for 5 minutes. Electroporation was performed for 5 ms at 1500 mV in a MicroPulser (BioRad). Right after the electronic impulse, 1 mL of ice-cold 1M sorbitol was added to the cells. The cells were transferred to a 15 mL sterile tube and incubated for 2 hours without shaking at 30°C. 1 mL of YPD medium was added to the cells and incubated for 3 hours at 30°C and 200 rpm. Afterwards, 200 µL of the culture were platted on YPDS agar, supplemented with the zeocin (25 µg mL^{-1}) and incubated for three days at 30°C until colonies appeared.

6.2 Cultivation and Protein Expression

6.2.1 Arginine kinase

Selected *E. coli* transformants were used for expression tests, in which different media, induction times and temperatures were optimised. The selected conditions were later used for the overexpression of ArgK in *E. coli* BL21 (DE3). For overexpression arginine kinase, 50 mL of Terrific Broth (TB) medium supplemented with kanamycin (50 µg mL^{-1}) was

inoculated with 500 µL of the corresponding overnight culture. 50 mL and cultivated at 37ºC and 150 rpm in a 250 mL Erlenmeyer flask with baffles. When the pre-culture reached the mid-log phase, the main culture was started. Hence, 400 mL of fresh TB medium in a 2L Erlenmeyer flask was inoculated with 20 mL of the *E. coli* pre-culture. After the culture reached an OD600 of 1.3 (optical density), protein expression was induced with 1mm of isopropyl-b-d-thiogalactopyranoside (IPTG). The main culture was shaken at 110rpm for 20h at 25ºC. The cells were harvested at 4500g for 30 min at 4°C. If not used directly, the cell pellets were stored at -20°C until further usage.

6.2.2 Shikimate kinase

Selected *E. coli* transformants were used for expression tests, in which different media and temperatures were optimised. The selected conditions were later used for the overexpression of AroL in *E. coli* BL21 (DE3). For overexpression shikimate kinase 50 mL of Terrific Broth (TB) medium supplemented with kanamycin (50 µg mL^{-1}) was inoculated with 500 µL of the corresponding overnight culture and cultivated at 37ºC and 150 rpm in a 250 mL Erlenmeyer flask with baffles. When the pre-culture reached the mid-log phase, the main culture was started. Hence, 400 mL of fresh TB medium in a 2L Erlenmeyer flask was inoculated with 20 mL of the *E. coli* pre-culture. After the culture reached an OD600 of 1.3 (optical density), protein expression was induced with 1mM of isopropyl-β-D-thiogalactopyranoside (IPTG). The main culture was shaken at 110rpm for 20h at 25ºC. The cells were harvested at 4500g for 30 min at 4°C. If not used directly, the cell pellets were stored at -20°C until further usage.

6.2.3 Argininosuccinate lyase

Selected *E. coli* transformants were used for expression tests, in which different media, induction times and temperatures were optimised. The selected conditions were later used for the overexpression of aroL in *E. coli* BL21 (DE3). For overexpression argininosuccinate lyase, 50 mL of Terrific Broth (TB) medium supplemented with kanamycin (50 µg mL^{-1}) was inoculated with 500 µL of the corresponding overnight culture and cultivated at 37ºC and 150 rpm in a 250 mL Erlenmeyer flask with baffles. When the pre-culture reached the mid-log phase, the main culture was started. Hence, 400 mL of fresh TB medium in a 2 L Erlenmeyer flask was inoculated with 20 mL of the *E. coli* pre-culture. After the culture reached an OD600 of 1.3 (optical density), protein expression was induced with 1mM of isopropyl-β-D-thiogalactopyranoside (IPTG). The main culture was shaken at 110rpm for 20h at 25ºC. The cells were harvested at 4500g for 30 min at 4°C. If not used directly, the cell pellets were stored at -20°C until further usage.

6.2.4 Monooxygenase P450_OleP

The pET28a(+) plasmid encoding the gene CYP107D1 was transformed via heat shock into the *E. coli* strain C43 (DE3) and co-transformed with the vector pACYCDuet, which contained the redox partner genes (putidaredoxin (CamA) and putidaredoxin reductase (CamB) from *Pseudomonas putida*). Positive transformants were used for expression tests, where different media, induction time, inducer concentrations and temperature were tested. The selected condition was later used for over-expression of CYP107D1 and redox partner genes. The transformants were grown overnight in 5 mL Lysogeny Broth medium (LB) with 50μg mL^{-1} kanamycin and 34μg mL^{-1} chloramphenicol at 37°C and 180rpm. The following morning 50mL Terrific Broth medium (TB) supplemented with chloramphenicol and kanamycin (35μg mL^{-1} and 50μg mL^{-1}, respectively) was inoculated with 500 μL of an overnight culture as a pre-culture in a 250mL shake flask. At mid-log phase, 400 mL of fresh TB medium in 2 L Erlenmeyer flask was inoculated with 20 mL of an *E. coli* pre-culture. After the absorbance reached an OD=1.3 at 600 nm, protein expression was induced with 1mM of isopropyl-β-D-thiogalactopyranoside (IPTG) and cells were supplemented with 5-aminolevulinic acid (84 μg mL^{-1}) as a precursor for the heme synthesis in *E. coli.* The cultures were shaken at 30°C at 110rpm for 20h and cells were harvested by centrifugation at (13300g for 30min at 4°C). Cells were washed once with ice-cold 50mM potassium phosphate buffer at pH7.4 and cell pellets were frozen at -20°C (Bracco et al. 2013b).

6.2.5 Monooxygenase P450_FG0067

6.2.5.1 Monooxygenase P450_FG0067 *E. coli* expression

The gene encoding P450_FG067 in pET24a(+) plasmid was transformed with heat shock method into the *E. coli* strain C43 (DE3). The transformants were grown overnight in 5 mL Lysogenic Broth medium (LB) with 50μg mL^{-1} kanamycin at 37°C and 180 rpm. The following morning 50 mL of Terrific Broth medium (TB) supplemented with kanamycin (50μg mL^{-1}) was inoculated with 500 μL of an overnight culture as a pre-culture in a 250 mL shake flask. At mid-log phase, 400 mL of fresh TB medium in a 2 L Erlenmeyer flask was inoculated with 20 mL of an *E. coli* pre-culture. After the absorbance reached OD=1.3 at 600 nm, protein expression was induced with 1mM of isopropyl-β-D-thiogalactopyranoside (IPTG) and cells were supplemented with 5-aminolevulinic acid (84 μg mL^{-1}) as a precursor for the heme synthesis in *E. coli.* The cultures were shaken at 30°C, and 110 rpm for 20 h and cells were harvested by centrifugation at 13300 g for 30 min at 4°C. Cells were washed once

with ice-cold 50mM potassium phosphate buffer at pH 7.4 and cell pellets were frozen at –20°C.

6.2.5.2 Monooxygenase P450_FG0067 *P. pastoris* expression

The *Pichia pastoris* strain BG10 was transformed by electroporation. The vector pPICZ(A)_P450-FG067 was linearised with the SacI restriction enzyme, purified via the QIAquick PCR Purification Kit (Qiagen, Germany) and transformed into *P. pastoris* BG10 using an electroporation method from the expression kit manual (Invitrogen). The recombinant strains were selected with the use of Zeocin, and the insertion of the fusion gene into the genomic DNA of the recombinants was confirmed by PCR method described in the expression kit manual (Invitrogen). Recombinant *P. pastoris* BG10 were cultivated in 400 mL. BMGY growth medium containing yeast extract (1%), peptone (2%), Yeast Nitrogen Base (1,34% (w/o AA)), biotin (4µg mL^{-1}) and glycerol (1%) in 100mM Potassium phosphate pH 6.0 was inoculated with single colonies of *P. pastoris* (50 mL). The cells were cultured at 30°C for 24 h. The cells were then collected by centrifugation for 10 min at 3000 g, 4°C and resuspended to an approximate OD_{600} of 2 in 400 mL of BMMY medium supplemented with 0.5 µM hemin chloride and zeocin (100 µg mL^{-1}). Cells were grown at 30°C with 110 rpm shaking and induced for 24 h by adding methanol (0.5%) every 24 h. After 96 h, the cells were harvested by centrifugation at 5000 g for 25 min at 4°C and washed once with an ice-cold 50 mM sodium phosphate buffer at pH 7.5. The *P. pastoris* cell pellets containing the overexpressed enzyme (rec. P450_FG067) were frozen at –20°C.

6.2.6 Cell disruption

For cell disruption of *E. coli* containing overexpressed arginine kinase, shikimate kinase and argininosuccinate lyase, frozen cells were adjusted to an OD600 of 40 in a buffer (50mM TrisHCl, pH7.5 for arginine kinase, shikimate kinase and potassium phosphate buffer 50mM, pH 7.5 for argininosuccinate lyase), mixed with glass beads (Ø 0.25-0.5 µm) at an approximate ratio of 1:1 and 10. The suspension was sonicated at 0°C for 20 min and interval pulsed at alternating cycles (Hielscher sonicator UP200St: 50% power and 50% pulse). Insoluble cell debris was removed by centrifugation at 13300g for 30 min at 4°C. The supernatant, which contained the soluble protein fraction, was immediately used for activity determination. A 50µl samples of whole-cell homogenate, supernatant and a cell pellet were mixed with 2× SDS sample buffer and thermally denaturated for 8 min at 95°C. The supernatant, which contained the soluble protein fraction, was immediately used for activity determination. For cell disruption of *E. coli* containing P450_OleP/putidaredoxin

(CamA)/putidaredoxin reductase (CamB) and P450_FG067, frozen cells were adjusted to an OD_{600} of 40 in potassium phosphate buffer (KPp: 50mM, pH7.4), the suspension was sonicated at 0°C for 20 min and pulsed intervally at alternating cycles (Hielscher sonicator UP200St: 50% power and 50% pulse). Insoluble cell debris was removed by centrifugation at 13300g for 30 min at 4°C. The supernatant, which contained the soluble protein fraction, was immediately used for activity determination.

For *P. pastoris* cell disruption containing P450_FG067, frozen cells were adjusted to an OD_{600} of 40 in potassium phosphate buffer (50 mM, pH7.5), mixed with glass beads (Ø 0.25-0.5 µm) at an approximate ratio of 1:1 and 10 U of lyticase was added. After incubation for 30 min on ice, the cells were disintegrated mechanically by a cell disruptor (Retsch Mixer Mill MM 200) 200) for cycles for 3 min full-speed vortexing followed by 1min cooling on ice. The samples were cooled on ice and insoluble cell debris was removed by centrifugation (13300 g, 30 min, 4°C). A 50µl samples of whole-cell homogenate, supernatant and a cell pellet were mixed with 2× SDS sample buffer and thermally denaturated for 8min at 95°C. The supernatant, which contained the soluble protein fraction, was immediately used for activity determination.

6.3 Molecular biology methods

6.3.1 Plasmid isolation

Plasmids were isolated by the usage of the innuPREP Plasmid Mini Kit (Analytik Jena). All steps were performed as described in the manufacturer's manual. The elution of plasmid DNA was conducted with 50 µL of elution buffer previously warmed up to 95°C and cooled down to 70°C.

6.3.2 PCR methods

6.3.2.1 Subcloning pUC_FG067-pET24FG-067

Table 23: Master Mix

Component	**5 samples [µL]**
10X Reaction Buffer + $MgCl_2$	50
dNTPs	5
FW-E15 primer (10 pmol/µl)	25
RV-E16 primer (10 pmol/µl)	25
MilliQ water	140
Template DNA	10
Phusion DNA Polymerase (0.05 U/µl)	2,5

Table 24: Temperature program used for the subcloning of p450-FG067.

Step	**Temperature**	**Time**	**Cycle**
Initial denaturation	98°C	1 min.	
Denaturation	98°C	10 sec.	30x
Annealing	53°C	30 sec.	
Extension	72°C	1 min 30 sec.	
Final Extension	72°C	10 min.	1x
	4°C	∞	

6.3.3 Colony PCR

In general, colony PCR was applied to identify clones harbouring the freshly introduced plasmid.

6.3.3.1 Verification of the plasmid integration via colony PCR in *P. pastoris*

This reaction was used as a control of the ligation processes to test *P. pastoris* clones for insertion of pPICZα-P450-FG067 by PCR. Briefly, the cells are lysed by a combined enzyme, freezing, and heating treatment. The genomic DNA was used directly as a PCR template. At least 20 colonies were analysed each time.

Table 25: Master Mix *P. pastoris* colony PCR.

Component	5 samples [µL]
10X Reaction Buffer	5
25 mM MgCl2	5
5'AOX1 primer (10 pmol/µl)	1
3'AOX1 primer (10 pmol/µl)	1
MilliQ water	28
Cell lysate	5
Taq polymerase (0.16 U/µl)	5

Table 26: Temperature program fort the colony PCR of *P. pastoris*

Step	Temperature	Time	Cycle
Denaturation	95°C	1 minute	30x
Annealing	54°C	1 minute	
Extension	72°C	1 minute	
Final Extension	72°C	7 minutes	1x

The reaction products were afterwards analysed by electrophoresis using 1% agarose.

6.3.3.2 Digestion of pPICZα-P450-FG067

The construct pPICZα-P450-FG067 was linearized by digestion with Sac I.

DNA was digested overnight at 37°C.

Table 27: Digestion mixture composition

Component	µL
10 x digestion buffer	10
40 µL DNA	40
10 µL Sac I	10
MilliQ water	40

This reaction was used for linearization of DNA to stimulate recombination when the plasmid is transformed into *P. pastoris.*

6.4 Quantification of DNA

6.4.1 Nano drop

Determination of DNA concentrations was achieved by the usage of UV-Vis photometer NanoDrop. The device measures absorbance at a wavelength of λ=260 nm. Additionally, other important wavelengths are measured to assure the purity of the DNA sample.

6.5 Agarose gel electrophoresis

For separation of DNA fragments or plasmids by size, agarose gel electrophoresis was applied. The agarose gel was prepared with TAE buffer, which was heated until boiling in the microwave oven to solve the appropriate amount of agarose. 5 µL of Roti-GelStain (Carl Roth) were added per 100 mL agarose solution for later visualisation of DNA. The gel was casted and left for cooling. Samples were prepared by mixing with 6x loading dye (1:6). After applying 6 µL of each sample and 5 µL DNA ladder (1kbp DNA ladder, Carl Roth), the gel was run at 110 V for 25 min. The final result was investigated after illumination on a UV table.

6.6 Biochemical methods

6.6.1 Protein purification

6.6.1.1 Hand columns

In general, approximately the same protocol was used for all proteins if hand columns were used for purification (arginine kinase, shikimate kinase, ASL). When the cell pellet was stored at -20°C, then it was thawed slowly on ice and washed two times with equilibration buffer. After cell lysis in equilibration buffer, by sonication, the crude cell lysate was separated by centrifugation at 10000g for 1h at 4°C. After filtering the supernatant with a 0.45 μm filter, the His-tagged enzyme was purified on a Ni-NTA hand column (Roti®garose-His/Ni Beads, Carl Roth GmbH & Co. KG, Germany). First, the column was washed and preequilibrated with five column volumes (5 CV) of equilibration buffer, followed by loading of the filtered supernatant. Secondly, after washing the column with 2 CV of wash buffer, the protein was eluted. The elution was obtained with 2 CV of elution buffer. Finally, the eluted protein sample was desalted and stored in storage buffer or used immediately.

6.6.1.2 ÄKTApurifier

To purify the recombinant P450 Monooxygenase OleP and P450 Monooxygenase FG0067 by IMAC (immobilised metal ion chromatography) with FPLC ÄKTA-purifier. In this research 1mL HiTrap IMAC HP prepacked columns with sepharose matrix functionalized with chelating groups charged with Ni^{2+} was used. The system was equilibrated with sodium phosphate buffer (pH 7.4) and supplemented with 500 mM NaCl. To prevent non-specific binding of protein, 30mM imidazole was included both in-sample and in binding buffer. In the purification procedure performed in native conditions. After equilibrating the whole system with the used buffer, the column was washed with 5 CV equilibration buffer. Afterwards, the protein was loaded onto the column and elution was accomplished by a linear gradient over 5 CV changing gradually from the equilibration buffer to the elution buffer. All the chromatographic steps were carried out at 1 mL min^{-1} flow rate.

6.6.1.3 Desalting

All obtained elution fractions from protein purification were desalted using PD-10 columns (GE Healthcare, Freiburg, Germany). Desalting was performed as suggested by the manufacturer. The buffer used for elution from the column was different for all proteins. In most cases, the storage buffer was used.

6.6.2 Protein quantification

6.6.2.1 BCA assay

Protein concentrations of samples was determined using the PierceTM BCA Assay Kit (Thermo Fisher Scientific, Waltham, USA). The assay performed according to the manufacturer's instructions for the 96-well plate format. After incubation for at least, 30 min at 37°C, the absorbance of all samples at λ=562nm was determined. BSA standard solutions were always prepared fresh with the same buffer that the samples contained.was

6.6.3 SDS-PAGE

According to general procedure, stacking and resolving gel were made and poured into the gel form. Soluble and insoluble fractions were always analysed separately. Soluble fraction: 10 µL samples were mixed with 5 µL loading buffer and heated at 95°C for 10 min. Insoluble fraction: The pellet was resuspended with 500 µL of 0.1% Triton X-100 solution and incubated at 37°C for 10 min. It was washed twice with 500 µL of 50 mM sodium phosphate buffer (pH 7.4) and resuspended in 20 µL loading buffer. This mixture was heated at 95°C for 10 min. The gels ran at 200 V until the bromophenol blue band reached the front of the gel. The protein bands were visualised by Coomassie Brilliant Blue staining. Standards for protein size were present in all gels.

6.6.4 Coomassie staining

For visualisation of the protein bands, SDS gels were stained by incubation in staining solution overnight (Coomassie staining). The next day the background of the gels was destained with destaining solution, which was exchanged at least twice. The gels were incubated in the destaining solution until clear protein bands, and only a little or no background colour could be observed.

6.6.5 Heme Staining

To facilitate in-gel detection of free or P450 associated heme, the method of Thomas et al. was utilized (Thomas et al. 1976). Briefly, 9% resolving gels were preelectrophoresed at 10°C overnight at low voltage to remove excess ammonium persulfate. Samples were boiled for 5 min in buffer containing 7% SDS prior to loading. The use of DTT or other thiol-containing agents was explicitly avoided due to their propensity to react with heme and potentially interfere with the heme peroxidase activity necessary for staining. Electrophoresis was carried out in fresh buffer over the course of 2-3 h at 10ºC. To stain gels for heme detection, a 1.5 mg mL^{-1} solution of TMBZ was freshly prepared in methanol. After the TMBZ dissolved fully, 3

parts of the resulting solution were mixed with 7 parts of 250 mM sodium acetate buffer (pH 5.0). Gels were immersed in this mixture for 1-2 h in the dark before the addition of hydrogen peroxide to a final concentration of 30 mM. Over the next 30 min, light blue bands emerged, indicating the presence of heme. Photographs were taken immediately after the gels were developed as the staining intensity eventually diminishes due to light sensitivity. Shortterm storage of stained gels could be achieved in 1:2:17 glacial acetic acid/2-propanol/water. Staining of gels for protein content was carried out with Coomassie R250 dye using standard procedures. Protein samples for Coomassie gels were treated identically to those for TMBZ staining so that results from the different staining techniques could be compared directly.

6.6.6 Western blot

Proteins were transferred from the respective SDS gel to nitrocellulose membranes by the wet blotting procedure. Therefore, for every gel to be blotted, two stacks of three blotting papers, cut to approximate gel size, were soaked in the blotting buffer. A nitrocellulose membrane was cut to the gel size and soaked in the blotting buffer for a short time. At the same time, the SDS gel had been incubated in blotting buffer before it was transferred onto one blotting paper stack in a wet blotting chamber. The equilibrated nitrocellulose membrane and the second blotting paper stack were piled on top, and potential air bubbles were removed by applying pressure gently onto the stack from the middle towards the border. Electroblotting was performed by administering 100 mA/blotted gel at 120V and 50W for 1h, thus pulling the negatively charged proteins from the SDS gel onto the nitrocellulose membrane towards the positively charged electrode of the blotting chamber. In order to prevent unspecific antibody binding during the following incubation steps, membranes were blocked in a blocking solution. The incubation was carried out under gentle agitation for 30 min at RT. For specific labelling of a given protein, the respective primary antibody (Anti-His6) was diluted (1:10000) in a washing solution. Samples were then incubated at RT for 1h or at 4°C overnight on a rocker. After that, membranes were washed three times for 10 minutes in a washing solution to eliminate unbound antibody residues and subsequently incubated with the anti-mouse AP, a secondary antibody diluted 1:10000 in a washing solution. After incubation at RT for 1h blots were again rinsed several times in a washing solution for residual antibody removal. The secondary antibodies were visualised for alkaline phosphatase. Alkaline Tris-buffer containing BCIP/NBT was used, and the colour reaction was stopped with ddH2O.

6.7 Activity determination

6.7.1 Arginine kinase Assay

This assay, for the quantification of arginine kinase in liquid medium, is based on the transformation of arginine and ATP into phospho-arginine and ADP by the enzyme. ADP is measured by two coupling reactions involving pyruvate kinase (EC 2.7.1.40) and lactate dehydrogenase (EC 1.1.1.27) with measurement of NADH consumption at 340 nm for 60 seconds. The amount of reagents required for the assay of arginine kinase is summarized in Table 28.

Table 28: Reagents for enzymatic assay of arginine kinase. A reaction cocktail was prepared by pipetting the following reagents into a suitable containers:

Components	Final concentration	Reagents
Tris-HCl pH 7,5	100mM	A
KCl	50mM	
$MgCl_2$	5mM	
ATP	250mM	B
PEP	100mM	
NADH	10mM	
LDH	82U mL^{-1}	C
Pyruvat-Kinase	40U mL^{-1}	
L-Arginine	1M	D

The reaction cocktail was prepared by pipetting (in µliters) reagents (Tab. 28) into a suitable cuvettes (Tab. 29).

Table 29: Procedure for enzymatic assay of arginine kinase

The reaction cocktail was prepared by pipetting (in µlliters) the following reagents into a suitable cuvettes.

Components	Reagents	µl
Tris-HCl pH 7,5 KCl $MgCl_2$	A	740
ATP PEP NADH	B	100
LDH Pyruvat-Kinase	C	100
L-Arginine	D	10
Arginine kinase	E	50

* blank: denaturized enzyme by heating at 95°C for 10 minutes

Decrease of absorbance at 340 nm is monitored for 60 sec. Arginine kinase activity can be calculated as:

$$\text{Activity}\left(\frac{\text{U}}{\text{mL}}\right) = \frac{\left(\Delta\text{A}\frac{340\text{nm}}{\text{min}}\text{Test} - \Delta\text{A}\frac{340\text{nm}}{\text{min}}\text{ blank}\right) * \text{df}}{\varepsilon * 0{,}05}$$

df = Dilution factor
ε =6.22- Millimolar extinction coefficient of ß-NADH at 340 nm
0.05 = Volume (in milliliter) of enzyme used

6.7.2 Shikimate kinase Assay

The enzymatic activity of Shikimate kinase was evaluated by using a double coupled assay involving pyruvate kinase (EC 2.7.1.40) and lactate dehydrogenase (EC 1.1.1.27). During the assay, the ADP generated by Shikimate kinase led to the oxidation of NADH to NAD+. All assays were conducted by measuring the decrease in absorbance at 340 nm. The amount of reagents required for the assay of shikimate kinase is summarised in Table 30.

Table 30: Reagents for enzymatic assay of shikimete kinase. A reaction cocktail was prepared by pipetting the following reagents into a suitable containers:

Components	Final concentration	Reagents
Tris-HCl pH 7,5	100mM	A
KCl	50mM	
$MgCl_2$	5mM	
ATP	2,5mM	B
PEP	1mM	
NADH	0,1- 0,15mM	
LDH	8U	C
Pyruvat-Kinase	4U	
Shikimic acid	1,6mM	D

Table 31: Procedure for enzymatic assay of shikimate kinase.

The reaction cocktail was prepared by pipetting (in µlliters) the following reagents into a suitable cuvettes.

Components	Reagents	µl
Tris-HCl pH 7,5 KCl MgCl2	A	740
ATP PEP NADH	B	100
LDH Pyruvat-Kinase	C	100
Shikimic acid	D	10
Shikimate kinase	E	50

* blank: denaturized enzyme by heating at 95°C for 10 minutes

$$\text{Activity}\left(\frac{\text{U}}{\text{mL}}\right) = \frac{\left(\Delta\text{A}\frac{340\text{nm}}{\text{min}}\text{Test} - \Delta\text{A}\frac{340\text{nm}}{\text{min}}\text{ blank}\right) * \text{df}}{\varepsilon * 0{,}05}$$

df = Dilution factor
ε =6.22- Millimolar extinction coefficient of ß-NADH at 340 nm
0.05 = Volume (in milliliter) of enzyme used

6.7.3 Argininosuccinate lyase Assay

The enzymatic activity of argininosuccinate lyase was assayed at room temperature by recording at 240nm formation of fumarate during the reaction. The amount of reagents required for the assay in the cuvette is summarised in Table 13.

Table 32: Procedure for enzymatic assay of argininosuccinate lyase. The reaction cocktail was prepared by pipetting (in µlliters) the following reagents into a suitable cuvette.

Components	Reagents	µl
50mM Potassium Phosphate Buffer	50mM final concentration	950
Argininosuccinate	10mM standard concentration	100
ASL	enzyme solution	50

Increase of absorbance at 240 nm is monitored for 60 sec. Argininosuccinate lyase activity can be calculated as:

$$\text{Activity}\left(\frac{\text{U}}{\text{mL}}\right) = \frac{\left(\Delta\text{A}\frac{240\text{nm}}{\text{min}}\text{Test} - \Delta\text{A}\frac{240\text{nm}}{\text{min}}\text{ blank}\right) * \text{df}}{\varepsilon * 0{,}05}$$

df = Dilution factor
ε = 2.42- Millimolar extinction coefficient of fumarate at 240 nm
0.05 = Volume (in milliliter) of enzyme used

6.7.4 Determination of P450 concentration

The finally obtained P450 concentration was determined using the CO assay as described by Guengerich et al. 2009 (Guengerich et al. 2009). Samples from fermentation and biotransformations were stored in the form of frozen cell pellet until the analysis. The final P450 concentration was obtained and then determined using the CO assay as described by Omura et al. 1964. The 2 mL sample was mixed with 2µM safranin T as a redox indicator, followed by the addition of one spatula tip of sodium dithionite. By inverting the tube slowly, the solution was mixed, and 1 mL each was transferred in a new cuvette. Approximately one bubble min-1 CO-gas is applied for 1 min in one cuvette. A different sample is measured as blank. Then, a spectrum is recorded between λ=400 nm and λ=500 nm. With this difference spectrum, the concentration of cytochrome P450 enzymes can be determined (Table. 14). With this difference spectrum, the concentration of cytochrome P450 enzymes can be determined (Equation 2).

$$\boldsymbol{C = \frac{A450nm - A490nm}{1cm * 91mM^{-1}cm^{-1}}}$$

Equation 2: Equation for calculating the concentration of correctly folded Cytochrome P450 enzyme, from values determined by the recorded difference spectrum.

Table 33: Settings used for the recording of CO difference spectra using the Jasco device.

Parameter	Setting
Wavelength	500 - 400 nm
Photometric mode	Abs
Response	medium
UV/Vis bandwidth	0.2 nm
Scan speed	200 nm/min
Delta interval	1nm
Scan mode	Continuous
Number of cycles	1
Vertical scale	Auto 1 - 0

6.7.5 Cytochrome c and DCPIP assay

Cytochrome c reductase activity of the fractions was assayed by using cytochrome c reductase (NADPH) assay kit (Sigma Aldrich). The reaction was initiated by addition of NADPH, and the reduction of cytochrome c is monitored by the increase of absorbance at 550 nm for 7 min with the kinetic program. With DCPIP, assays were performed in 20 mM Tris-HCl buffer 7.4 at 25°C in the presence of 70 μM DCPIP. Reduction of the DCPIP colour indicator (an artificial one electron acceptor) was quantified by rates of decrease in absorbance at 600 nm over 10 min (Gray et al. 2010).

6.8 Biocatalysis

6.8.1 Whole-cell biocatalysis with the OleP

With *E. coli* C43 (DE3) cells harbouring the pET-28a-oleP and pACYC-*pdR/pdX* coding the CYP107D1 and reductase/ferredoxin system PdR/PdX, whole-cell biocatalysis according to Glazyrina et al. was performed (Glazyrina et al. 2010). Cells were resuspended in resting cell medium (200mM KH_2PO_4/K_2HPO_4, 20mM NaCl, 1% (*w/v*) glucose, 0.4% (*w/v*) glycerol, pH 7.4) and adjusted to a cell dry weight of 6.6 $g \cdot L^{-1}$. The substrate was added to a final concentration of 2$mg \cdot mL^{-1}$ from a 100$mg \cdot mL^{-1}$ stock solution in DMSO. Reactions were incubated at 28°C with shaking at 160rpm. Samples (1mL) were taken over a period of 24 h and centrifuged (13300*g*, 5min) to remove cells. The supernatants were used for quantification of bile acids.

6.8.2 Whole-cell biocatalysis with the P450_FG67

One gram of *P. pastoris* cell pellet was suspended in 10 mL potassium phosphate buffer (50 mM, pH 7.4). Preparative-scale bioconversions were carried out in 2 mL potassium phosphate buffer (50 mM, pH 7.4) using resting whole cells of *P. pastoris* strain BG10, with the addition of 10 % of glycerol and 0.5 M NaCl. Co-factors like NADPH are recruited for the CYP dependent reaction by addition of glycerol to the reaction mix. NADPH-regeneration is ensured by the activity of metabolic enzymes (Bracco et al. 2013b; Brixius-Anderko et al. 2015). The substrate was added to a final concentration of 1$mg \cdot mL^{-1}$ from a 10 $mg \cdot mL^{-1}$ stock solution in DMSO. Reactions were incubated at 30°C with shaking at 850rpm. Control reactions were carried out in parallel with wild type of *P. pastoris* strain. Samples for TLC analysis were taken after 24 h, extracted twice with 1 mL of ethyl acetate. The organic phase was taken for TLC analysis using Polygram Sil G/UV 254 plates (stationary phase), *Cer* (2 g cerium sulfate in 200 mL H_2O, 5g Molybdatophosphoric acid and 16mL concentrated H_2SO_4) for staining and a mixture of cyclohexane, ethyl acetate, acetic acid (7:3:0.1, v/v/v) as mobile phase.

6.8.3 In vitro biocatalysis with arginine kinase

Biocatalysis with the arginine kinase enzyme was in general performed in 30 mL water containing 1000 mg of L-arginine, adjusted to pH 8.0 with 0.1 M acetic acid (55mL) and the pH again adjusted to 8.0. As to the L-arginine, which was adjusted to pH 8.0, $MgCl_2$ (345 mg Magnesium chloride), ATP(158 mg ATP (0.05 equivalents)) and PEP (1124 mg PEP (0.95 equivalents)) were added. The pH increased to 8.6 and had to be readjusted to pH 8.0 before

adding the kinases. Then pyruvate kinase (200 U) and arginine kinase solution (200 mL) were added, and the reaction mixture was again adjusted to pH 8 by addition of a small amount of 0.1 M acetic acid with stirring. The reaction progress was monitored by ^{31}P-NMR; the reaction mixture was concentrated after two days and dried.

6.8.4 *In vitro* biocatalysis with shikimate kinase

Biocatalysis with the shikimate kinase was performed in 900mL scale. To a solution of 4.6 g (26.4 mmol) shikimic acid in 90 mL H_2O 3.4 g KCl, 1.9 g $MgCl_2$-hydrate, 4.9 g phosphoenolpyruvate (PEP) and 0.47 g ATP were added and the resulting solution was then adjusted to pH 7 with 1 M NaOH. To this mixture, 900 units of pyruvate kinase and 900 mL of the soluble protein fraction of recombinant shikimate kinase AroL were added. After 18 h of stirring at room temperature, NMR analysis of a sample of the reaction mixture showed complete consumption of PEP.

6.8.5 *In vitro* biocatalysis with argininosuccinate lyase

Biocatalysis with the argininosuccinate lyase was performed in 100 mL of H_2O containing a mixture of 5 mmol L-arginine and fumaric acid.The pH was adjusted to 7.5 with 1 M LiOH. 500 µL of the soluble fraction of the *E. coli* purified cell extract were added to this solution, overexpressing recombinant argininosuccinate lyase (Arg4). The solution was stirred at room temperature and the progress of the reaction was monitored periodically by ^{1}H-NMR and TLC.

6.9 Analytics

6.9.1 OleP

Samples (1mL) were extracted twice with 1mL of ethyl acetate. The combined organic phases were dried over anhydrous Na_2SO_4. After complete evaporation of ethyl acetate, the residue was dissolved in 200µL of ethanol. Samples (20 µL) were then analyzed using a Hitachi LaChrom Elite® HPLC System (Hitachi High-Technologies, Krefeld, Germany) with a Luna® Omega 5 µm/100Å PS C18 column (Phenomenex, Aschaffenburg, Germany). The mobile phase was acetonitrile:water (50:50)% (v/v) containing 0.1% of trifluoroacetic acid. An isocratic method ($1mL \cdot min^{-1}$) was employed at room temperature. The bile acids were detected using a LaChrom Elite L-2490 RI Detector (Hitachi High-Technologies, Krefeld, Germany). NMR spectra were recorded with a Bruker Avance III HD 600 spectrometer equipped with an inverse $^{1}H/^{13}C/^{15}N/^{31}P$ quadruple resonance cryoprobe head and z-field gradient (Bruker BioSpin GmbH, Rheinstetten, Germany). Products were dissolved in deuterated methanol and the identification was based on 2D-NMR techniques. The quantification of the observed products was done by HLC-RI using the by NMR-spectroscopy confirmed off white powder resulting from the preparative scale biotransformations of MDCA as well as commercially available LCA. Different concentration ranging from 4 $mg \cdot mL^{-1}$ to 0.1 $mg \cdot mL^{-1}$ of MCA and LCA were prepared and measured by HPLC-RI. The resulting equation was used to calculate the amount of produced MCA over time. The internal standard was used to evaluate the quality of the extraction process. The results of the standard series are displayed in appendix Figure A 5, Figure A 6, Figure A 7.

6.9.2 P450-FG067

Biotransformation reaction mixtures were extracted twice with ethyl acetate. The organic phase was dried under vacuum. Samples were derivatized for GC-MS measurement as follows. Part of the crude product was redissolved in 450 µl of MeOH and 10 ul BF3*Et2O was added to form the methyl ester. The mixture was heated at 60°C for 45 min. Then MeOH was evaporated, 500 µl of $CHCl_3$ and 200 µl of water were added. The phases were mixed thoroughly; the chloroform phase was separated and evaporated. The residue was redissolved in 300 µl of BSTFA, heated at 80°C for 45 min in order to trimethylsilylate the hydroxy functional groups.

6.9.3 Arginine kinase

345 mg of magnesium chloride, 158 mg of ATP (0.05 equivalents) and 1124 mg of PEP (0.95 equivalents) were added to a solution of 1000 mg of L-arginine in 30 mL of water, adjusted to pH 8.0 with 0.1 M acetic acid (55 mL). The pH was again adjusted to 8.0. As to the L-arginine, which was also adjusted to pH 8.0, $MgCl_2$, ATP and PEP were added, the pH increased to 8.6 and had to be readjusted to pH 8.0 before adding the kinases. Then pyruvate kinase (200 U) and arginine kinase solution (200 mL, see above) were added and the reaction mixture was again adjusted to pH 8 by addition of a small amount of 0.1 M acetic acid with stirring. The reaction progress was monitored by ^{31}P-NMR, and the reaction mixture was concentrated after 2 days and dried.The product was worked up by normal phase (NP) column chromatography on silica gel (methanol/water1:1). The strong acidic ion exchanger Dowex 50 WX8 was loaded with LiOH, then washed again until neutral and the product was subsequently converted to the lithium salt, yielding 410 mg (28%) of N_ω-phospho-L-arginine. Analytical data: Single spot on TLC (silica gel, Rf=0.67 with eluent H_2O/1-Propa-nol/NH_4OH 25% =11:6:3; Rf=0.05 with eluent 1-Propanol/NH_4OH 25%/ H_2O=6:3:1); ^{1}H-NMR (D_2O, 400 MHz): δ = 3.45 (dd, 1H, *J*1,*J*2 ~ 6 Hz), 3.17 (t, 2H, *J* = 6.8 Hz), 1.82 (m, 2H), 1.60 ppm (m, 2H); ^{31}P-NMR (D_2O, 162 MHz, CPD): δ = 3.26 ppm.

6.9.4 Shikimate kinase

To a solution of shikimic acid (4.6 g, 26.4 mmol) in H_2O (90 mL) KCl (3.4 g), $MgCl_2$-hydrate (1.9 g), phosphoenolpyruvate (PEP) (4.9 g), and ATP (0.47 g) were added and the resulting solution then was adjusted to pH 7 with 1 M aqueous NaOH. Pyruvate kinase (900 units) and the soluble protein fraction of recombinant shikimate kinase AroL (900 mL) were added to this mixture. After 18 h stirring at room temperature, NMR analysis of a sample of the reaction mixture showed complete consumption of PEP. The mixture was then adjusted to pH 4 with 1 M aqueous HCl and microfiltrated after 1 h. While stirring a solution of calcium acetate (23 g) in H_2O (100mL) was added to the filtrate. Then acetone (400 mL) was added slowly. After 2 h, the suspension was filtrated, the residue dried at room temperature on high vacuum and taken up in H_2O (200 mL). A cation exchanger (Dowex) in its H^+-form (50 g) was added with stirring to this suspension. After 1/2 h, the resulting thin suspension was passed through a column with 250 g of the same ion exchanger, the eluate partially concentrated on a rotary evaporator and was transformed to the lithium salt by addition of an appropriate amount of 1 M LiOH to adjust to pH 7. It resulted in 3.83 g (53% yield) of a white solid after lyophilization. Analytical data for the final isolated shikimic acid 3-phosphate lithium salt: ^{1}H-NMR (D_2O, 400 MHz, δ): 6.36 (m, 1H, H(2)), ~4.7 (m, 1H, H(3),

covered by HDO signal), 3.95 (m, 1H, H(5)), 3,69 (dd, 1H, H(4)), 2.60 (dd, 1H, H(6)), 2.08 (dd, 1H, H(6')) ^{31}P-NMR (D_2O, 162 MHz, proton decoupled, δ): 4.32; 13C-NMR (D2O, 101 MHz, proton decoupled, 31P coupled, δ):175.4(s), 135.3 (s), 130.6 (d), 71.4(d), 69.2 (d), 67.3 (s), 31.9(s). Purity by TLC (silica gel 60 on glass plates, n-propanol/H_2O/AcOH = 6:3:1), R_f (shikimic acid) 0.85, and R_f (shikimic acid 3-phosphate) 0.72. Purity by HPLC: >97%.

6.9.5 Argininosuccinate Lyase

A mixture of L-arginine (876 mg, 5 mmol) and fumaric acid (89 mg, 5 mmol) in H_2O (100 mL) was adjusted to pH 7.5 with 1 M aqueous LiOH. A soluble fraction of the purified cell extract of *E. coli* overexpressing recombinant argininosuccinate lyase (Arg4) (500 µL) was added to this solution. The solution was stirred at room temperature and the progress of the reaction was monitored periodically by ^{1}H-NMR and TLC (silica plates with n-propanol : H_2O = 2:1 as a solvent and detection by ninhydrin and by exposing to short wave UV-light at 254 nm. After the conversion was ceased (6 days), the mixture was concentrated on a rotary evaporator at high vacuum and room temperature, giving a white solid. This was dissolved in H_2O (5 mL) and then n-propanol (10 mL) was added. The resulting emulsion was flash-chromatographed on silica with n-propanol:H_2O = 2:1. The early fractions contained unreacted fumarate followed by the L-argininosuccinate in later fractions. Fractions containing the product L-argininosuccinate were pooled, filtered, frozen and lyophilised to give 1.07 g (~70%) of the pure product N-(([(4S)-4-amino-4-carboxy-butyl]amino)-iminomethyl)-L-aspartic acid lithium salt (L-argininosuccinic acid lithium salt) in the form of a colorless solid. Analytical data for N-(([(4S)-4-amino-4-carboxy-butyl]amino) imino-methyl)-L-aspartic acid lithium salt (L-Argininosuccinic acid mono-lithium salt)

NMR: δ_H (400 MHz; D_2O) 4.14 (1H, dd, *J*1 3.4, *J*2 9.9, succinyl–CH–NH), 3.65 (1H, dd, *J*1 = *J*2 6.2, arginyl-CαH), 3.17 (2H, t, *J* 6.8, arginyl-CδH2), 2.71 (1H, dd, *J*1 3.4, *J*2 16.1, succinyl-CH), 2.41 (1H, dd, *J*1 9.9, *J*2 16.1, succinyl-CH´), 1.80 (2H, m, arginyl-CbH2), 1.58 (2H, m, arginyl-CgH2); dC (100.6 MHz; D2O) 178.9, 177.1, 174.4 (3 COOH), 155.8 (guanidino-C), 55.1, 54.3 (2 NH2–C–COOH), 40.6 (succinyl-CH2 and arginyl-Cd), 27.6 (arginyl-Cb), 23.9 (arginyl-Cg). H2O content (Karl Fischer titration): 14.1% elemental analysis, found: C, 33.3; H, 6.2; N, 15.5%. Calcu-lated for $C_{10}H_{16}N_4O_6Li_2$. 14.1% H2O: C, 35.2; H, 6.2; N 16.4%; TLC, purity: 95.1% (n-propanol:NH_4OH(25%):H_2O = 6:3:1; ninhydrin; R_f 0.4); qNMR, content: 94.4% (calculated as di-lithium salt including 14.1% H_2O).

6.10 Bioinformatic methods

6.10.1 Used software

Table 34: List of used important software

Software	Purpose	Developer
Chem Draw 12.0	Creation of chemical molecule structures and reaction schemes	Cambridge Soft
Geneious	Construction of primers and virtual cloning, DNA sequence analysis and management	Biomatters, Ltd
Snapgene	Construction of primers and virtual cloning, DNA sequence analysis and management	GSL Biotech LLC
GelAnalyzer Freeware	1D gel electrophoresis image analysis software	GelAnalyzer

7 Literature

A. Schmid, J. S. Dordick, B. Hauer, A. Kiener MWBW (2001) Industrial biocatalysis today and tomorrow. Nature 409:258–269. doi: 10.1016/0300-483x(87)90052-7

Agematu H, Matsumoto N, Fujii Y, et al Hydroxylation of Testosterone by Bacterial Cytochromes P450 Using the Escherichia coli Expression System

Ajouz H, Mukherji D, Shamseddine A (2014) Secondary bile acids: An underrecognized cause of colon cancer. World J Surg Oncol 12:1–5. doi: 10.1186/1477-7819-12-164

Albertolle ME, Peter Guengerich F (2018) The relationships between cytochromes P450 and H 2 O 2 : Production, reaction, and inhibition. J Inorg Biochem 186:228–234. doi: 10.1016/j.jinorgbio.2018.05.014

Andexer JN, Richter M (2015) Emerging enzymes for ATP regeneration in biocatalytic processes. ChemBioChem 16:380–386. doi: 10.1002/cbic.201402550

Anzenbacher P, Anzenbacherová E Cytochromes P450 and metabolism of xenobiotics

Arakawa K, Kodama K, Tatsuno S, et al (2006) Analysis of the loading and hydroxylation steps in lankamycin biosynthesis in Streptomyces rochei. Antimicrob Agents Chemother 50:1946–1952. doi: 10.1128/AAC.00016-06

Araya Z, Wikvall K (1999) 6α-Hydroxylation of taurochenodeoxycholic acid and lithocholic acid by CYP3A4 in human liver microsomes. Biochim Biophys Acta - Mol Cell Biol Lipids 1438:47–54. doi: 10.1016/S1388-1981(99)00031-1

Arnold T, Linke D (2008) The use of detergents to purify membrane proteins. Curr Protoc Protein Sci 1–30. doi: 10.1002/0471140864.ps0408s53

Ascher B, Fellmann J, Monheit G (2016) ATX-101 (deoxycholic acid injection) for reduction of submental fat. Expert Rev Clin Pharmacol 9:1131–1143. doi: 10.1080/17512433.2016.1215911

Atalla SMM, EL Gamal NG, Awad HM, Ali NF (2019) Production of pectin lyase from agricultural wastes by isolated marine Penicillium expansum RSW_SEP1 as dye wool fiber. Heliyon 5:e02302. doi: 10.1016/j.heliyon.2019.e02302

Attwood P V. (2013) Histidine kinases from bacteria to humans. Biochem Soc Trans 41:1023–1028. doi: 10.1042/BST20130019

Baltussen LL, Rosianu F, Ultanir SK (2018) Kinases in synaptic development and neurological diseases. Prog Neuro-Psychopharmacology Biol Psychiatry 84:343–352. doi: 10.1016/j.pnpbp.2017.12.006

Bartlett PA, Mcquaid LA (1984) dY. 7854–7860

Bartsch S, Bornscheuer UT (2010) Mutational analysis of phenylalanine ammonia lyase to improve reactions rates for various substrates. Protein Eng Des Sel 23:929–933. doi: 10.1093/protein/gzq089

Bernhardt R (2006) Cytochromes P450 as versatile biocatalysts. J Biotechnol 124:128–145. doi: 10.1016/j.jbiotec.2006.01.026

Bernhardt R, Urlacher VB (2014) Cytochromes P450 as promising catalysts for biotechnological application: Chances and limitations. Appl Microbiol Biotechnol 98:6185–6203. doi: 10.1007/s00253-014-5767-7

Bernstein H, Bernstein C, Payne CM, et al (2005) Bile acids as carcinogens in human gastrointestinal cancers. Mutat Res - Rev Mutat Res 589:47–65. doi: 10.1016/j.mrrev.2004.08.001

Bhattacharya SS, Yadav JS (2017) Microbial P450 Enzymes in Bioremediation and Drug Discovery: Emerging Potentials and Challenges. Curr Protein Pept Sci 19:. doi: 10.2174/1389203718666161122105750

Boddupalli SS, Pramanik BC, Slaughter CA, et al (1992) Fatty acid monooxygenation by P450BM-3: Product identification and proposed mechanisms for the sequential

hydroxylation reactions. Arch Biochem Biophys 292:20–28. doi: 10.1016/0003-9861(92)90045-X

Booth WT, Schlachter CR, Pote S, et al (2018) Impact of an N-terminal polyhistidine tag on protein thermal stability. ACS Omega 3:760–768. doi: 10.1021/acsomega.7b01598

Bornscheuer UT, Huisman GW, Kazlauskas RJ, et al (2012) Engineering the third wave of biocatalysis. Nature 485:185–194. doi: 10.1038/nature11117

Bortolini O, Medici A, Poli S (1997) Biotransformations on steroid nucleus of bile acids. Steroids 62:564–577. doi: 10.1016/S0039-128X(97)00043-3

Bracco P, Janssen DB, Schallmey A (2013a) Selective steroid oxyfunctionalisation by CYP154C5, a bacterial cytochrome P450. Microb Cell Fact 12:1–11. doi: 10.1186/1475-2859-12-95

Bracco P, Janssen DB, Schallmey A (2013b) Selective steroid oxyfunctionalisation by CYP154C5, a bacterial cytochrome P450. Microb Cell Fact 12:1. doi: 10.1186/1475-2859-12-95

Brixius-Anderko S, Schiffer L, Hannemann F, et al (2015) A CYP21A2 based whole-cell system in Escherichia coli for the biotechnological production of premedrol. Microb Cell Fact 14:1–14. doi: 10.1186/s12934-015-0333-2

Buller R, Hecht K, Mirata AM, Meyer H-P (2017) Context and Challenges for Industrial Biocatalysis

Butler CF, Peet C, Mason AE, et al (2013) Key mutations alter the cytochrome P450 BM3 conformational landscape and remove inherent substrate bias. J Biol Chem 288:25387–25399. doi: 10.1074/jbc.M113.479717

Calderini E, Wessel J, Süss P, et al (2019) Selective Ring-Opening of Di-Substituted Epoxides Catalysed by Halohydrin Dehalogenases. ChemCatChem 11:2099–2106. doi: 10.1002/cctc.201900103

Cánovas M, Torroglosa T, Iborra JL (2005) Permeabilization of Escherichia coli cells in the biotransformation of trimethylammonium compounds into L-carnitine. Enzyme Microb Technol 37:300–308. doi: 10.1016/j.enzmictec.2004.07.023

Cao Y, Zhang X (2013) Production of long-chain hydroxy fatty acids by microbial conversion. Appl Microbiol Biotechnol 97:3323–3331. doi: 10.1007/s00253-013-4815-z

Cereghino JL, Cregg JM (2000) Heterologous protein expression in the methylotrophic yeast Pichia pastoris. FEMS Microbiol Rev 24:45–66. doi: 10.1016/S0168-6445(99)00029-7

Chang TKH, Teixeira J, Gil G, Waxman DJ (1993) The lithocholic acid 6β-hydroxylase cytochrome P-450, CYP 3A10, is an active catalyst of steroid-hormone 6β-hydroxylation. Biochem J 291:429–433. doi: 10.1042/bj2910429

Chanshetti U (2014) GREEN CHEMISTRY : CHALLENGES AND OPPORTUNITIES REVIEW ARTICLE GREEN CHEMISTRY : CHALLENGES AND OPPORTUNITIES IN SUSTAINABLE DEVELOPMENT * Umakant Chanshetti

Chen Y, Li Y, Liu P, et al (2014) Optimized expression in Pichia pastoris eliminates common protein contaminants from subsequent His-tag purification. Biotechnol Lett 36:711–718. doi: 10.1007/s10529-013-1411-3

Choi JM, Han SS, Kim HS (2015) Industrial applications of enzyme biocatalysis: Current status and future aspects. Biotechnol Adv 33:1443–1454. doi: 10.1016/j.biotechadv.2015.02.014

Ciaramella A, Minerdi D, Gilardi G (2017) Catalytically self-sufficient cytochromes P450 for green production of fine chemicals. Rend Lincei 28:169–181. doi: 10.1007/s12210-016-0581-z

Clark JH (1999) Green chemistry: Challenges and opportunities. Green Chem 1:1–8. doi: 10.1039/a807961g

Cohen P (2002) Protein kinases — the major drug target of twenty century? Nat Rev Drug

Discov 1:
Cook DJ, Finnigan JD, Cook K, et al (2016) Cytochromes P450: History, Classes, Catalytic Mechanism, and Industrial Application, 1st edn. Elsevier Inc.
de Souza ROMA, Miranda LSM, Bornscheuer UT (2017) A Retrosynthesis Approach for Biocatalysis in Organic Synthesis. Chem - A Eur J 23:12040–12063. doi: 10.1002/chem.201702235
Delcarte J, Fauconnier ML, Jacques P, et al (2003) Optimisation of expression and immobilized metal ion affinity chromatographic purification of recombinant (His)6-tagged cytochrome P450 hydroperoxide lyase in Escherichia coli. J Chromatogr B Anal Technol Biomed Life Sci 786:229–236. doi: 10.1016/S1570-0232(02)00815-2
Dias MVB, Faím LM, Vasconcelos IB, et al (2007) Effects of the magnesium and chloride ions and shikimate on the structure of shikimate kinase from Mycobacterium tuberculosis. Acta Crystallogr Sect F Struct Biol Cryst Commun 63:1–6. doi: 10.1107/S1744309106046823
Dubey KD, Shaik S (2019) Cytochrome P450 - The Wonderful Nanomachine Revealed through Dynamic Simulations of the Catalytic Cycle. Acc Chem Res 52:389–399. doi: 10.1021/acs.accounts.8b00467
Dumon-Seignovert L, Cariot G, Vuillard L (2004) The toxicity of recombinant proteins in Escherichia coli: A comparison of overexpression in BL21(DE3), C41(DE3), and C43(DE3). Protein Expr Purif 37:203–206. doi: 10.1016/j.pep.2004.04.025
Durairaj P, Malla S, Nadarajan SP, et al (2015) Fungal cytochrome P450 monooxygenases of Fusarium oxysporum for the synthesis of ω-hydroxy fatty acids in engineered Saccharomyces cerevisiae. Microb Cell Fact 14:1–16. doi: 10.1186/s12934-015-0228-2
Durairaj P, Malla S, Nadarajan SP, et al Fungal cytochrome P450 monooxygenases of Fusarium oxysporum for the synthesis of ω-hydroxy fatty acids in engineered Saccharomyces cerevisiae. doi: 10.1186/s12934-015-0228-2
Erdogan H (2019) One small step for cytochrome P450 in its catalytic cycle, one giant leap for enzymology. J Porphyr Phthalocyanines 23:358–366. doi: 10.1142/S1088424619300040
Fry AM, O'Regan L, Sabir SR, Bayliss R (2012) Cell cycle regulation by the NEK family of protein kinases. J Cell Sci 125:4423–4433. doi: 10.1242/jcs.111195
Fujii Y, Kabumoto H, Nishimura K, et al (2009) Purification, characterization, and directed evolution study of a vitamin D3 hydroxylase from Pseudonocardia autotrophica. Biochem Biophys Res Commun 385:170–175. doi: 10.1016/j.bbrc.2009.05.033
Fulco J, Miura Y (1974) System from Bacillus of Fatty Acids meguterium * by a Soluble. J Biol Chem 249:1880–1888
Furuya T, Nishi T, Shibata D, et al (2008) Characterization of Orphan Monooxygenases by Rapid Substrate Screening Using FT-ICR Mass Spectrometry. Chem Biol 15:563–572. doi: 10.1016/j.chembiol.2008.05.013
Galante Y, Formantici C (2005) Enzyme Applications in Detergency and in Manufacturing Industries. Curr Org Chem 7:1399–1422. doi: 10.2174/1385272033486468
Ghisalba, O., Meyer, H. P., & Wohlgemuth R (2010) Industrial biotransformation.
Glazyrina J, Materne EM, Dreher T, et al (2010) High cell density cultivation and recombinant protein production with Escherichia coli in a rocking-motion-type bioreactor. Microb Cell Fact 9:1–11. doi: 10.1186/1475-2859-9-42
Gray JP, Mishin V, Heck DE, et al (2010) Inhibition of NADPH cytochrome P450 reductase by the model sulfur mustard vesicant 2-chloroethyl ethyl sulfide is associated with increased production of reactive oxygen species. Toxicol Appl Pharmacol 247:76–82. doi: 10.1016/j.taap.2010.05.015
Grinkova Y V., Denisov IG, McLean MA, Sligar SG (2013) Oxidase uncoupling in heme

monooxygenases: Human cytochrome P450 CYP3A4 in Nanodiscs. Biochem Biophys Res Commun 430:1223–1227. doi: 10.1016/j.bbrc.2012.12.072

Grobe S, Wszołek A, Brundiek H, et al (2020) Highly selective bile acid hydroxylation by the multifunctional bacterial P450 monooxygenase CYP107D1 (OleP). Biotechnol Lett 4:. doi: 10.1007/s10529-020-02813-4

Gruenke LD, Konopka K, Cadieu M, Waskell L (1995) The stoichiometry of the cytochrome P-450-catalyzed metabolism of methoxyflurane and benzphetamine in the presence and absence of cytochrome b5. J Biol Chem 270:24707–24718. doi: 10.1074/jbc.270.42.24707

Guengerich FP, Martin M V., Sohl CD, Cheng Q (2009) Measurement of cytochrome P450 and NADPH-cytochrome P450 reductase. Nat Protoc 4:1245–1251. doi: 10.1038/nprot.2009.121

Guengerich FP, Munro AW (2013) Unusual cytochrome P450 enzymes and reactions. J Biol Chem 288:17065–17073. doi: 10.1074/jbc.R113.462275

Gupta A, Rao G (2003) A study of oxygen transfer in shake flasks using a non-invasive oxygen sensor. Biotechnol Bioeng 84:351–358. doi: 10.1002/bit.10740

Hammerer L, Winkler CK, Kroutil W (2018) Regioselective Biocatalytic Hydroxylation of Fatty Acids by Cytochrome P450s. Catal Letters 148:787–812. doi: 10.1007/s10562-017-2273-4

Hannemann F, Bichet A, Ewen KM, Bernhardt R (2007) Cytochrome P450 systems-biological variations of electron transport chains. Biochim Biophys Acta - Gen Subj 1770:330–344. doi: 10.1016/j.bbagen.2006.07.017

Hawkes DB, Adams GW, Burlingame AL, et al (2002) Cytochrome P450cin (CYP176A), isolation, expression, and characterization. J Biol Chem 277:27725–27732. doi: 10.1074/jbc.M203382200

Hayashi K, Yasuda K, Sugimoto H, et al (2010) Three-step hydroxylation of vitamin D3 by a genetically engineered CYP105A1: Enzymes and catalysis. FEBS J 277:3999–4009. doi: 10.1111/j.1742-4658.2010.07791.x

Hernández-Martín A, Von Bühler CJ, Tieves F, et al (2014) Whole-cell biotransformation with recombinant cytochrome P450 for the selective oxidation of Grundmannâ€™s ketone. Bioorg Med Chem 22:5586–5592. doi: 10.1016/j.bmc.2014.06.005

Honda Malca S, Scheps D, Kühnel L, et al (2012) Bacterial CYP153A monooxygenases for the synthesis of omega-hydroxylated fatty acids. Chem Commun 48:5115–5117. doi: 10.1039/c2cc18103g

Ide M, Ichinose H, Wariishi H (2012) Molecular identiWcation and functional characterization of cytochrome P450 monooxygenases from the brown-rot basidiomycete Postia placenta. Arch Microbiol 194:243–253. doi: 10.1007/s00203-011-0753-2

Iida T, Momose T, Nambara T, Chang FC (1986) Potential Bile Acid Metabolites. X. Syntheses of Stereoisomeric 3,7-Dihydroxy-5a-cholanic Acids. Chem Pharm Bull 34:1929–1933. doi: 10.1248/cpb.34.1929

Iliuta I, Garnier A, Iliuta MC (2015) Enzymatic Fatty Acid Hydroxylation in a Liquid-Liquid Slug Flow Microreactor. Ind Eng Chem Res 54:7787–7799. doi: 10.1021/acs.iecr.5b01498

Isin EM, Guengerich FP (2008) Substrate binding to cytochromes P450. Anal Bioanal Chem. doi: 10.1007/s00216-008-2244-0

Iyer P V., Ananthanarayan L (2008) Enzyme stability and stabilization-Aqueous and non-aqueous environment. Process Biochem 43:1019–1032. doi: 10.1016/j.procbio.2008.06.004

Jackson CJ, Lamb DC, Marczylo TH, et al (2002) A novel sterol 14α-demethylase/ferredoxin

fusion protein (MCCYP51FX) from Methylococcus capsulatus represents a new class of the cytochrome P450 superfamily. J Biol Chem 277:46959–46965. doi: 10.1074/jbc.M203523200

Jennewein S, Schürmann M, Wolberg M, et al (2006) Directed evolution of an industrial biocatalyst: 2-deoxy-d-ribose 5-phosphate aldolase. Biotechnol J 1:537–548. doi: 10.1002/biot.200600020

Jeong H, Barbe V, Lee CH, et al (2009) Genome Sequences of Escherichia coli B strains REL606 and BL21(DE3). J Mol Biol 394:644–652. doi: 10.1016/j.jmb.2009.09.052

Jung H, Jung K, Kleber HP (1989) Purification and properties of carnitine dehydratase from Escherichia coli - a new enzyme of carnitine metabolization. Biochim Biophys Acta (BBA)/Lipids Lipid Metab 1003:270–276. doi: 10.1016/0005-2760(89)90232-4

Kashyap R, Mishra P (2011) Application of enzymes in textile processing. Text Trends 53:27–29

Kelly SL, Kelly DE, Jackson CJ, et al The Diversity and Importance of Microbial Cytochromes P450

Kim KR, Oh DK (2013) Production of hydroxy fatty acids by microbial fatty acid-hydroxylation enzymes. Elsevier B.V.

Kim SH, Roh KH, Kim KS, et al (2014) Coexpression of multiple genes reconstitutes two pathways of very long-chain polyunsaturated fatty acid biosynthesis in Pichia pastoris. Biotechnol Lett 36:1843–1851. doi: 10.1007/s10529-014-1550-1

Kirschner A, Bornscheuer UT (2008) Directed evolution of a Baeyer-Villiger monooxygenase to enhance enantioselectivity. Appl Microbiol Biotechnol 81:465–472. doi: 10.1007/s00253-008-1646-4

Kitazume T, Takaya N, Nakayama N, Shoun H (2000) Fusarium oxysporum fatty-acid subterminal hydroxylase (CYP505) is a membrane-bound eukaryotic counterpart of Bacillus megaterium cytochrome P450BM3. J Biol Chem 275:39734–39740. doi: 10.1074/jbc.M005617200

Kitazume T, Tanaka A, Takaya N, et al (2002) Kinetic analysis of hydroxylation of saturated fatty acids by recombinant p450foxy produced by an Escherichia coli expression system. Eur J Biochem 269:2075–2082. doi: 10.1046/j.1432-1033.2002.02855.x

Kitazume T, Yamazaki Y, Matsuyama S, et al (2008) Production of hydroxy-fatty acid derivatives from waste oil by Escherichia coli cells producing fungal cytochrome P450foxy. Appl Microbiol Biotechnol 79:981–988. doi: 10.1007/s00253-008-1513-3

Kizawa H, Tomura D, Oda M, et al (1991) Nucleotide sequence of the unique nitrate/nitrite-inducible cytochrome P-450 cDNA from Fusarium oxysporum. J Biol Chem 266:10632–10637

Lamb DC, Waterman MR Unusual properties of the cytochrome P450 superfamily. doi: 10.1098/rstb.2012.0434

Lan Y, Zhang X, Liu Z, et al (2017) Overexpression and characterization of two types of nitrile hydratases from Rhodococcus rhodochrous J1. PLoS One 12:1–14. doi: 10.1371/journal.pone.0179833

Lee EC, Ohk SO, Suh BY, et al (2010) Cloning and expression in Pichia pastoris of a new cytochrome P450 gene from a dandruff-causing Malassezia globosa. Toxicol Res 26:47–52. doi: 10.5487/TR.2010.26.1.047

Lee K (2006) p-Hydroxylation reactions catalyzed by naphthalene dioxygenase. FEMS Microbiol Lett 255:316–320. doi: 10.1111/j.1574-6968.2005.00079.x

Lewis JC, Mantovani SM, Fu Y, et al (2010) Combinatorial alanine substitution enables rapid optimization of cytochrome P450BM3 for selective hydroxylation of large substrates. ChemBioChem 11:2502–2505. doi: 10.1002/cbic.201000565

Li M, Wang X-Y, Bai J-G (2006) Purification and Characterization of Arginine Kinase from

Locust. Protein Pept Lett 13:405–410. doi: 10.2174/092986606775974375
Li QS, Ogawa J, Schmid RD, Shimizu S (2005) Indole hydroxylation by bacterial cytochrome P450 BM-3 and modulation of activity by cumene hydroperoxide. Biosci Biotechnol Biochem 69:293–300. doi: 10.1271/bbb.69.293
Li S, Yang X, Yang S, et al (2012) Technology prospecting on enzymes: Application, marketing and engineering. Comput Struct Biotechnol J 2:e201209017. doi: 10.5936/csbj.201209017
Li T, Apte U (2015) Bile Acid Metabolism and Signaling in Cholestasis, Inflammation, and Cancer, 1st edn. Elsevier Inc.
Li T, Chiang JYL (2014) Bile acid signaling in metabolic disease and drug therapy. Pharmacol Rev 66:948–983. doi: 10.1124/pr.113.008201
Lisowska K, Szemraj J, Rózalska S, Długoński J (2006) The expression of cytochrome P-450 and cytochrome P-450 reductase genes in the simultaneous transformation of corticosteroids and phenanthrene by Cunninghamella elegans. FEMS Microbiol Lett 261:175–180. doi: 10.1111/j.1574-6968.2006.00339.x
Liu H, Chen BS, Ribeiro de Souza FZ, Liu L (2018) A comparative study on asymmetric reduction of ketones using the growing and resting cells of marine-derived fungi. Mar Drugs 16:1–15. doi: 10.3390/md16020062
Lundemo MT, Notonier S, Striedner G, et al (2016) Process limitations of a whole-cell P450 catalyzed reaction using a CYP153A-CPR fusion construct expressed in Escherichia coli. Appl Microbiol Biotechnol 100:1197–1208. doi: 10.1007/s00253-015-6999-x
Lundemo MT, Notonier S, Striedner G, et al (2015) Process limitations of a whole-cell P450 catalyzed reaction using a CYP153A-CPR fusion construct expressed in Escherichia coli. Appl Microbiol Biotechnol. doi: 10.1007/s00253-015-6999-x
Lundemo MT, Woodley JM (2015) Guidelines for development and implementation of biocatalytic P450 processes. Appl Microbiol Biotechnol 99:2465–2483. doi: 10.1007/s00253-015-6403-x
Luthra A, Denisov IG, Sligar SG (2011) Spectroscopic features of cytochrome P450 reaction intermediates. Arch Biochem Biophys 507:26–35. doi: 10.1016/j.abb.2010.12.008
Macauley-Patrick S, Fazenda ML, McNeil B, Harvey LM (2005) Heterologous protein production using the Pichia pastoris expression system. Yeast 22:249–270. doi: 10.1002/yea.1208
Mahdi JG, Kelly DR (2008) Lyases. Biotechnol Second Complet Revis Ed 8–12:41–171. doi: 10.1002/9783527620999.ch2i
Makris TM, Denisov I, Schlichting I, Sligar SG (2005) Activation of molecular oxygen by cytochrome P450. Cytochrome P450 Struct Mech Biochem Third Ed 149–182. doi: 10.1007/0-387-27447-2_5
Martínez AT, Ruiz-Dueñas FJ, Camarero S, et al (2017) Oxidoreductases on their way to industrial biotransformations. Biotechnol Adv 35:815–831. doi: 10.1016/j.biotechadv.2017.06.003
Martinez S, Kuhn ML, Russell JT, et al (2014) Acrylamide production using encapsulated nitrile hydratase from Pseudonocardia thermophila in a sol-gel matrix. J Mol Catal B Enzym 100:19–24. doi: 10.1016/j.molcatb.2013.11.014
Martins M, Silva C, Cavaco-Paulo A (2019) Enzyme stabilization for biotechnological applications. Elsevier Ltd
May SW (1999) Applications of oxidoreductases. Curr Opin Biotechnol 10:370–375. doi: 10.1016/S0958-1669(99)80067-6
May SW, Padgette SR (1983) Oxidoreductase enzymes in biotechnology: Current status and future potential. Bio/Technology 1:677–686. doi: 10.1038/nbt1083-677
Meesapyodsuk D, Chen Y, Ng SH, et al (2015) Metabolic engineering of Pichia pastoris to

produce ricinoleic acid, a hydroxy fatty acid of industrial importance. J Lipid Res 56:2102–2109. doi: 10.1194/jlr.M060954

Meunier B, de Visser SP, Shaik S (2004) Mechanism of oxidation reactions catalyzed by cytochrome P450 enzymes

Milhim M, Putkaradze N, Abdulmughni A, et al (2016) Identification of a new plasmid-encoded cytochrome P450 CYP107DY1 from Bacillus megaterium with a catalytic activity towards mevastatin. J Biotechnol 240:68–75. doi: 10.1016/j.jbiotec.2016.11.002

Millar G, Lewendon A, Hunter MG, Coggins JR (1986) The cloning and expression of the aroL gene from Escherichia coli K12. Purification and complete amino acid sequence of shikimate kinase II, the aroL-gene product. Biochem J 237:427–437

Monte MJ, Marin JJG, Antelo A, Vazquez-Tato J (2009) Bile acids: Chemistry, physiology, and pathophysiology. World J Gastroenterol 15:804–816. doi: 10.3748/wjg.15.804

Montemiglio LC, Parisi G, Scaglione A, et al (2015) Functional analysis and crystallographic structure of clotrimazole bound OleP, a cytochrome P450 epoxidase from Streptomyces antibioticus involved in oleandomycin biosynthesis. BBA - Gen Subj. doi: 10.1016/j.bbagen.2015.10.009

Morlock LK, Böttcher D, Bornscheuer UT (2018) Simultaneous detection of NADPH consumption and H 2 O 2 production using the Ampliflu^{TM} Red assay for screening of P450 activities and uncoupling. Appl Microbiol Biotechnol 102:985–994. doi: 10.1007/s00253-017-8636-3

Munro AW, Girvan HM, Mason AE, et al (2013) What makes a P450 tick? Trends Biochem Sci 38:140–150. doi: 10.1016/j.tibs.2012.11.006

Munro AW, Leys DG, Mclean KJ, et al (2002) 2002 Munro P450 bm3 the verz model of a modern flavocytochrome. 27:250–257

Murakami-Murofushi K, Ratner S (1979) Argininosuccinase from bovine brain: Isolation and comparison of catalytic, physical, and chemical properties with the enzymes from liver and kidney. Anal Biochem 95:139–155. doi: 10.1016/0003-2697(79)90197-0

Nakajima T, Sf- TA, Carcinogenesis M, et al (1994) CYP2Cll AND CYP2Bl ARE MAJOR CYTOCHROME P450 AND LUNG MICROSOMES FROM UNTREATED RATS ,. 48:637–642

Nakayama N, Takemae A, Shoun H (1996) Cytochrome P450foxy, a catalytically self-sufficient fatty acid hydroxylase of the fungus Fusarium oxysporum. J Biochem 119:435–440. doi: 10.1093/oxfordjournals.jbchem.a021260

Nebert DW, Russell DW (2002) Clinical importance of the cytochromes P450. Lancet 360:1155–1162. doi: 10.1016/S0140-6736(02)11203-7

Nolan LC, O'Connor KE (2008) Dioxygenase- and monooxygenase-catalysed synthesis of cis-dihydrodiols, catechols, epoxides and other oxygenated products. Biotechnol Lett 30:1879–1891. doi: 10.1007/s10529-008-9791-5

O'Reilly E, Köhler V, Flitsch SL, Turner NJ (2011) Cytochromes P450 as useful biocatalysts: Addressing the limitations. Chem Commun 47:2490–2501. doi: 10.1039/c0cc03165h

Oliveira JS, Pinto C a, Basso L a, Santos DS (2001) Cloning and overexpression in soluble form of functional shikimate kinase and 5-enolpyruvylshikimate 3-phosphate synthase enzymes from Mycobacterium tuberculosis. Protein Expr Purif 22:430–5. doi: 10.1006/prep.2001.1457

Ostrowski J, Barber MJ, Rueger DC, et al (1989) Characterization of the flavoprotein moieties of NADPH-sulfite reductase from Salmonella typhimurium and Escherichia coli. Physicochemical and catalytic properties, amino acid sequence deduced from DNA sequence of cysJ, and comparison with NADPH-cytochrom. J Biol Chem 264:15796–15808

Palaniappan N, Kim BS, Sekiyama Y, et al (2003) Enhancement and selective production of

phoslactomycin B, a protein phosphatase IIa inhibitor, through identification and engineering of the corresponding biosynthetic gene cluster. J Biol Chem 278:35552–35557. doi: 10.1074/jbc.M305082200

Parajuli N, Basnet DB, Lee HC, et al Genome analyses of Streptomyces peucetius ATCC 27952 for the identification and comparison of cytochrome P450 complement with other Streptomyces. doi: 10.1016/j.abb.2004.03.011

Parisi G, Montemiglio LC, Giuffrè A, et al (2019) Substrate-induced conformational change in cytochrome P450 OleP. FASEB J 33:1787–1800. doi: 10.1096/fj.201800450RR

Park J, Lee S, Choi J, et al (2008) Fungal cytochrome P450 database. BMC Genomics 9:1–11. doi: 10.1186/1471-2164-9-402

Park SY, Yamane K, Adachi SI, et al (2002) Thermophilic cytochrome P450 (CYP119) from Sulfolobus solfataricus: High resolution structure and functional properties. J Inorg Biochem 91:491–501. doi: 10.1016/S0162-0134(02)00446-4

Patel AK, Singhania RR, Pandey A (2016) Novel enzymatic processes applied to the food industry. Curr Opin Food Sci 7:64–72. doi: 10.1016/j.cofs.2015.12.002

Pereira CA (2014) Arginine Kinase: A Potential Pharmacological Target in Trypanosomiasis. 12–14

Pinske C, Bönn M, Krüger S, et al (2011) Metabolic deficiences revealed in the biotechnologically important model bacterium Escherichia coli BL21(DE3). PLoS One 6:. doi: 10.1371/journal.pone.0022830

Poliakoff M, Fitzpatrick JM, Farren TR, Anastas PT (2002) Green chemistry: Science and politics of change. Science (80-) 297:807–810. doi: 10.1126/science.297.5582.807

Rasor JP, Voss E (2001) Enzyme-catalyzed processes in pharmaceutical industry. Appl Catal A Gen 221:145–158. doi: 10.1016/S0926-860X(01)00804-3

Resnick SM, Zehnder AJB (2000) In vitro ATP regeneration from polyphosphate and AMP by polyphosphate:AMP phosphotransferase and adenylate kinase from Acinetobacter johnsonii 210A. Appl Environ Microbiol 66:2045–2051. doi: 10.1128/AEM.66.5.2045-2051.2000

Ridlon JM, Kang DJ, Hylemon PB, Bajaj JS (2015) Bile Acids and the Gut Microbiome Introduction: The Human Gut Microbiome. 30:332–338. doi: 10.1097/MOG.0000000000000057

Roberts GA, Grogan G, Greter A, et al (2002) Identification of a new class of cytochrome P450 from a Rhodococcus sp. J Bacteriol 184:3898–3908. doi: 10.1128/JB.184.14.3898-3908.2002

Rodriguez AM, Olano C, Méndez C, et al (1995) A cytochrome P450-like gene possibly involved in oleandomycin biosynthesis by Streptomyces antibioticus. FEMS Microbiol Lett 127:117–120. doi: 10.1016/0378-1097(95)00047-9

Rosano GL, Ceccarelli EA (2014) Recombinant protein expression in Escherichia coli: Advances and challenges. Front Microbiol 5:1–17. doi: 10.3389/fmicb.2014.00172

Rotunda AM, Ablon G, Kolodney MS (2005) Lipomas treated with subcutaneous deoxycholate injections. J Am Acad Dermatol 53:973–978. doi: 10.1016/j.jaad.2005.07.068

Rotunda AM, Suzuki H, Moy RL, Kolodney MS (2004) Detergent effects of sodium deoxycholate are a major feature of an injectable phosphatidylcholine formulation used for localized fat dissolution. Dermatologic Surg 30:1001–1008. doi: 10.1111/j.1524-4725.2004.30305.x

Roy S, Vega MV, Harmer NJ (2019) Carbohydrate kinases: A conserved mechanism across differing folds. Catalysts 9:1–19. doi: 10.3390/catal9010029

Russell DW (2009) Fifty years of advances in bile acid synthesis and metabolism. J Lipid Res 50:120–125. doi: 10.1194/jlr.R800026-JLR200

Schoenenberger B, Wszolek A, Meier R, et al (2017a) Biocatalytic asymmetric Michael addition reaction of l-arginine to fumarate for the green synthesis of: N -(([(4 S)-4-amino-4-carboxy-butyl]amino)iminomethyl)-l-aspartic acid lithium salt (l-argininosuccinic acid lithium salt). RSC Adv 7:48952–48957. doi: 10.1039/c7ra10236d

Schoenenberger B, Wszolek A, Meier R, et al (2018) Recombinant AroL-Catalyzed Phosphorylation for the Efficient Synthesis of Shikimic Acid 3-Phosphate. Biotechnol J 13:. doi: 10.1002/biot.201700529

Schoenenberger B, Wszolek A, Meier R, et al (2017b) Biocatalytic asymmetric Michael addition reaction of l-arginine to fumarate for the green synthesis of: N -(([(4 S)-4-amino-4-carboxy-butyl]amino)iminomethyl)-l-aspartic acid lithium salt (l-argininosuccinic acid lithium salt). RSC Adv 7:48952–48957. doi: 10.1039/c7ra10236d

Schoenenberger B, Wszolek A, Milesi T, et al (2017c) Synthesis of Nω-Phospho-l-arginine by Biocatalytic Phosphorylation of l-Arginine. ChemCatChem 9:121–126. doi: 10.1002/cctc.201601080

Sevrioukova IF, Poulos TL (2011) Structural biology of redox partner interactions in P450cam monooxygenase: A fresh look at an old system. Arch Biochem Biophys 507:66–74. doi: 10.1016/j.abb.2010.08.022

Shin J, Kim JE, Lee YW, Son H (2018) Fungal cytochrome p450s and the p450 complement (Cypome) of fusarium graminearum. Toxins (Basel) 10:76–91. doi: 10.3390/toxins10030112

Singh R, Kumar M, Mittal A, Mehta PK (2016) Microbial enzymes: industrial progress in 21st century. 3 Biotech 6:1–15. doi: 10.1007/s13205-016-0485-8

Staudt S, Bornscheuer UT, Menyes U, et al (2013) Direct biocatalytic one-pot-transformation of cyclohexanol with molecular oxygen into ε-caprolactone. Enzyme Microb Technol 53:288–292. doi: 10.1016/j.enzmictec.2013.03.011

Straathof AJJ, Panke S, Schmid A (2002) The production of fine chemicals by biotransformations. Curr Opin Biotechnol 13:548–556. doi: 10.1016/S0958-1669(02)00360-9

Strong SJ, Ellington WR (1993) Horseshoe crab sperm contain a unique isoform of arginine kinase that is present in midpiece and flagellum. J Exp Zool 267:563–571. doi: 10.1002/jez.1402670603

Strong SJ, Ellington WR (1996) Expression of horseshoe crab arginine kinase in Escherichia coli and site-directed mutations of the reactive cysteine peptide. Comp Biochem Physiol - B Biochem Mol Biol 113:809–816. doi: 10.1016/0305-0491(95)02104-3

Strong SJ, Ellington WR (1995) et Biophysica Isolation and sequence analysis of the gene for arginine kinase from the important residues ". Cloning 1246:197–200

Takahashi S, Fukami T, Masuo Y, et al (2016) Cyp2c70 is responsible for the species difference in bile acid metabolism between mice and humans. J Lipid Res 57:2130–2137. doi: 10.1194/jlr.M071183

Teixeiras J, Gilg G (1991) THE JOURNAL OF BIOLOGICAL CHEMISTRY Cloning, Expression, and Regulation of Lithocholic Acid G@-Hydroxylase*. 266:21030–21036

Thakare R, Alamoudi JA, Gautam N, et al (2018) Species differences in bile acids II. Bile acid metabolism. J Appl Toxicol 38:1336–1352. doi: 10.1002/jat.3645

Thomas PE, Ryan D, Levin W (1976) An improved staining procedure for the detection of the peroxidase activity of cytochrome P-450 on sodium dodecyl sulfate polyacrylamide gels. Anal Biochem 75:168–176. doi: 10.1016/0003-2697(76)90067-1

Thomas SM, DiCosimo R, Nagarajan V (2002) Biocatalysis: Applications and potentials for the chemical industry. Trends Biotechnol 20:238–242. doi: 10.1016/S0167-7799(02)01935-2

Timson DJ (2019) Four challenges for better biocatalysts. Fermentation 5:1–9. doi:

10.3390/fermentation5020039
Tonin F, Arends IWCE (2018) Latest development in the synthesis of ursodeoxycholic acid (UDCA): A critical review. Beilstein J Org Chem 14:470–483. doi: 10.3762/bjoc.14.33
Trauner M, Claudel T, Fickert P, et al (2010) Bile acids as regulators of hepatic lipid and glucose metabolism. Dig Dis 28:220–224. doi: 10.1159/000282091
Truppo MD (2017) Biocatalysis in the Pharmaceutical Industry: The Need for Speed. ACS Med Chem Lett 8:476–480. doi: 10.1021/acsmedchemlett.7b00114
Urlacher VB, Girhard M (2019) Cytochrome P450 Monooxygenases in Biotechnology and Synthetic Biology. Trends Biotechnol 37:882–897. doi: 10.1016/j.tibtech.2019.01.001
Urlacher VB, Girhard M (2012) Cytochrome P450 monooxygenases: An update on perspectives for synthetic application. Trends Biotechnol 30:26–36. doi: 10.1016/j.tibtech.2011.06.012
Urlacher VB, Girhard M (2011) Cytochrome P450 monooxygenases: an update on perspectives for synthetic application. Trends Biotechnol 30:26–36. doi: 10.1016/j.tibtech.2011.06.012
Van Den Brink HM, Van Gorcom RFM, Van Den Hondel CAMJJ, Punt PJ (1998) Cytochrome P450 enzyme systems in fungi. Fungal Genet Biol 23:1–17. doi: 10.1006/fgbi.1997.1021
van der Werf MJ, van den Tweel WJJ, Kamphuis J, et al (1994) The potential of lyases for the industrial production of optically active compounds. Trends Biotechnol 12:95–103. doi: 10.1016/0167-7799(94)90112-0
Virtanen E, Kolehmainen E (2004) Use of bile acids in pharmacological and supramolecular applications. European J Org Chem 3385–3399. doi: 10.1002/ejoc.200300699
Wang X, Fu X, Van Ness C, et al (2013) Bile Acid Receptors and Liver Cancer. Curr Pathobiol Rep 1:29–35. doi: 10.1007/s40139-012-0003-6
Werck-reichhart D, Feyereisen R (2000) Protein family review Cytochromes P450 : a success story. Genome Biol 1:1–9
Williams MG, Olson PE, Tautvydas KJ, et al (1990) The application of toluene dioxygenase in the synthesis of acetylene-terminated resins. Appl Microbiol Biotechnol 34:316–321. doi: 10.1007/BF00170050
Wohlgemuth R (2009) The locks and keys to industrial biotechnology. N Biotechnol 25:204–213. doi: 10.1016/j.nbt.2009.01.002
Wohlgemuth R (2017) Horizons of systems biocatalysis and renaissance of metabolite synthesis. 169–172. doi: 10.13546/j.cnki.tjyjc.2017.23.040
Wohlgemuth R, Liese A, Streit W (2017) Biocatalytic Phosphorylations of Metabolites: Past, Present, and Future. Trends Biotechnol 35:452–465. doi: 10.1016/j.tibtech.2017.01.005
Xiao K, Yue XH, Chen WC, et al (2018) Metabolic engineering for enhanced medium chain omega hydroxy fatty acid production in Escherichia coli. Front Microbiol 9:. doi: 10.3389/fmicb.2018.00139
Xu F (2005) Applications of oxidoreductases: Recent progress . Ind Biotechnol 1:38–50. doi: 10.1089/ind.2005.1.38
Yadav JS, Soellner MB, Loper JC, Mishra PK (2003) Tandem cytochrome P450 monooxygenase genes and splice variants in the white rot fungus Phanerochaete chrysosporium: Cloning, sequence analysis, and regulation of differential expression. Fungal Genet Biol 38:10–21. doi: 10.1016/S1087-1845(02)00508-X
Yin YC, Yu HL, Luan ZJ, et al (2014) Unusually Broad Substrate Profile of Self-Sufficient Cytochrome P450 Monooxygenase CYP116B4 from Labrenzia aggregata. ChemBioChem 15:2443–2449. doi: 10.1002/cbic.201402309
Yu B, Howell PL (2000) Intragenic complementation and the structure and function of argininosuccinate lyase. Cell Mol Life Sci 57:1637–1651. doi: 10.1007/PL00000646

Zelasko S, Palaria A, Das A (2013) Optimizations to achieve high-level expression of cytochrome P450 proteins using Escherichia coli expression systems. Protein Expr Purif 92:77–87. doi: 10.1016/j.pep.2013.07.017

Zhao Y, Yuan Y, Zhang X, et al (2018) Screening of a novel polysaccharide lyase family 10 pectate lyase from paenibacillus polymyxa KF-1: Cloning, expression and characterization. Molecules 23:. doi: 10.3390/molecules23112774

Zhou G, Somasundaram T, Blanc E, et al (1998a) Transition state structure of arginine kinase: implications for catalysis of bimolecular reactions. Proc Natl Acad Sci U S A 95:8449–8454. doi: 10.1073/pnas.95.15.8449

Zhou G, Somasundaram T, Blanc E, et al (1998b) Transition state structure of arginine kinase: Implications for catalysis of bimolecular reactions. Proc Natl Acad Sci U S A 95:8449–8454. doi: 10.1073/pnas.95.15.8449

Tsuei et al. - 2014 - Bile acid dysregulation, gut dysbiosis, and gastrointestinal cancer.pdf

(1975) Preparation and physicochemical properties of argininosuccinase. 397:478–488

Curriculum vitae

Name and Surname:	Agata Wszołek (Bednarczyk)
Date of birth:	16.10.1987
Adsress:	Kazimierska 1h/6, 71-043 Szczecin, Poland
Phone number:	+48 600 431 454
E-mail:	wszolek.agata@gmail.com

Education

1/10/2006 – 30/06/2009	**Biotechnology engineering** Technical University of Szczecin, Faculty of biotechnology and animal breeding. Engineering studies
1/10/2009 – 30/06/2011	**Biotechnology, Master.** Technical University of Szczecin, Faculty of Biotechnology and animal breeding.

Work Experience

1/01/2012 –28/02/2019	BTA; Enzymicals AG, Greifswald Germany
1/03/2019 – present	Teaching Research Assistant, The University of Szczecin, Szczecin, Poland

Published papers:

Kuzajewska, D., **Wszołek, A**., Żwierełło, W., Kirczuk, L., & Maruszewska, A. (2020). Magnetotactic Bacteria and Magnetosomes as Smart Drug Delivery Systems: A New Weapon on the Battlefield with Cancer?.*Biology*,*9*(5), 102.

Grobe, S., **Wszołek, A**., Brundiek, H., Fekete, M., & Bornscheuer, U. T. (2020). Highly selective bile acid hydroxylation by the multifunctional bacterial P450 monooxygenase CYP107D1 (OleP). *Biotechnology Letters* (2020): 42(5) 819-826. DOI: 10.1007/s10529-020-02813-4

Schoenenberger B.,**Wszolek A.**, Meier R., Brundiek H., Obkircher M., Wohlgemuth R. (2018).
Recombinant AroL-Catalyzed Phosphorylation for the Efficient Synthesis of Shikimic Acid 3-Phosphate. *Biotechnol. J.*, 13.8 (2018): 1700529; DOI: 10.1002/biot.201700529

B. Schoenenberger, **A. Wszolek**, R. Meier, H. Brundiek, M. Obkircher,and R. Wohlgemuth (2017),
Biocatalytic asymmetric Michael addition reaction of L-arginine to fumarate for the green synthesis of *N*-(([(4 S)-4-amino-4-carboxy-butyl] amino) iminomethyl)-L-aspartic acid lithium salt (L-argininosuccinic acid lithium salt). *RSC advances* 7(77) (2017): 48952-48957; DOI: 10.1039/c7ra10236d

Schoenenberger B.,**Wszolek A.**, Milesi T., Obkircher M., Brundiek H., Wohlgemuth R. (2016),
Synthesis of Nω-Phospho-L-arginine by Biocatalytic Phosphorylation of L-Arginine, *ChemCatChem*, 9, 121–126 (2017), DOI: 10.1002/cctc.201601080.

Wardenga, R., **Bednarczyk, A.,** Höhne, M. (2013),
Asymmetric Synthesis of Chiral Amines from Ketones: How to Apply Biocatalysis and Find a Suitable Enzyme. *ChemInform* 45(49) (2014)

Contributions to conferences:

03/2015	Conference: “Transam 2.0”; Greifswald; Poster: “Tailor-made Transamination” A. Wszołek, S. Borchert, H. Brundiek, R. Wardenga
11/2015	Conference: “Scottish Metabolomics Network Inaugural Meeting“ ;Edinburgh, Poster: ”Synthesis of Shikimic acid-3-phosphate by Biocatalytic Phosphorylation of Shikimic acid” Bernhard Schönenberger, **Agata Wszołek,** Roland Meier, Markus Obkircher, Henrike Brundiek, Roland Wohlgemuth
07/2016	Conference: “Biocat2016”; Hamburg Poster (#312): „Argininosuccinate Lyase-catalyzed Condensation of L-arginine and Fumarate” Bernhard Schoenenberger, **Agata Wszolek**, Roland Meier, Henrike Brundiek, Markus Obkircher, Roland Wohlgemuth Poster (#308): „Shikimate Kinase-catalyzed Phosphorylation of Shikimate” Bernhard Schönenberger, **Agata Wszołek,** Roland Meier, Markus Obkircher, Henrike Brundiek, Roland Wohlgemuth

Acknowledgement

And at this point, the PhD journey is at an end with the completion of this thesis. There are many people that helped me to achieve this milestone, and I would like to thank all of them.

First of all, I would like to thank my promotor Prof. Dr. Uwe T. Bornscheuer. Thank you so much for all the time you invested not only towards the end while critically reading my thesis, but also for all your constant patience, support and understanding.

I would also like to thank Dr. Ulf Menyes and Dr. Rainer Wardenga for giving me an opportunity to work at Enzymicals AG. It has been a great honour to be able to work together with you.

I would like to express my deepest gratitude to my supervisor Dr. Henrike Brundiek who provided me the best academic supervision I have ever had. Thank you for the trust in me and giving me the opportunity to work on several of projects. Henrike, you accepted me into your group, where I really enjoyed to work and where I have learnt many things about so many different topics. You were always available for my questions and gave me instant feedback. Thank you for your patience with me. Your comments and corrections have been fundamental to improve the quality of my manuscript. You are truly a mother of this PhD thesis! …and my great mentor!

Besides to my supervisors, I would also like to give special thanks to the members of Enzymicals Team. In particular, to Pauline, Sabine, Melinda, who together with Eric have created the best atmosphere in the lab. Thank you for all the company and friendship, and for all the fun! I would further like to thank Dr. Melinda Fekete for her help and guidance regarding mass spectrometric analysis.

I would like to say thanks to all the co-operation partners I have been working with during my Ph.D. I am particularly thankful to Dr. Roland Wohlgemuth (Merck) for fruitful collaboration.

Thanks to Sascha Grobe, especially for the fact that you have carried out the last experiments.

Next I would like to thank my best friends, in particular Paula and Wiktoria. They always knew when to encourage or kick butt, as I needed! I am very thankful and honored to have you in my life!!

Last but foremost, I whole heartedly thank my family, especially my husband Kuba (He is my soulmate, best friend, and means the world to me) and my lovely almost 3-year-old daughter Ada. Kids do not make things easier. But they do give you a reason to keep going. During dark periods of the PhD, she was always there to put a smile on my face.

I also wish to express my greatest gratitude to the best and wisest woman, my mom. Her love, courage, and wisdom have shaped me into what I am today.

Appendix

7.1 CYP107D1

Table A 1: Substrate scope of P450 monooxygenase OleP

Steroids and fatty acids tested in this study as substrates for CYP107D1. Twenty two steroids were screened using the whole-cell biotransformation, out of which two (LCA and DCA) were investigated further.

No	Substrate	Conversion
1	**Testosterone**	**+**
2	Androstendione	-
3	Progesterone	-
4	Dehydroepiandrosterone	-
5	7-Dehydrocholesterol	-
6	Cholesterol	-
7	β-Sitosterol	-
8	Cortisone	-
9	Corticosterone	-
10	4,5α-Dihydrotestosterone,	-
11	Androstanolone	-
12	Stanolone	-
13	**DCA (Deoxycholic acid)**	**+**
14	**LCA (Lithocholic acid)**	**+**
15	Chenodeoxycholic acid (CDCA)	-
16	Ursodeoxycholic acid (UDCA)	-
17	iso_LCA (3α-hydroxy-5α-cholan-24-oic acid)	-
18	Hyodeoxycholic acid (HDCA)	-
19	Chlorzoxazone	-
20	Canrenone	-
21	Daidzein	-
22	dexamethasone	-
23	C10 Decanoic acid (capric acid)	-
24	C12 Lauric	-
25	C14 Myristic acid	-
26	C16 Palmitic acid	-

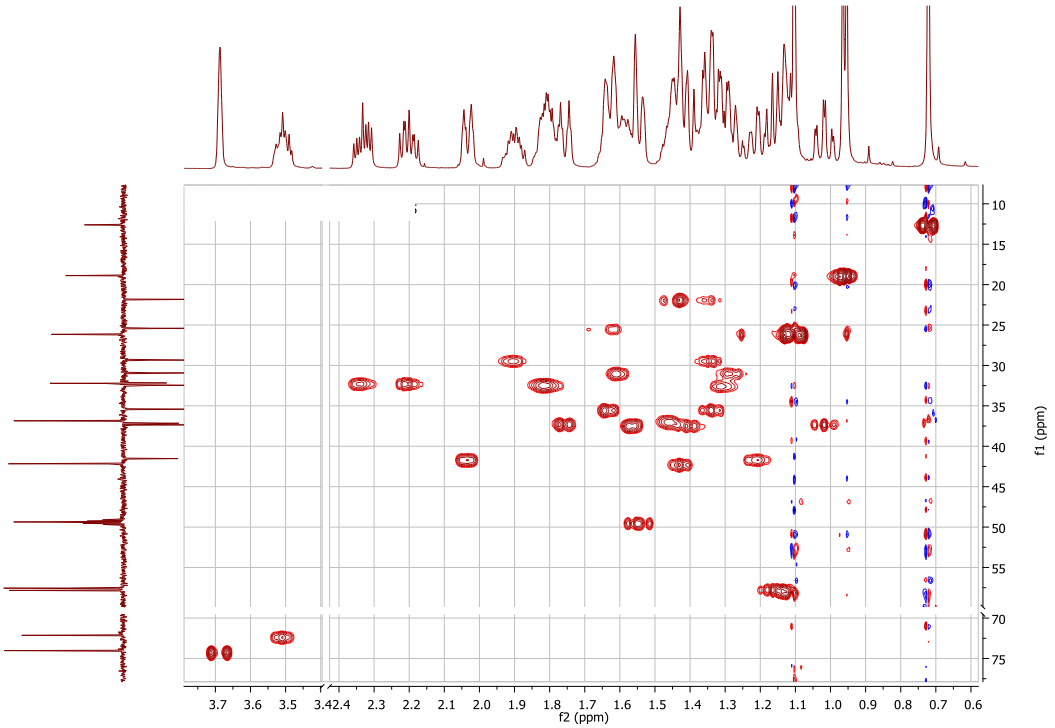

Figure A. 1: 2D-NMR of the purified MCA (3α,6β-dihydroxy-5β-cholan-24-oic acid) 3α,6β-dihydroxy-5β-cholan-24-oic acid. [M^-]: 391.5; ^{1}H-NMR δ (ppm, MeOD): 0.72 (s, 18-Me), 1.10 (s, 19-Me), 3.51 (tt, J=4.7, 11Hz, 3-H), 3.69 (H-6); ^{13}C-NMR δ (ppm, MeOD): 12.6 (C-18), 26.16 (C-19), 72.1 (C-3), 74.04 (C-6).

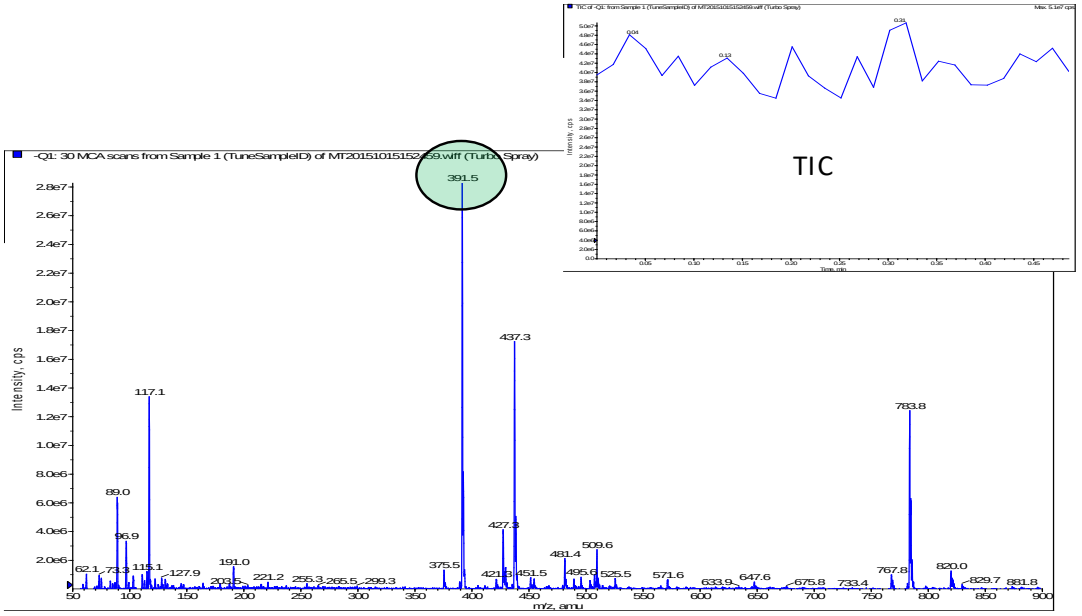

Figure A. 2: MS verification of MCA (Grobe et al. 2020).

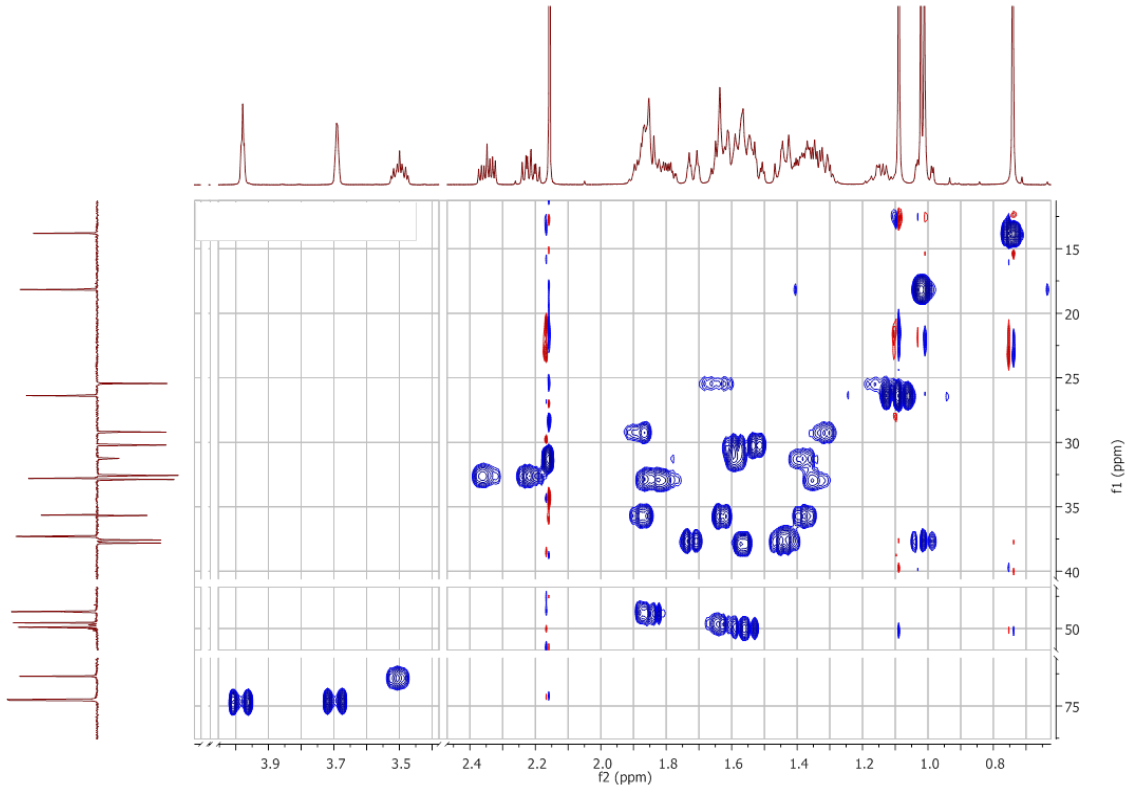

Figure A. 3: 2D NMR of the purified 3α,6β,12α-trihydroxy-5β-cholan-24-oic acid. 3α,6β,12α-trihydroxy-5b-cholan-24-oic acid. [M$^-$]: 407.4; 1H-NMR δ (ppm, MeOD): 0.74 (s, 18-Me), 1.09 (s, 19-Me), 3.50 (tt, J=4.7, 11Hz, 3-H), 3.69 (q, J=2.60Hz, H-6), 3.98 (t, J=2.70Hz, H-12); 13C-NMR δ (ppm, MeOD): 13.80 (C-18), 26.40 (C-19), 72.83 (C-3), 74.55 (C-6), 74.60 (C-12).(Grobe et al. 2020)

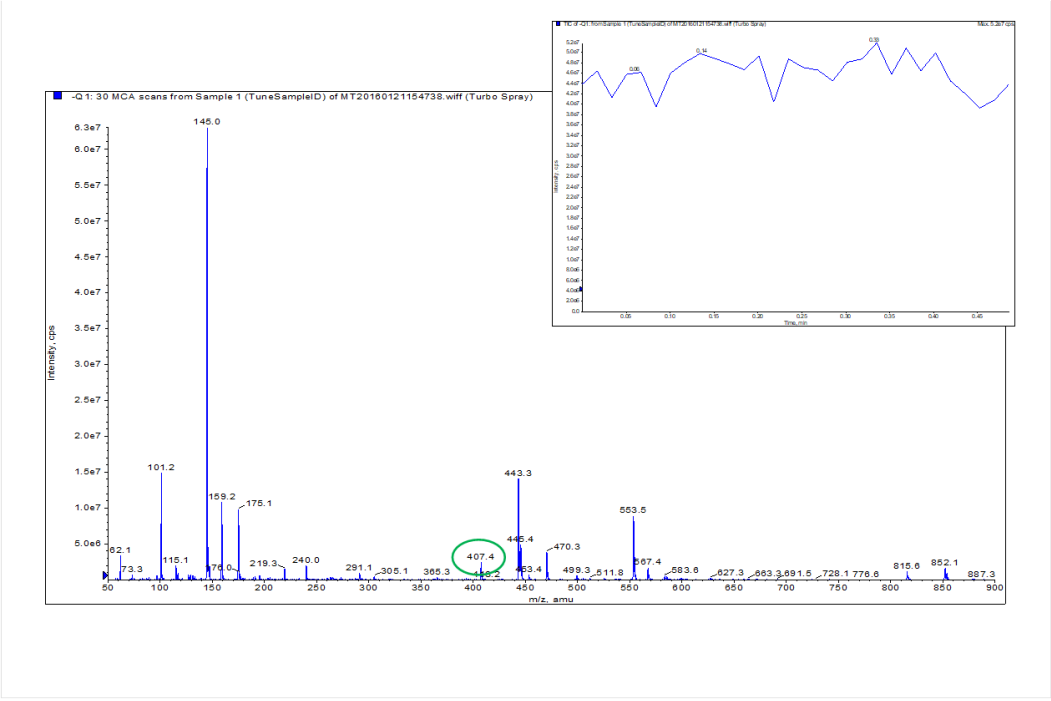

Figure A. 4: MS verification of 3α,6β,12α-trihydroxy-5β-cholan-24-oic acid (Grobe et al. 2020).

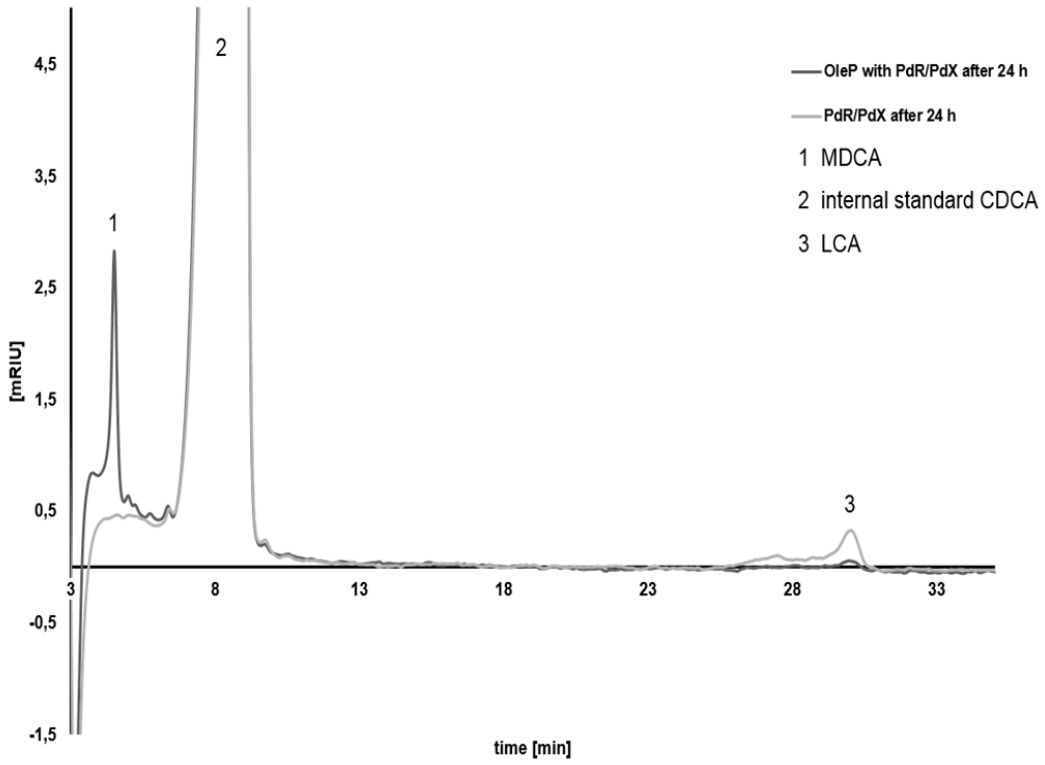

Figure A. 5: HPLC-RI chromatograms of *E. coli* C43 (DE3) pET-28a *oleP*, pACYC *pdR/pdX* (black) and *E. coli* C43 (DE3) pACYC *pdR/pdX* (grey) are overlayed. Peaks marked with numbers 1 correspond to MCA, 2 corresponds to the internal standard used CDCA and 3 corresponds to LCA (Grobe et al. 2020).

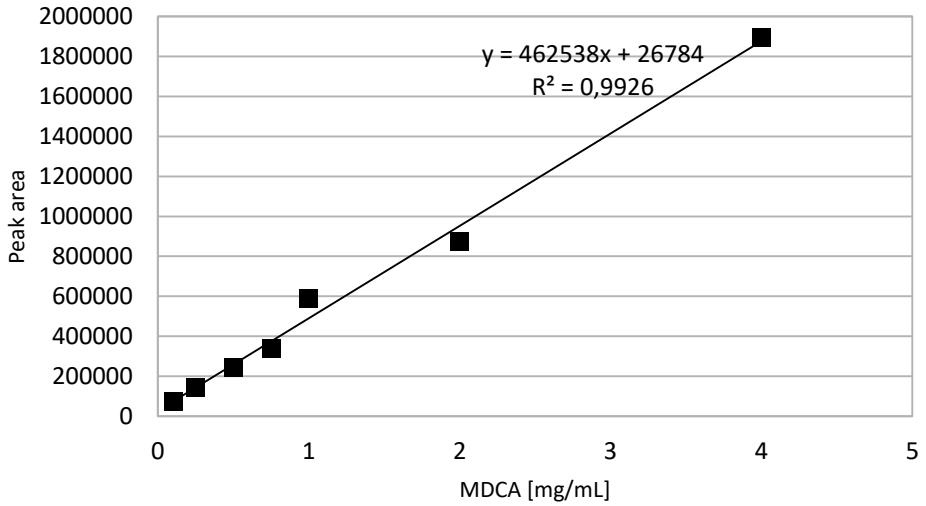

Figure A. 6.: Product quantification of MDCA based on HPLC-RI measurements(Grobe et al. 2020).

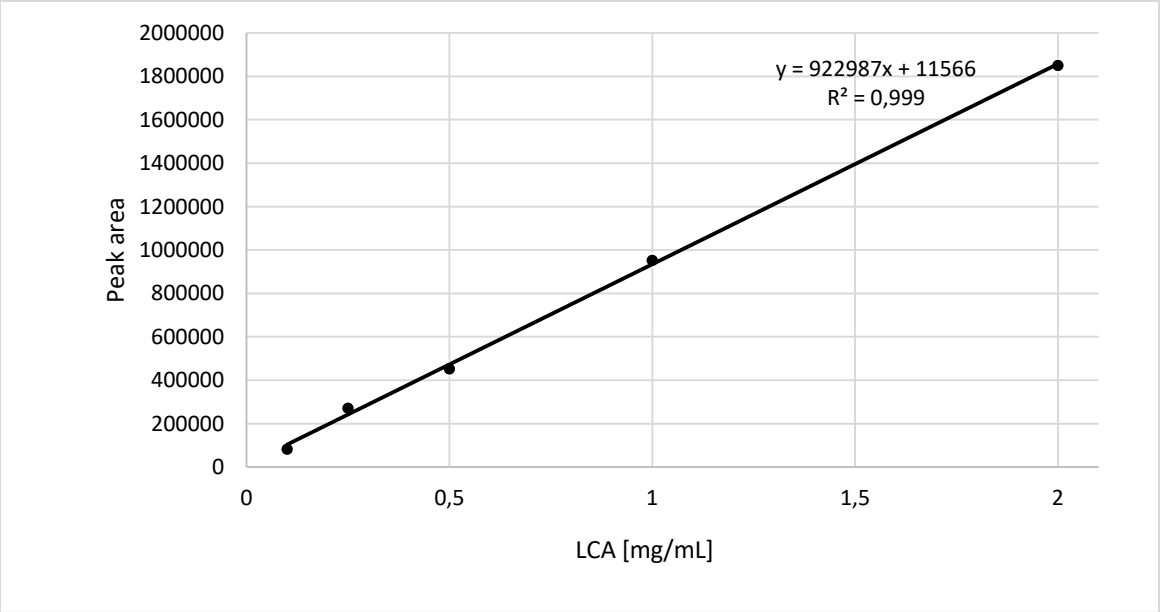

Figure A. 7: Substrate quantification of LCA based on HPLC-RI measurements (Grobe et al. 2020).

7.2 P450_FG067

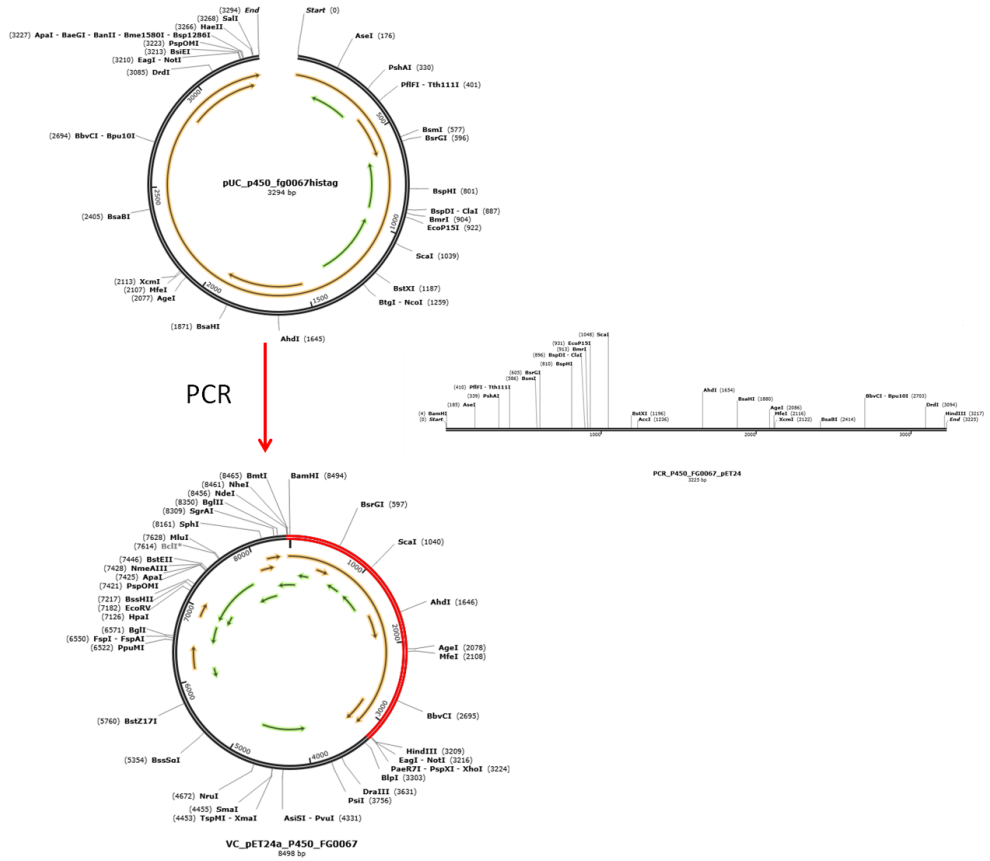

Figure A. 8: Strategy of subcloning P450-FG067 from pUC vector to the pET24 vector, contains a kanamycin resistance gene, an IPTG inducible promoter system.

.

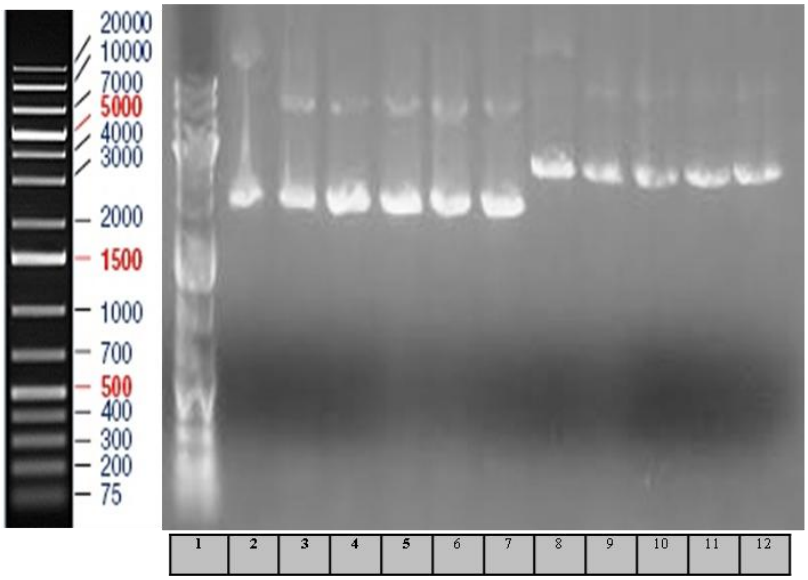

Figure A. 9: PCR amplification of P450-FG067.Amplicons are shown on a 1% agarose gel corresponding to: (1) marker lanes containing a 1 kb ladder (Thermo). (8) P450 –FG067 positive control, (9-12) PCR products with the expected sizes in kb for PCR products 3330 bp.

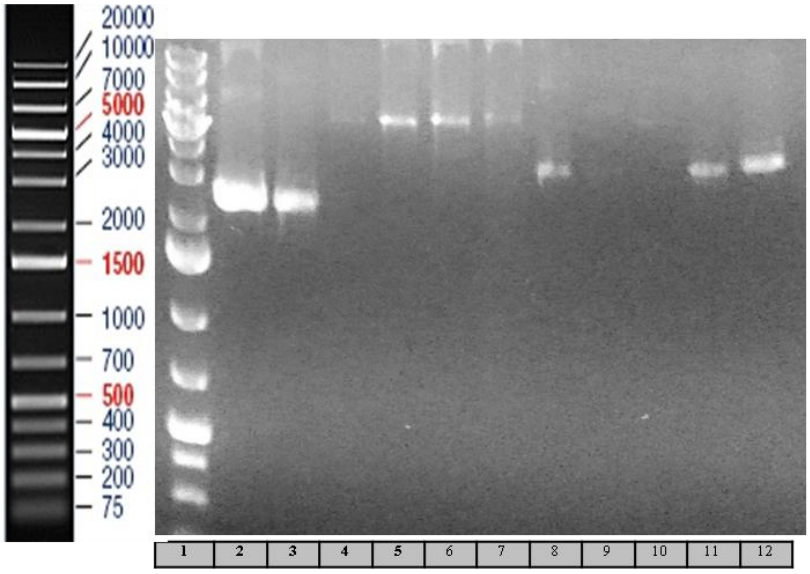

Figure A. 10: PCR control to monitor the integrity of P450-FG067 amplicons in PET24a vector.PCR products are shown on a 1% agarose gel corresponding to: (1) marker lanes containing a 1 kb ladder (Thermo). (8) P450 –FG067 positive control (PUC-FG0067), (9-12) PCR products with the expected sizes in kb for PCR products 3330 bp.

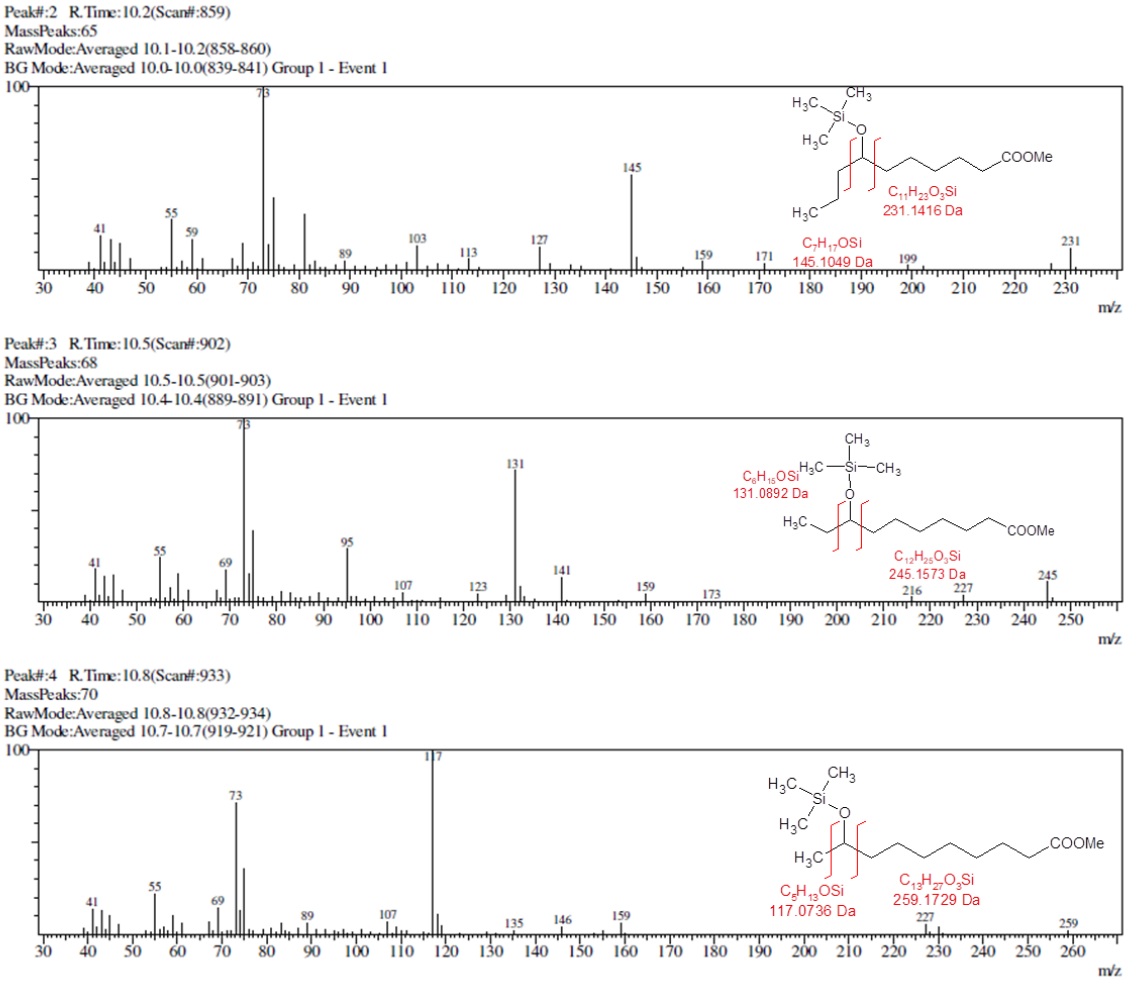

Figure A. 11: MS verificationof hydroxylated C10 fatty acids after derivatization

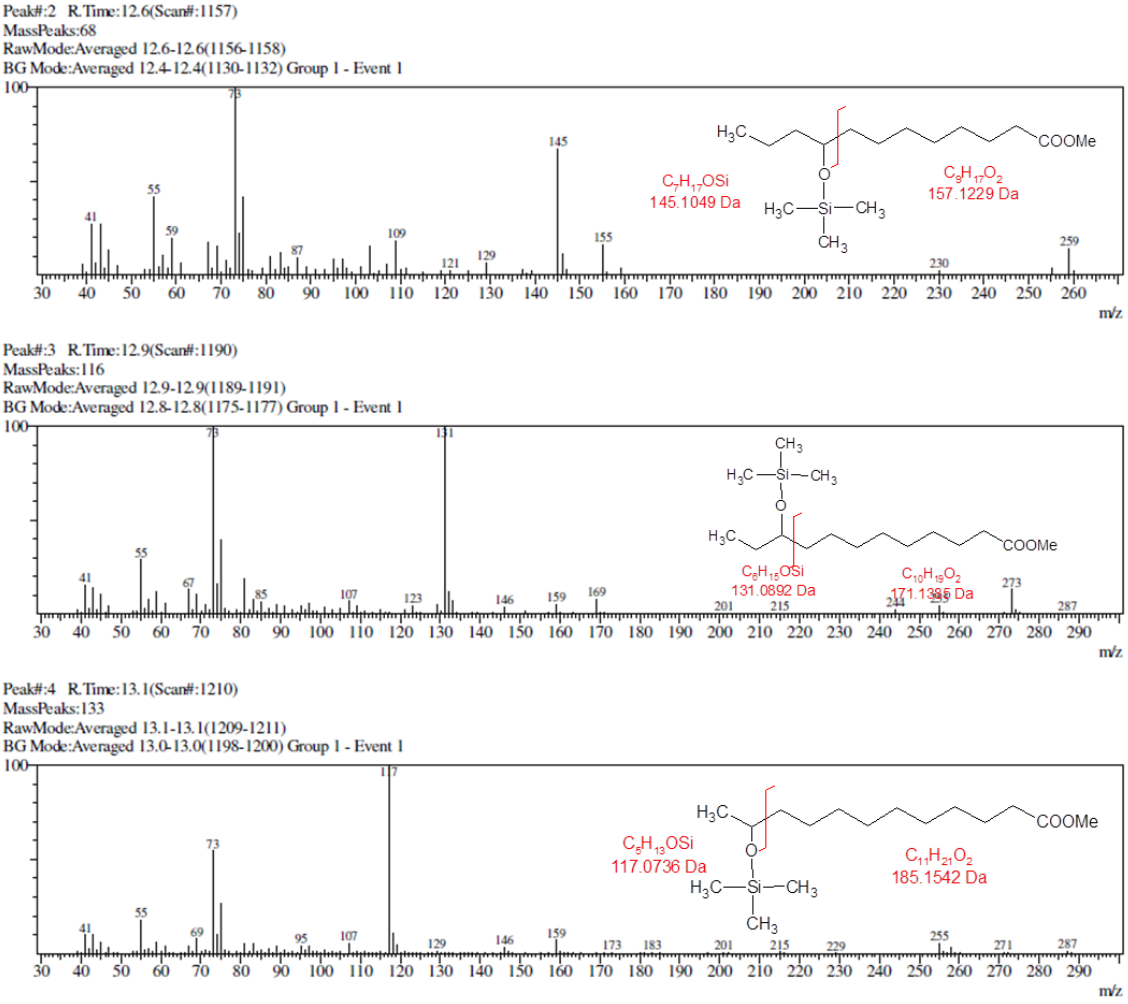

Figure A. 12. MS verification of of hydroxylated C12 fatty acids after derivatization

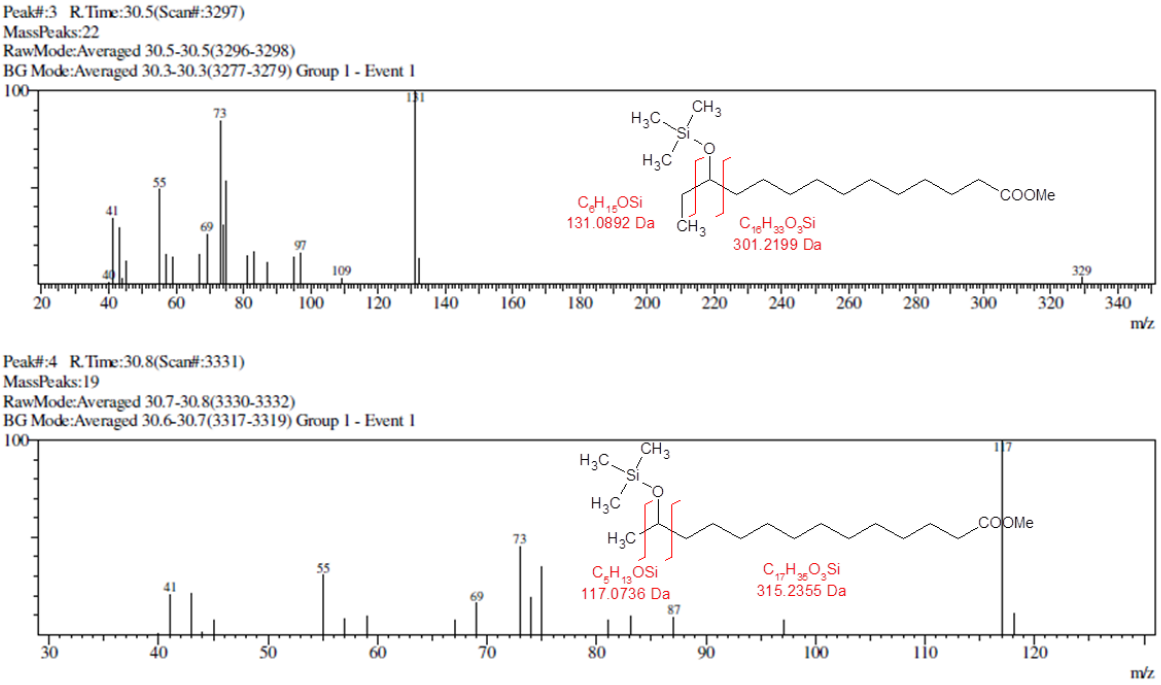

Figure A. 13: MS verificationof of hydroxylated C14 fatty acids after derivatization

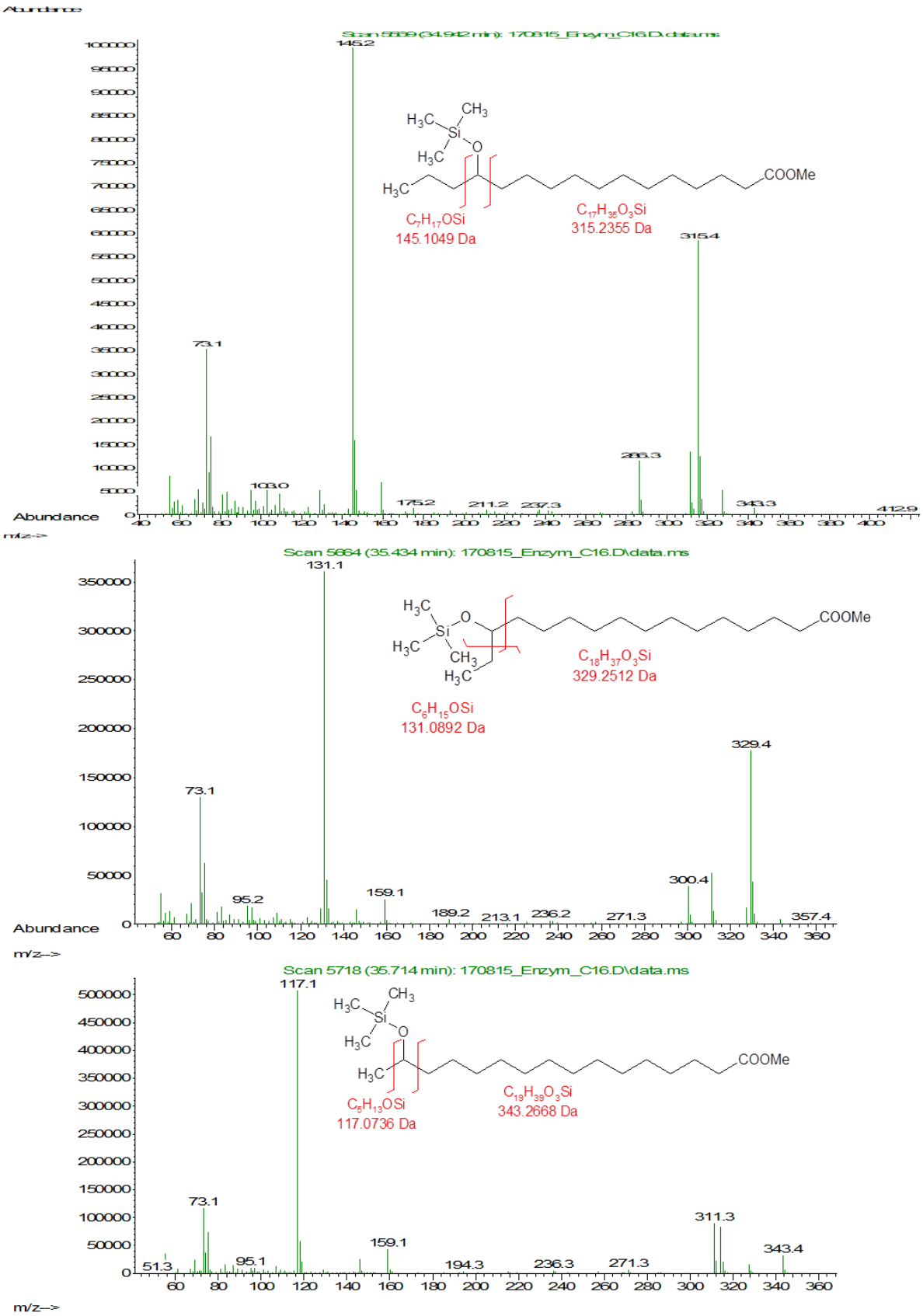

Figure A. 14. MS verificationof of hydroxylated C16 fatty acids after derivatization

Eigenständigkeitserklärung

Hiermit erkläre ich, dass diese Arbeit bisher von mir weder an der Mathematisch Naturwissenschaftlichen Fakultät der Universität Greifswald noch einer anderen wissenschaftlichen Einrichtung zum Zwecke der Promotion eingereicht wurde. Ferner erkläre ich, dass ich diese Arbeit selbstständig verfasst und keine anderen als die darin angegebenen Hilfsmittel und Hilfen benutzt und keine Textabschnitte eines Dritten ohne Kennzeichnung übernommen habe.

Unterschrift des Promovenden